

Post-transcriptional regulation of virulence gene expression in enterohemorrhagic

***E. coli* O157:H7**

Elizabeth McKenney Melson

Fairfax, Virginia

B.S., University of Maryland, 2009

M.S., George Mason University, 2011

A Dissertation presented to the Graduate Faculty
of the University of Virginia in Candidacy for the Degree of
Doctor of Philosophy

Department of Microbiology, Immunology, and Cancer Biology

University of Virginia

December 2019

TABLE OF CONTENTS

List of abbreviations	i
Abstract	iii
Acknowledgments	v
Chapter 1: Introduction to post-transcriptional regulation and enterohemorrhagic <i>Escherichia coli</i> O157:H7	1
Small RNAs.....	2
RNA-binding proteins.....	7
<i>Escherichia coli</i>	9
Enterohemorrhagic <i>E. coli</i> O157:H7.....	10
Transcriptional regulation of the LEE.....	12
Post-transcriptional regulation of the LEE.....	14
Project rationale.....	16
Figures.....	18
Chapter 2: A multicopy sRNA integrates oxygen sensing to modulate host-pathogen interactions	21
Abstract.....	22
Introduction.....	23
Results.....	25
Discussion and future directions.....	33
Materials and methods.....	37
Figures.....	44
Chapter 3: RNA helicases promote virulence gene expression in EHEC	62
Abstract.....	63
Introduction.....	64
Results.....	65
Discussion and future directions.....	71
Materials and methods.....	76
Figures.....	80
Chapter 4: Summary and implications to the field	95
Summary.....	96
Implications to the field.....	97
Figures.....	100
Appendix	101
Table 1. Bacterial strains used in Chapter 2.....	102
Table 2. Plasmids used in Chapter 2.....	103
Table 3. Oligonucleotides used in Chapter 2.....	104
Table 4. Bacterial strains used in Chapter 3.....	109
Table 5. Plasmids used in Chapter 3.....	110
Table 6. Oligonucleotides used in Chapter 3.....	111
References	116

LIST OF ABBREVIATIONS

AE: attaching and effacing

cDNA: complementary DNA

CDS: coding sequence

CFU: colony-forming unit

CTD: C-terminal domain

DMEM: Dulbecco's Modified Eagle Medium

EHEC: enterohemorrhagic *Escherichia coli* O157:H7

EMSA: electrophoretic mobility shift assay

EPEC: enteropathogenic *Escherichia coli*

FAS: fluorescein actin staining

GI: gastrointestinal

H-NS: histone-like nucleoid structuring protein

HUS: hemolytic uremic syndrome

IPTG: isopropyl β -d-1-thiogalactopyranoside

LEE: locus of enterocyte effacement

mRNA: messenger RNA

PNPase: polynucleotide phosphorylase

qPCR: quantitative PCR

RBS: ribosome binding site

RNase: ribonuclease

rRNA: ribosomal RNA

SCFA: short-chain fatty acid

SD: Shine-Dalgarno

sRNA: small RNA

Stx: Shiga toxin

Tir: translocated intimin receptor

T3SS: type III secretion system

UTR: untranslated region

ABSTRACT

Pathogenic bacteria must be able to withstand harsh conditions in environmental reservoirs until the opportune time of infecting a host. Foodborne pathogens survive within distinct niches in the environment and adapt methods to persist during food processing and preparation until ultimately infecting a human host. Once inside the gastrointestinal (GI) tract, foodborne pathogens combat host defense mechanisms to finally colonize the small or large intestines. Virulence genes required for colonization must be precisely controlled to ensure expression at the appropriate location. To accomplish these feats, pathogens integrate signals from the environment into outputs that modulate gene expression to adapt to changing conditions. These outputs affect transcription, as well as post-transcriptional and post-translational regulation. Post-transcriptional regulation, in particular, allows for rapid adaptation to changing environments. Post-transcriptional regulation occurs through the activity of small non-coding RNAs (sRNAs) and/or RNA-binding proteins.

The foodborne pathogen enterohemorrhagic *Escherichia coli* O157:H7 (EHEC) causes GI illness associated with consuming undercooked meats and contaminated produce. EHEC encodes the locus of enterocyte effacement (LEE), a pathogenicity island critical for tight adherence of EHEC to the epithelial barrier of the colon. The infectious dose of EHEC is unusually low, requiring as few as 50 bacteria to cause disease, suggesting that EHEC evolved mechanisms to tightly control virulence gene expression. LEE expression in EHEC responds to different signals that lead to transcriptional and post-transcriptional outputs to control this critical virulence factor and promote expression when appropriate.

In this dissertation, we characterize two pathways that promote LEE expression post-transcriptionally in EHEC. We identify a new mechanism of sRNA activation of gene

expression, describing an sRNA that promotes LEE expression in response to low oxygen conditions, which mimic the environment EHEC encounters when establishing infection in the colon. In addition, we characterize an RNA helicase that promotes LEE expression by repressing the expression of a negative LEE-regulator. In total, we describe complex regulatory pathways that control virulence gene expression, providing new insights into post-transcriptional gene regulation in bacteria.

ACKNOWLEDGMENTS

First, I would like to thank my mentor Melissa Kendall. Melissa has always provided an environment in which I could explore any idea that came to mind. I had the independence that I needed to become a successful scientist under Melissa's guidance. Melissa was also a great resource for the exchange of ideas. She also gave me the opportunity to explore opportunities outside of the lab, which allowed me to figure out what I want to do with my life after lab. I will always be grateful for her support over the past 5.5 years!

I would also like to acknowledge the members of the Kendall Lab, both past and present. Overall, the members of the Kendall Lab have helped me work through various issues with my projects, and the end product would not have been possible without them. To the OG lab - David Clark, Laura Gonyar, Debi Luzader, and CJ Anderson - thank you for your support, encouragement, friendship, and advice during the early years of graduate school. Laura - your friendship since the Goldberg Lab days has always meant a lot to me. Debi and CJ - you were my closest workplace proximity associates. To current lab members Brooke Sauder, Carol Rowley, and John Satkovich - I appreciate all of your support and good ideas over the last few years. I particularly enjoyed our conversations about science and other random topics.

Thank you to the members of my committee - David Rekosh, David Brautigan, Alison Criss, and Jim Nataro. I always felt challenged in a way that made me a better scientist and I appreciate all of your helpful comments and advice.

Alexandra Bettina, your friendship for the last 8.5 years (!!!) has meant more to me than you will ever know. I could not have done this without you. Thank you for being the best, most non-judgmental friend that anyone could ask for. I am so glad that I

responded to that initial e-mail during your search for a roommate. Things have changed so much since then, but also so much has stayed the same. LYFLYFAALAILMBYB.

To my parents, thank you for always supporting me, literally and figuratively, for my entire life. I definitely would not be where I am today if it were not for you.

To my husband, Tim - thank you for everything that you do for our family and me every day. Your support means more to me than you will ever know. I am so thankful that we found each other and I can't imagine my life without you in it.

And finally, to my daughter, Avery - how did this world ever exist without you in it? You are the light of my life and I hope that you will always know that I will always have your back.

**Chapter 1: Introduction to post-transcriptional gene
regulation and enterohemorrhagic *Escherichia coli*
O157:H7**

The ability to sense and respond to changing environments by modulating gene expression is key to bacterial survival and proliferation. The expression of a gene depends on transcriptional responses, mRNA stability and/or translation efficiency, and post-translational modifications. Pathogenic bacteria, in particular, are exposed to many harsh conditions, and adaptation to a host niche is required to establish colonization and promote disease. In order to adapt, bacteria respond to signals that lead to changes in transcriptional and post-transcriptional outputs. While transcriptional responses are important for gene regulation, post-transcriptional modulation of gene expression allows for more rapid adaptation to new environments (1, 2). Post-transcriptional regulation involves direct effects on messenger RNA (mRNA) that lead to changes in transcription termination, transcript stability, and translation of mRNA into protein. These effects are modulated by non-coding small RNAs (sRNAs) and/or RNA-binding proteins (3). In this dissertation, we identify new mechanisms of an sRNA and an RNA-binding protein that post-transcriptionally regulate virulence gene expression in the bacterial pathogen enterohemorrhagic *Escherichia coli* O157:H7 (EHEC). This introduction will cover general concepts of sRNAs, RNA-binding proteins, and EHEC.

Small RNAs

sRNAs affect gene expression by directly binding to mRNAs through complementary base-pairing. sRNAs are typically 50-300 nucleotide non-coding RNAs and are either transcribed from their own promoters or processed from larger transcripts (4, 5). sRNAs are either *cis*-encoded or *trans*-encoded. *Cis*-encoded sRNAs are transcribed from the opposite strand of their target transcript, and thus are 100% complementary to target mRNA (6). On the other hand, *trans*-encoded sRNAs are transcribed from chromosomal locations unrelated to the target transcripts and display

imperfect complementarity to targets (6). *Trans*-encoded sRNAs typically bind to targets through a short 7-10 base-pair seed region and require chaperone proteins, such as Hfq, to affect target expression (6). As regulatory sRNAs do not rely on translation into protein for their activity, post-transcriptional regulation by sRNAs is typically faster than transcriptional responses (2). Indeed, sRNAs are often involved in responses to stressful conditions, such as nutrient limitation, membrane stress, and host responses to infection (7).

Mechanisms of sRNA Activity

sRNAs are involved in all aspects of gene regulation and affect transcription termination, translation, and transcript stability through direct base-pairing to target transcripts. DNA that is transcribed into mRNA is subjected to transcription termination. There are two types of transcription termination in bacteria classified based on the requirement (or not) for extrinsic factors such as Rho. Intrinsic termination depends on a GC-rich stem-loop followed by a stretch of uridines (polyU) at the 3' end of the elongating transcript (8). The stem-loop causes RNA polymerase to pause and the weak association between adenines (DNA) and uridines (RNA) leads to dissociation of the mRNA from the DNA and RNA polymerase (8, 9). In general, the 3' ends of sRNAs are generated by intrinsic termination (10).

In contrast, Rho-dependent termination requires the RecA family helicase, Rho, which binds non-specifically to mRNA to terminate transcription (11). Rho preferentially binds to unstructured cytidine-rich sequences, but a single Rho-utilization site consensus sequence has not been identified (11, 12). Binding of Rho to RNA, in combination with other factors, leads to dissociation of RNA polymerase from the transcript and termination of transcription (13). Rho is responsible for terminating 20-50% of

transcription in *E. coli* (13). To prevent Rho-dependent termination, sRNAs bind to elongating transcripts in the 5' untranslated region (5' UTR) and block Rho binding sites, allowing transcription elongation to continue (Fig. 1-1A) (14, 15). Alternatively, sRNAs can promote Rho-dependent transcription termination through binding to the 5' end of a bicistronic operon and inhibiting translation of the upstream gene, which allows Rho to bind to the elongating transcript and terminate transcription prematurely (Fig. 1-1B) (16).

An abundance of studies have also demonstrated a role for sRNAs in promoting and inhibiting target transcript translation and stability (6) (Fig. 1-1C-F). These two processes are often linked, as transcripts that are not translated are usually rapidly degraded due to lack of protection by ribosomes (17). In general, sRNAs activate or inhibit translation by affecting binding of the 30S ribosomal subunit to the ribosomal binding site (RBS) on target transcripts (Fig. 1-1C and D) (18). The 16S ribosomal RNA (rRNA) includes a sequence that binds to a complementary sequence in the RBS of mRNAs, known as the Shine-Dalgarno (SD) sequence, to initiate ribosome loading (19). sRNAs activate translation initiation by removing mRNA secondary structures that block the SD sequence and prevent ribosome loading on the RBS (Fig. 1-1C) (20–29). Historically, these interactions were demonstrated to occur in the 5' UTR of target transcripts (26). The major focus of Chapter 2 of this dissertation demonstrates an sRNA binding to the coding sequence (CDS) of its target to promote translation initiation (30). In contrast, the most common mechanism of translation inhibition by sRNAs is by direct binding of the sRNA to the RBS through the fifth codon of the open reading frame of a transcript to occlude these sites from the ribosome (31–34) (Fig. 1-1D). However, two recent studies also demonstrated sRNAs binding to the CDS to inhibit translation (35, 36). In the first example, an sRNA binding to the CDS of its target recruited the sRNA chaperone Hfq to a site near the mRNA RBS where Hfq interfered with the formation of

the translation initiation complex (35). In the second example, sRNAs binding to the CDS of a target transcript disrupted secondary structures in the mRNA that were important for translation initiation (36).

In addition to affecting transcription termination and translation initiation of targets, sRNAs also affect stability of the mRNAs to which they bind by either blocking degradation by or recruiting ribonucleases (RNases) (Fig. 1-1E and F). To stabilize transcripts, sRNAs bind to the 5' UTR of targets and protect the transcript from degradation, which is typically linked to promoting translation (23, 37–39). Alternatively, sRNAs destabilize target transcripts by binding either to the 5' UTR or the CDS and recruiting RNases (40–43). Overall, sRNAs are important mediators of transcription, translation, and transcript stability in bacteria (Fig. 1-1).

The *rpoS* transcript often serves as a model for sRNA activity as it is subjected to tight post-transcriptional control. RpoS is an alternative sigma factor (σ^{38}) that binds RNA polymerase core enzyme during stress conditions and is the master regulator of the general stress response in Gram-negative bacteria (44). The *rpoS* transcript includes a long >500 nucleotide 5' UTR that forms an inhibitory secondary structure that occludes its own RBS (20). Direct binding of the sRNAs DsrA, RprA, or ArcZ to the *rpoS* 5' UTR both inhibits Rho-dependent termination at this site and relieves the inhibitory secondary structure, allowing the ribosome to bind the RBS to initiate translation (14, 20–23). These sRNAs are produced under distinct conditions and promote expression of RpoS in response to different stresses (20–23). A related effect of this positive regulation of *rpoS* translation is stabilization of the *rpoS* transcript (23). Altogether, post-transcriptional control of this stress response regulator by sRNAs is crucial for the general stress response.

Sibling sRNAs

One of the processes that sRNAs affect is the regulation of virulence genes in pathogenic bacteria. In particular, sRNAs that exist in multiple copies in the genome of a bacterium are often referred to as “sibling sRNAs” and are frequently involved in virulence gene regulation of pathogens (45). Sibling sRNAs exist in 2-7 copies in the genome, are highly similar either at the nucleotide level or by secondary structure, and are generally thought to have arisen by gene duplication events (46–51). Sibling sRNAs in pathogenic bacteria regulate processes important for colonization of host niches, such as the blood or cerebrospinal fluid (46, 48, 49, 52). Depending on the sRNA and target, the activities of sibling sRNAs are either redundant or additive (46, 53). The existence of multiple copies of an sRNA may support the integration of several regulatory inputs (i.e. different signaling molecules) to modulate the same output (i.e. virulence gene regulation) (53), suggesting that it is beneficial for pathogens to acquire and maintain multiple copies of the same gene.

The sRNA DicF is multicopy in pathogenic strains of *E. coli*, while non-pathogenic strains encode 0-1 copy (33, 54), suggesting that DicF may be involved in virulence gene regulation. Interestingly, the different copies of DicF in pathogenic *E. coli* are encoded within different prophages integrated into the genomes (33, 55), indicating that the multiple copies of DicF were acquired by horizontal gene transfer rather than by gene duplication. That pathogenic *E. coli* evolved to maintain multiple copies of the same foreign DNA suggests that DicF provides a fitness advantage. However, a role for DicF in modulating gene expression in pathogenic *E. coli* had not been identified before this study. In Chapter 2, we describe how the multiple copies of DicF promote the expression of a critical virulence factor in a pathogenic strain of *E. coli* (30).

RNA-binding Proteins

Proteins that bind to and modulate RNA are also important contributors to post-transcriptional regulation of gene expression. Hfq and ProQ are sRNA chaperones that both stabilize sRNAs and assist with sRNA-mRNA interactions. Initially identified as a host factor required for bacteriophage $\text{Q}\beta$ replication (56), Hfq is a member of the Sm/LSm family of proteins and is encoded within many sequenced bacterial genomes (57). Hfq is a global regulator; deletion of Hfq often leads to pleiotropic effects in bacteria as most *trans*-acting sRNAs require Hfq for stabilization and activity (57–59). Hfq is highly abundant and co-localizes with ribosomes in the cytoplasm of the bacterial cell (60). The functional Hfq protein is a homohexamer and forms a ring-like structure (61, 62). Hfq binds to sRNAs and mRNAs on different surfaces of the hexamer ring, via short A/U-rich regions of the sRNA and $(\text{ARN})_n$ motifs of the mRNAs, which enhances interactions between the sRNA and target transcripts (61, 63). The intrinsic polyU terminators of sRNAs are essential for Hfq binding (64). Although Hfq exists in high copy numbers, Hfq is a limiting factor for sRNA function, as binding to many different sRNAs and mRNAs leads to competition (65). When sRNAs and their targets are not present in equal amounts, Hfq is sequestered in sRNA-Hfq or mRNA-Hfq complexes, leading to decreased availability of Hfq for other interactions (65). Thus, it is important for sRNAs and their targets to be transcriptionally expressed under similar conditions to limit competition for Hfq.

ProQ was originally identified as an activator of a proline transporter in *E. coli* (66), and more recently was demonstrated to be another RNA chaperone that facilitates interactions between sRNAs and their targets (67, 68). While Hfq recognizes RNA targets through short sequences, ProQ binds to targets based on secondary structure

(69). Additionally, ProQ primarily binds mRNAs at the 3' end and protects transcripts from degradation by RNases (69).

In addition to the sRNA chaperones, the RNA-binding protein CsrA (carbon storage regulator) is involved in central metabolism, stress responses, and virulence gene regulation (70). The recognized consensus sequence for CsrA contains a GGA motif, which is often found in the SD sequences of the RBS (70). CsrA typically binds to mRNA targets in this region to activate or repress translation, similar to the activity of some sRNAs. CsrA is sequestered by two sRNAs, CsrB and CsrC, which mimic this consensus sequence and prevent CsrA from binding to other targets, thus controlling CsrA activity (71, 72). Altogether, Hfq, ProQ, and CsrA bind to >30% of all transcripts, indicating that the activities of these proteins are critical for global modulation of gene expression (69).

RNA helicases are another class of RNA-binding proteins involved in post-transcriptional regulation. RNA helicases are ubiquitous in all kingdoms of life, and are involved in virtually all aspects of RNA metabolism, including ribosome maturation, rRNA processing, RNA stability, and translation initiation (73). RNA helicases unwind RNA duplexes by an ATP-dependent mechanism (73). In bacteria, RNA helicases are often produced in response to cold shock to disrupt mRNA secondary structures that are stabilized in low temperatures (74–77). Although some RNA helicases have been reported to regulate virulence processes in pathogens (78–80), the involvement of RNA helicases in bacterial pathogenesis is relatively unexplored. In Chapter 3, we describe an RNA helicase that affects virulence gene expression in EHEC.

As previously discussed, a result of post-transcriptional regulation is the stabilization or destabilization of transcripts. RNase E is the major RNase in *E. coli*, controlling the majority of RNA processing and decay (81). RNase E is an endonuclease

that preferentially cleaves mRNA in A/U-rich sequences (82). The N-terminal domain is responsible for the catalytic activity of RNase E (83, 84). Additionally, the N-terminal domain is involved in tethering RNase E to the cytoplasmic membrane, which is important for catalytic activity (85, 86). The C-terminal domain of RNase E contains binding sites for the accessory proteins RNA helicase B (RhlB), polynucleotide phosphorylase (PNPase), and the glycolytic enzyme enolase, which together with RNase E form the RNA degradosome (81, 87). PNPase is an exonuclease that cleaves transcripts in the 3' → 5' direction (88). Under low oxygen growth conditions, RNase E is released from the membrane and becomes cytoplasmic, a process that is dependent on enolase in the degradosome, leading to destabilization of the protein and subsequent stabilization and accumulation of the sRNA DicF (54).

Altogether, sRNAs and RNA-binding proteins are critically important to shaping the transcriptome in bacteria.

Escherichia coli

Commensal strains of *E. coli* colonize the human gastrointestinal (GI) tract and form a mutually beneficial relationship with the host (89). Commensal *E. coli* are generally non-pathogenic, are the most abundant facultative anaerobes of the microbiota, and establish colonization in the mucus layer of the colon (89). Commensal *E. coli* differ from pathogenic strains of *E. coli* that have acquired virulence genes that allow for the ability to cause disease (55, 89, 90). Extraintestinal pathogenic *E. coli* cause infections outside of the GI tract, such as uropathogenic *E. coli* (urinary tract infections) and meningitis-associated *E. coli*. There are at least six types of *E. coli* that cause infections in the GI tract: enterohemorrhagic *E. coli* (EHEC), enteropathogenic *E. coli* (EPEC), enterotoxigenic *E. coli*, enteroaggregative *E. coli*, enteroinvasive *E. coli*, and diffusely

adherent *E. coli*, all of which use different virulence factors to colonize the GI tract and cause disease (89).

EHEC and EPEC share the ability to form attaching and effacing (AE) lesions on intestinal epithelial cells due to the acquisition of a 35.6 kb pathogenicity island known as the locus of enterocyte effacement (LEE), which encodes 41 genes (91, 92). However, the two pathogens are distinct due to location of colonization in the GI tract and the infectious dose. EHEC establishes its niche in the colon and leads to severe bloody diarrhea, has a very low infectious dose (as few as 50 bacteria are sufficient to cause disease (93)), and encodes a potent Shiga toxin (Stx), which is responsible for the severe morbidity and mortality associated with these infections (89, 94). The low infectious dose is a result of efficient stress resistance mechanisms employed by EHEC, particularly acid resistance that is necessary for passage through the acidic environment of the stomach (95, 96). In contrast, EPEC infections require a dose of 10^8 - 10^{10} bacteria to cause disease, and EPEC colonizes the small intestine, leading to profuse watery diarrhea (92). Although some regulatory pathways of the LEE are conserved in EHEC and EPEC, and are highlighted where appropriate, the majority of this dissertation focuses on EHEC.

Enterohemorrhagic *E. coli* O157:H7

EHEC is a foodborne pathogen that causes a self-limiting hemorrhagic colitis, but results in hemolytic uremic syndrome (HUS) in 5-10% of cases (97). EHEC was first recognized as a cause of GI illness after an outbreak of hemorrhagic colitis associated with eating undercooked beef at McDonald's in 1982 (98). Currently, EHEC causes an estimated 95,400 infections in the United States (cdc.gov) and 60 deaths each year (99). Moreover, EHEC infections are responsible for an estimated \$1 billion per year in

economic costs due to associated food recalls (99). Asymptomatically colonized cattle are the main reservoir of EHEC and human infections are caused by ingestion of contaminated meat products and produce (100–102). EHEC is one of the most common causes of foodborne illness associated with fresh produce (101, 102).

The recommended treatment for EHEC infections is supportive care; antibiotics are not recommended due to the potential induction of Stx (103–105). Stx is the causative agent of HUS, a syndrome characterized by renal damage and failure that is responsible for the mortality associated with EHEC infections (94). Stx is encoded by a chromosome-integrated prophage, and is produced and released by lysis of the bacterial cell when the prophage enters the lytic cycle (97, 106). Damage of bacterial DNA (for example, by antibiotics, nitric oxide, hydrogen peroxide, stationary phase growth) triggers a stress response that induces the production of Stx (97). Stx is an AB₅ bacterial toxin, which are characterized by an A subunit that contains the catalytic activity and a B subunit that forms a pentamer for binding specific receptors on target cells (97, 107–109). The globotriasylceramide receptor expressed on intestinal Paneth cells and kidney epithelial cells is the receptor for Stx (110). After internalization, Stx exerts a toxic effect on host cells by cleaving 28S rRNA and inactivating the 60S subunit of the ribosome, thereby halting protein synthesis and ultimately causing cell death (111).

In addition to Stx, the formation of AE lesions on colonic epithelial cells is a hallmark of EHEC infection (Fig.1-2A) (89). The genes required for this adhesion are encoded within the LEE and are organized into five operons known as *LEE1-LEE5* (Fig. 1-2B) (91, 112). AE lesions are characterized by the destruction of microvilli and the rearrangement of the host actin cytoskeleton into pedestals that “cup” the bacteria (Fig. 1-2A) (91). The translocated intimin receptor (Tir) is secreted through the LEE-encoded type three secretion system (T3SS) apparatus (Fig. 1-2C) and inserts into the host cell

membrane, where it acts as a receptor for the bacterial adhesin, intimin (113). The interaction between Tir and intimin initiates a signaling cascade within the host cell that leads to the reorganization of the host actin cytoskeleton and the formation of AE lesions (113). The intimate attachment of EHEC to colonic epithelial cells allows the bacterium to survive and proliferate within an optimal environment.

Transcriptional Regulation of the LEE

LEE-Encoded Regulators

In order to tightly regulate the expression of virulence factors, EHEC must integrate signals from the external environment into transcriptional and post-transcriptional outputs to express these factors when they are required for colonization. The transcriptional regulator Ler is encoded by the first gene in the *LEE1* operon and is responsible for activating transcription of the *LEE2-LEE5* operons (Fig. 1-3A) (114). Ler is required for the formation of AE lesions on enterocytes in both EHEC and EPEC (115). Ler is homologous to the DNA-binding protein histone-like nucleoid-structuring protein (H-NS) and activates transcription of LEE operons by counteracting H-NS repression (116). H-NS is a repressor of gene expression that binds non-specifically to AT-rich DNA sequences, such as those found in horizontally acquired genes, including the LEE (116–118). Ler does not directly activate transcription of *LEE1* in the absence of other regulators, but genes encoded within *LEE1* exhibit decreased expression in a *ler*-deletion strain, indicating that *ler* is directly or indirectly required for transcription of all LEE operons (114, 115). Ler activates transcription of its own LEE-encoded positive (GrlA) and negative (GrlR) regulators (Fig. 1-3A) (119). GrlA and GrlR are encoded within an operon that is not one of the major *LEE1-LEE5* operons (Fig. 1-3A) (119). GrlA and GrlR interact with each other (120) and are both required to activate *LEE2* and

LEE4 in a Ler-independent manner (121). GrIR acts as a repressor of *ler* by binding to GrIA and preventing GrIA binding to the *ler* promoter (119, 122). GrIA activates expression of Ler, and Ler activates expression of the *grIRA* operon (Fig. 1-3A); therefore, GrIA and Ler exist in a positive transcriptional feedback loop (123). Additionally, GrIR protein levels are under the control of the protease ClpXP, which increases LEE expression by degrading GrIR (as well as the non-LEE-encoded regulator RpoS) (124).

Non-LEE-Encoded Regulators

Many non-LEE-encoded transcription factors converge on the *ler* promoter to regulate LEE expression, dependent on different environmental signals and growth conditions. Over thirty non-LEE-encoded transcription factors activate or repress LEE expression (125). The examples described here, PerC/Pch and RpoS, are the subjects of Chapters 2 and 3, respectively.

PerC is a plasmid-encoded transcription factor in EPEC that activates the *LEE1* promoter (Fig. 1-3A) (126). The PerC homologs (Pch) were originally identified in EHEC strain Sakai as three genes that are highly similar to PerC (127). At the nucleotide level, *pchA*, *pchB*, and *pchC* are 99% identical to each other, and at the protein level, PchA, B, and C are 47% identical and 67% similar to PerC (127). Resembling PerC in EPEC, the effects of Pch on LEE expression in EHEC are dependent on Ler, as Pch positively regulates *ler* transcription (127). Furthermore, the additive effect of Ler and PchA on the *LEE2* promoter is much greater than either protein on its own, suggesting that both Ler and PchA are required for LEE transcription (128). Additionally, when Pch is introduced into EPEC, Pch activates the *LEE1* promoter, indicating that the homologous proteins share a similar function (126). The expression of *pch* in EHEC is slightly lower than that

of *perC* in EPEC, suggesting that the cumulative effect of multiple *pch* genes contributes to *LEE1* production in an additive manner (126).

The alternative sigma factor RpoS (σ^{38}), master regulator of the general stress response (44), is a LEE regulator. There are conflicting reports on whether RpoS enhances or represses LEE expression (Fig. 1-3A). In one study, adherence to epithelial cells was negatively affected in strains of EHEC that encoded inactivating point mutations in *rpoS* (129). Furthermore, RpoS promoted transcription of *LEE3* and *LEE4* (130, 131). Alternatively, other studies demonstrated that RpoS negatively affected LEE expression in EHEC, possibly by downregulating *pchA* transcription; however, a direct effect was not demonstrated (124, 132). The seemingly contradictory effects of RpoS on LEE expression are most likely due to strain differences and distinct growth conditions, as levels and activity of RpoS are sensitive to different stresses. Transcription of *rpoS* is relatively stable under most growth conditions (133). However, under various stress conditions, translation of *rpoS* is increased due to the activity of sRNAs, as described above (14, 20–23), and RpoS degradation by the ClpXP protease is inhibited, leading to accumulation of RpoS protein (44). Therefore, the effects of RpoS on LEE expression seem to be dependent on different environmental conditions that post-transcriptionally and post-translationally regulate RpoS production.

Post-transcriptional Regulation of the LEE

Most of the post-transcriptional regulation of the LEE that has been characterized to date either affects transcription of all LEE operons through Ler, or affects *LEE4*, which encodes the structural components of the T3SS (*sepL-espADB*) (Fig. 1-3B). The sRNA chaperone Hfq modulates LEE expression and exhibits different effects depending on the strain (Fig. 1-3B). For example, in EHEC strain 86-24, Hfq is a positive regulator of

the LEE (134), but is a negative regulator of the LEE in strains EDL933 and Sakai (135, 136). This variation in Hfq regulation is likely due to genetic differences between the strains. The transcription of *ler* is under the control of a proximal and a distal promoter and different EHEC strains control *ler* expression via one promoter or the other (137–139). The effect of Hfq on LEE expression in strain 86-24 is likely mediated through *ler*, as all LEE transcripts displayed decreased expression in an *hfq*-deletion strain (134). However, in strain EDL933, Hfq negatively affected *ler* indirectly through repression of *grlA* (135). Additionally, a deletion of *csrA* resulted in increased LEE expression and adherence of EHEC to epithelial cells, although the precise mechanism is unknown (Fig. 1-3B) (140). In EPEC, overexpression of CsrA resulted in repression of *grlA* and CsrA directly bound to the *grlA* transcript *in vitro* (Fig. 1-3B) (141). However, the physiological relevance of these studies is not clear, as overexpression of CsrA may cause off-target effects.

Post-transcriptional regulation of some LEE operons may be necessary because different proteins are required in distinct stoichiometric proportions (142). For example, the *LEE4* operon undergoes RNase E-dependent processing to produce individual *sepL* and *espADB* transcripts (143). This post-transcriptional processing could be a way to control precise levels of protein production for different LEE genes (142, 143). Regulation of LEE operons by sRNAs has also been demonstrated. The sRNAs GlmY and GlmZ bind to and destabilize the *LEE4* and *LEE5* transcripts, leading to decreased AE lesion formation (144) and a recent study to identify sRNAs encoded within the EHEC genome but absent in non-pathogenic *E. coli* identified three sRNAs that modulate LEE expression: sRNA56, sRNA103, and sRNA350 (145). These sRNAs all promoted *espA* expression, likely through indirect mechanisms as the sRNAs were not predicted to directly bind the *LEE4* operon (145). In addition, the sRNA Spot42 acted as

a toggle ON-OFF switch with CsrA to affect *sepL* translation and control protein levels of LEE4 (146). In this study it was shown that Spot42, chaperoned by Hfq, bound to the *sepL* 5' UTR in an overlapping location with CsrA to inhibit translation (the "OFF" state), while CsrA binding activated translation (146). There is also a report that Hfq promoted global LEE expression in EHEC strain 86-24 (134), suggesting the involvement of an sRNA, but the precise mechanisms by which this occurred were unknown. The major focus of Chapter 2 of this dissertation is the demonstration that an Hfq-dependent sRNA (DicF) globally affects LEE expression by promoting translation of the non-LEE-encoded transcriptional regulator, PchA (30).

Project Rationale

EHEC outbreaks cause significant morbidity as well as economic concerns due to food recalls. Currently, treatment of EHEC infections with antibiotics is not recommended due to the possible induction of Stx (103–105). Therefore, it is important to study the ways this pathogen senses the environment and causes disease to identify new approaches to treat infections. Low oxygen levels, such as those found near the epithelial layer of the colon, were previously demonstrated to promote LEE expression and subsequent AE lesion formation (147). However, how EHEC sensed and responded to low oxygen to modulate virulence genes was unknown. Furthermore, how the sRNA chaperone Hfq contributed to global LEE regulation remained to be elucidated. Recently, low oxygen conditions were found to promote expression of the sRNA DicF in non-pathogenic *E. coli* (54). DicF is multicopy in pathogenic strains of *E. coli*, including EHEC (33, 54), and multicopy sRNAs are involved in virulence gene expression in other pathogens (45). DicF expression was Hfq-dependent in EHEC based on microarray analysis (134). Thus, we hypothesized that DicF would affect EHEC virulence under low

oxygen conditions. In Chapter 2, we demonstrate that under microaerobic conditions, DicF targets a transcriptional regulator the LEE, *pchA*, promoting its translation and leading to increased LEE transcription (30). Additionally, in Chapter 3 we identify an alternative pathway for LEE regulation involving an RNA helicase that post-transcriptionally represses expression of RpoS, a negative transcriptional regulator of the LEE. Altogether, these studies highlight the importance of post-transcriptional regulation in controlling critical virulence factor expression.

FIGURES

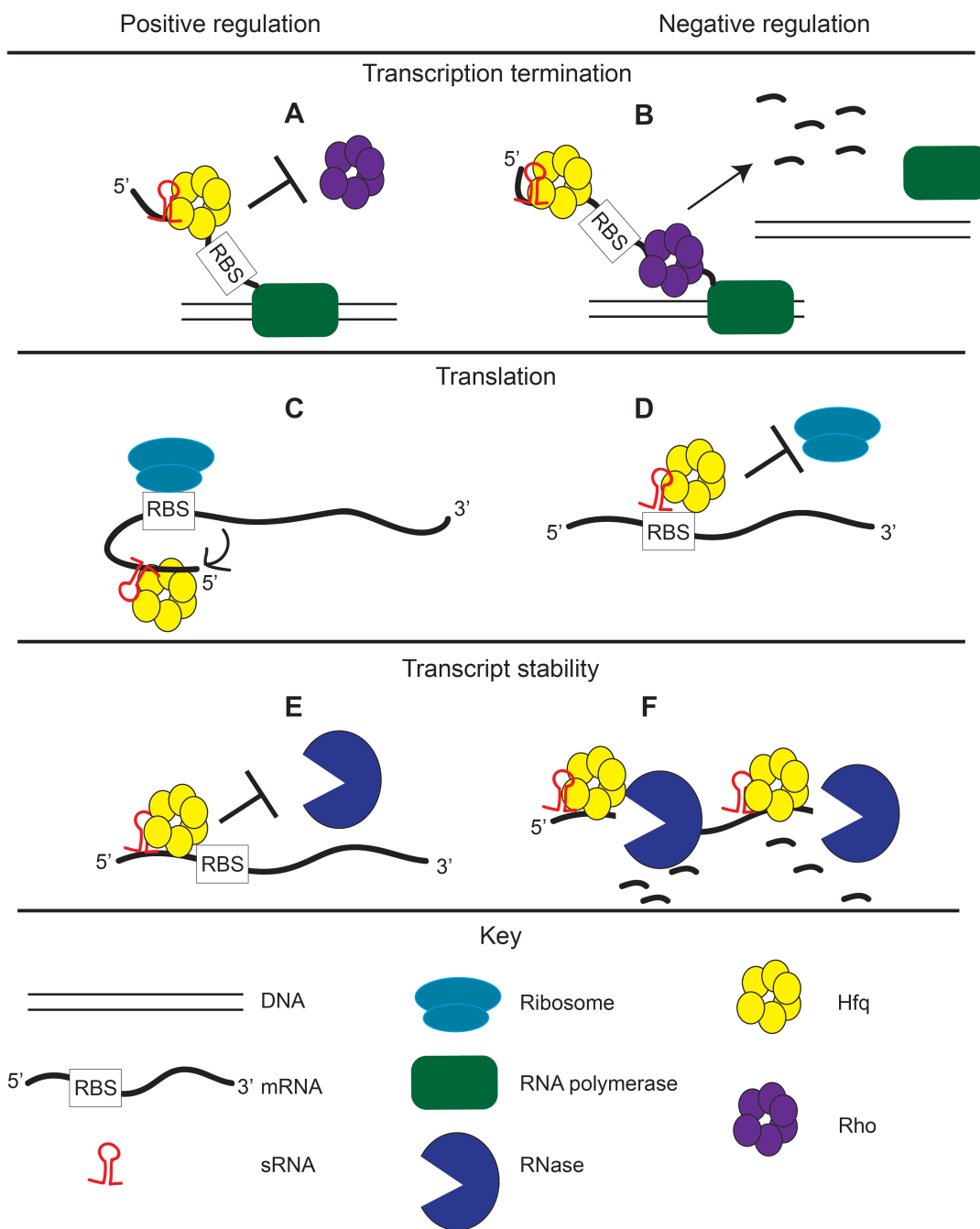


Fig. 1-1. Regulatory mechanisms of sRNAs. sRNAs both positively and negatively regulate target transcripts, and affect transcription termination, translation, and transcript stability. See text for detailed descriptions.

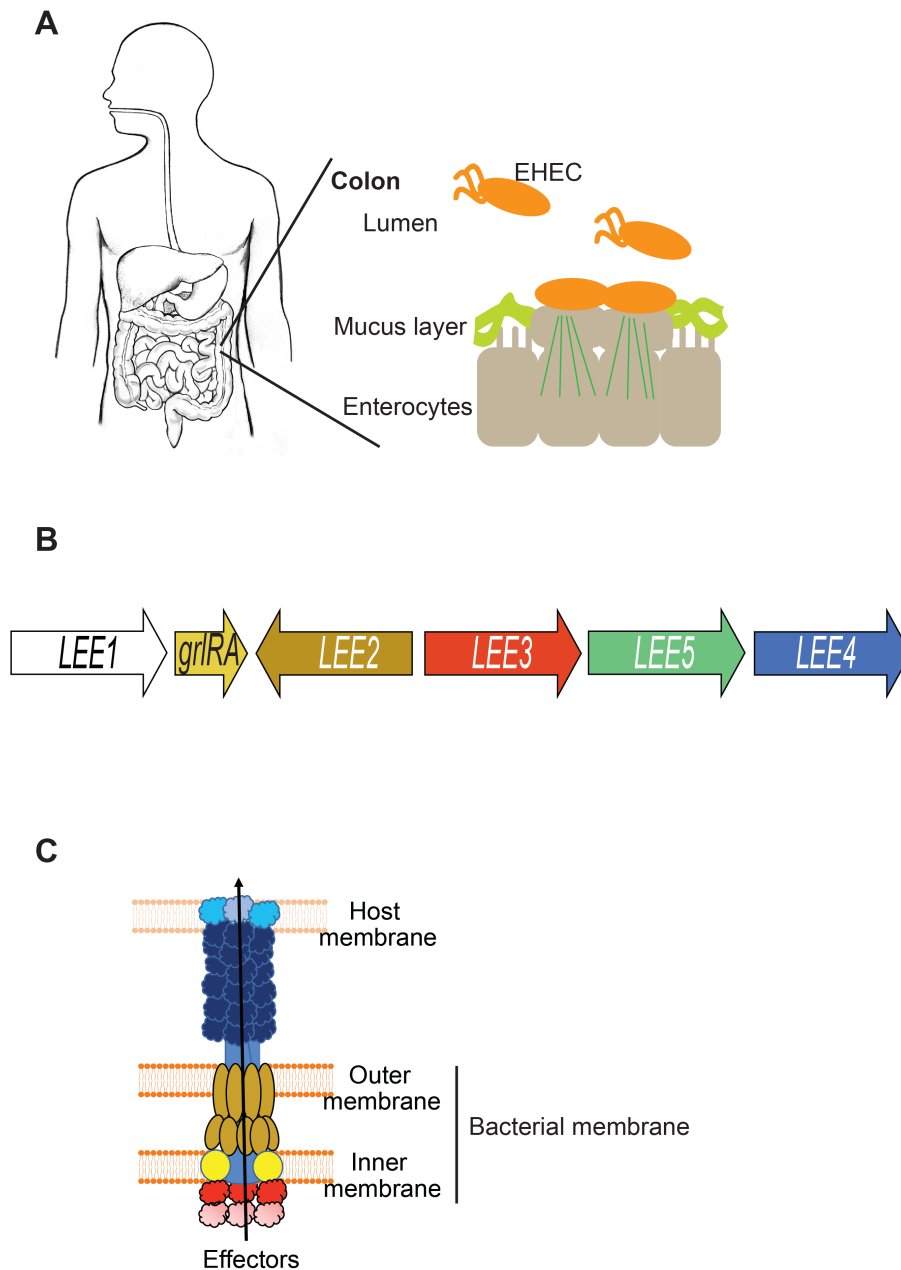
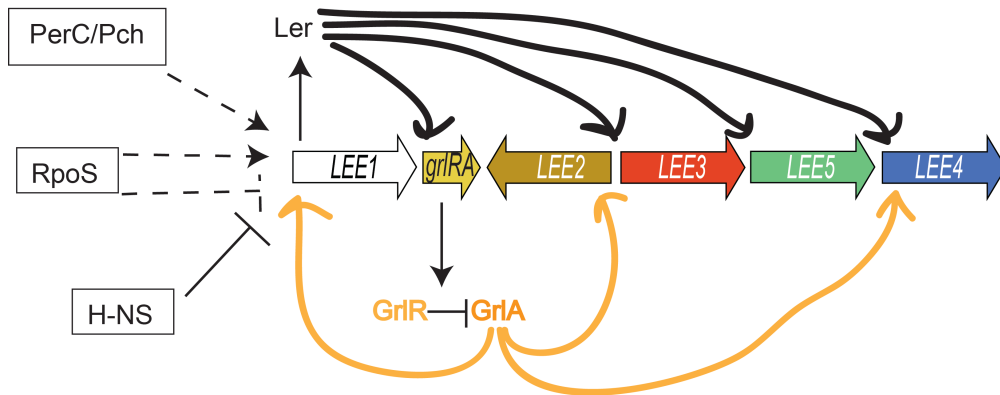


Fig. 1-2. EHEC forms AE lesions in the colon where it expresses the LEE, which encodes genes required for the production of a T3SS. (A) EHEC forms AE lesions in the colon, which are pedestal-like structures on enterocytes that “cup” the bacterium. (B) Schematic of the operon organization of the LEE pathogenicity island. (C) Schematic of the T3SS that connects the bacterial membrane to the host membrane.

A



B

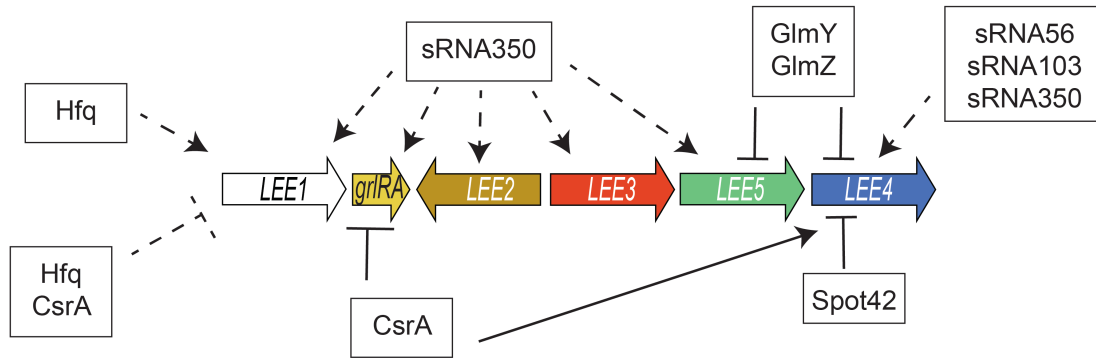


Fig. 1-3. Transcriptional and post-transcriptional regulation of the LEE. (A)

Transcriptional regulation of the LEE. (B) Post-transcriptional regulation of the LEE.

Detailed descriptions are provided in the text. \rightarrow indicate activation of expression, and \perp indicate inhibition of expression. Dashed lines represent indirect regulation.

Chapter 2: A multicopy sRNA integrates oxygen sensing to modulate host-pathogen interactions

Part of this chapter has been adapted from “The sRNA DicF integrates oxygen sensing to enhance enterohemorrhagic *Escherichia coli* virulence via distinctive RNA control mechanisms.”

Elizabeth M. Melson and Melissa M. Kendall. 2019. *Proceedings of the National Academy of Sciences*. 116(28):14210-14215.

ABSTRACT

To establish infection, enteric pathogens integrate environmental cues to navigate the gastrointestinal (GI) tract and precisely control expression of virulence determinants. During passage through the GI tract, pathogens encounter relatively high levels of oxygen in the small intestine before transit to the oxygen-limited environment of the colon. However, how bacterial pathogens sense oxygen availability and coordinate expression of virulence traits is not resolved. Here, we demonstrate that enterohemorrhagic *Escherichia coli* O157:H7 (EHEC) regulates virulence via the oxygen-responsive sRNA DicF. Under oxygen-limited conditions, DicF enhances global expression of the EHEC type three secretion system, which is a key virulence factor required for host colonization, through the transcriptional activator PchA. Mechanistically, the *pchA* coding sequence (CDS) base-pairs with the 5' untranslated region of the mRNA to sequester the ribosome binding site (RBS) and inhibit translation. DicF disrupts *pchA cis*-interactions by binding to the *pchA* CDS, thereby unmasking the *pchA* RBS and promoting PchA expression. These findings uncover a feed-forward regulatory pathway that involves novel mechanisms of RNA-based regulation and that provides spatiotemporal control of EHEC virulence.

INTRODUCTION

Host- and microbiota-dependent metabolic and chemical reactions shape the environmental landscape of the gastrointestinal (GI) tract including distribution of microbes (148). Invading bacterial pathogens navigate microenvironments within the GI tract to effectively compete with the microbiota for nutrients and coordinate virulence gene expression (149). Molecular oxygen plays a major role in establishment of bacterial communities in the gut (150, 151). Oxygen diffuses from the intestinal tissue into the GI tract. In the colon, oxygen is readily consumed by the resident microbiota that reside close to the mucosal interface (150). This generates oxygen gradients in which the lumen is anaerobic and niches more proximal to the epithelial border are microaerobic. In contrast, the small intestine harbors significantly lower numbers of bacteria, and oxygen is not entirely consumed (152). These data support a model in which, during transit through the GI tract, pathogens encounter a relatively oxygenated environment within the small intestine before progressing to the oxygen-limited environment of the colon. Therefore, sensing oxygen availability is a key strategy for pathogens to gauge their location within the host and effectively deploy their virulence arsenals (153); however, it is not fully understood how pathogens respond to oxygen levels to regulate virulence.

Enterohemorrhagic *Escherichia coli* O157:H7 (EHEC) is a food-borne pathogen that colonizes the colon and causes major outbreaks of bloody diarrhea and hemolytic uremic syndrome (HUS) (89). EHEC encodes several important virulence factors, including Shiga toxin (Stx) that causes HUS (154) and the locus of enterocyte effacement (LEE) pathogenicity island. The LEE-encoded genes are required for attaching and effacing (AE) lesion formation on enterocytes (91). The LEE is comprised of five major operons that encode a type three secretion system (T3SS) and effectors

(89, 112). The LEE-encoded *ler* gene encodes the master regulator of the LEE (114). EHEC uses the T3SS to translocate LEE- and non-LEE encoded effectors to hijack the host machinery, culminating in AE lesion formation, which is required for host colonization and overall pathogenesis (155).

The very low infectious dose of EHEC is a major factor contributing to outbreaks (89) and suggests that EHEC has evolved mechanisms to efficiently regulate traits important for host colonization. Indeed, *ler* is a hub of transcriptional regulation that is responsive to numerous signals, such as metabolites and hormones (156, 157). Besides transcription factors, the RNA chaperone Hfq also modulates Ler expression (134), suggesting that RNA-based regulation is central to controlling global LEE expression. Whereas RNA regulatory mechanisms that control expression of specific T3SS apparatus proteins have been described (e.g. (144)), in-depth mechanistic insights into how RNA regulation affects global LEE expression and the consequence(s) to T3SS expression are lacking.

Here, we show that under low-oxygen conditions, the sRNA DicF is expressed and plays an extensive role in modulating EHEC gene expression, including Stx and LEE expression. Mechanistically, DicF promotes T3SS expression through the Ler-transcriptional activator PchA. The *pchA* transcript contains a *cis*-acting regulatory element in which the CDS base-pairs to the 5' UTR. This interaction sequesters the Shine-Dalgarno (SD) site and inhibits translation. DicF relieves this interaction by binding to the *pchA* anti-SD site within the CDS to unmask the *pchA* SD site and promote PchA expression. These data reveal a feed-forward pathway involving new mechanisms of RNA-based regulation that spatiotemporally controls virulence in response to oxygen availability.

RESULTS

DicF is an oxygen-responsive sRNA that globally modulates EHEC gene expression

In non-pathogenic *E. coli* strains, the Hfq-dependent sRNA DicF influences expression of genes encoding cell division and metabolic processes (33, 35, 54, 158–160). Overexpression of DicF inhibits cell division and causes filamentation in non-pathogenic *E. coli* (158, 160). DicF inhibits translation of FtsZ, a protein important for cell division, by binding to the RBS of the *ftsZ* mRNA via an Hfq-dependent mechanism (33, 161). Significantly, environmental cues that promoted DicF expression were not known, and these original studies relied on plasmid-based, heterologous expression of DicF. The *dicF* gene is transcribed from the *dicA-ydfABC-dicF-dicB* operon (159). The only promoter found in this operon is upstream of the *dicA* gene, and signals that activate transcription from this promoter have not been identified (159). RNase E-mediated processing generates the 5' end of the DicF sRNA, and the 3' end is generated by intrinsic transcription termination as well as RNase III-mediated processing (159). Recent work demonstrated that DicF is exquisitely stabilized under low oxygen conditions (54) that are reflective of the colon. Under oxygen-limiting conditions, enolase bound to the degradosome causes changes in cellular localization of RNase E, from the cytoplasmic membrane to the cytoplasm. This redistribution results in decreased stability and activity of RNase E and concomitant stabilization of DicF (54, 85). Under aerobic conditions, this process is reversed (54), and thus DicF-dependent gene regulation is responsive to oxygen availability. We examined DicF expression in WT and Δhfq EHEC strains grown aerobically or under microaerobic conditions. Consistent with previous findings in nonpathogenic *E. coli*, DicF expression in EHEC required Hfq and was only detected following growth under microaerobic conditions (Fig. 2-1A).

EHEC shares a core set of genes with nonpathogenic *E. coli*. DicF is conserved in the core *E. coli* genome. However, during its evolution EHEC acquired > 1 Mb of distinct DNA, including three additional copies of *dicF* that are located within different, EHEC-specific pathogenicity islands (55, 90). One copy (named *dicF1*) shares 100% identity to nonpathogenic *E. coli* K-12 *dicF*, whereas the other alleles (arbitrarily labeled *dicF2*, *dicF3*, and *dicF4*) contain distinct sequence variations (Fig. 2-1B). Because EHEC has acquired and maintained multiple *dicF* copies, we hypothesized that DicF may be important for coordinating oxygen-dependent virulence responses. To investigate how EHEC sensing of environmental oxygen through DicF is linked with virulence expression, we generated a quadruple *dicF* deletion EHEC strain ($\Delta dicF1-4$, Fig. 2-1A). Of note, loss of *dicF* in EHEC did not impact bacterial growth or replication (Fig. 2-2), indicating that the deletion of chromosomal *dicF* does not lead to nonspecific defects in fitness or replication. Subsequently, we compared the transcriptomes of three biological replicates of WT and the $\Delta dicF1-4$ strains grown under microaerobic conditions in DMEM. More than 300 genes were differentially expressed in the $\Delta dicF1-4$ strain compared to WT (Fig. 2-3A). Of these, we measured expression differences of genes carried in the core genome, including genes encoding metabolic enzymes (*nar*, *adhE*, *tnaA*), regulatory factors (*hnr*, *csrB*), and fimbriae (*ecpR*, *yehD*) (Fig. 2-3B). Notably, we also measured differences in EHEC-specific genes, including *stx2A* that encodes Shiga toxin (Fig. 2-3B and C). *Trans* complementation with plasmid-expressed *dicF1* restored expression to near WT levels (Fig. 2-3C). Moreover, all *dicF* alleles rescued expression of *narL* and *hnr* in the $\Delta dicF1-4$ strain (Fig. 2-3D and E). These data revealed an extensive role for DicF under conditions that recapitulate EHEC virulence gene expression *in vivo* (162).

DicF enhances EHEC virulence

The LEE pathogenicity island carries 41 genes that are mostly organized into five major operons (Fig. 2-4A). *LEE1* encodes Ler that activates expression of all of the LEE genes (114). *LEE4* encodes EspA which forms the filament of the T3SS apparatus (163). The transcriptomic data revealed at least a 2-fold decrease in expression of 37 LEE genes in the $\Delta dicF1-4$ strain compared to WT (Fig. 2-4B). We further analyzed LEE transcripts by qPCR, confirming that LEE expression required DicF (Fig. 2-4C). Furthermore, Western blot analysis confirmed that levels of EspA were decreased in the $\Delta dicF1-4$ strain compared to WT EHEC (Fig. 2-4D and E).

Identical or nearly identical sRNAs may have redundant as well as non-redundant targets and cause differential regulation of a specific target (45). To test the contribution of the DicF copies to LEE expression, we measured EspA expression in the $\Delta dicF1-2$, $\Delta dicF1-3$, and $\Delta dicF1-4$ strains. These data indicated that DicF promoted LEE expression in an additive manner, as the double *dicF* deletion ($\Delta dicF1-2$) resulted in less EspA expression compared to WT, which became further decreased in correlation with the number of *dicF* genes deleted (Fig. 2-4D and E). In agreement with the expression data, the $\Delta dicF1-4$ strain was attenuated for AE lesion formation (Fig. 2-5A and B). Together, these data revealed that DicF plays an important role in EHEC virulence.

DicF and PchA function in a feed-forward pathway to regulate LEE expression

How does DicF promote LEE expression? Considering that nearly all of the LEE genes were decreased in expression in the $\Delta dicF1-4$ strain, we reasoned that DicF directly modulated Ler expression or expression of a Ler transcriptional regulator. Unbiased, *in silico* analysis predicted the *pch* genes as potential DicF targets. The Pch (PerC homologue) family of proteins are horizontally acquired transcriptional activators carried by pathogenic members of the Enterobacteriaceae (114). In enteropathogenic *E.*

coli or EHEC, PerC or Pch, respectively, promotes transcription of *ler*, to activate expression of the T3SS (116, 126, 127, 164, 165). EHEC encodes three *pch* genes (*pchA*, *pchB*, and *pchC*) located within distinct pathogenicity islands (127). To examine whether *pch* is a regulatory target of DicF, we measured *pch* transcript levels in the WT and $\Delta dicF1-4$ strains grown under microaerobic conditions. These data indicated that Pch expression required DicF, as *pch* mRNA levels were ~3-fold decreased in the $\Delta dicF1-4$ strain compared to WT EHEC (Fig. 2-6A).

In accordance with DicF modulating oxygen-dependent responses in EHEC, we measured increased levels of *pch* mRNA in WT EHEC grown under microaerobic conditions compared to aerobic conditions, and this increase required Hfq (Fig. 2-6B). Moreover, EspA was only detected after growth under microaerobic conditions (Fig. 2-6C and D), highlighting the importance of low oxygen availability as a signal for EHEC virulence expression. Although overexpression of any *pch* gene results in increased levels of LEE expression, PchA is the major contributor to LEE activation (127, 166). Therefore, to test how PchA contributes to oxygen-dependent LEE expression, we generated a *pchA* deletion EHEC strain ($\Delta pchA$). Significantly, EspA expression was decreased in the $\Delta pchA$ and $\Delta dicF1-4$ strains compared to WT EHEC (Fig. 2-6C and D; Fig. 2-7), indicating that DicF and PchA are required for coordinating oxygen sensing and virulence responses.

Next, we investigated whether DicF- and Pch-dependent regulation of the LEE is functionally linked. For this assay, we generated a $\Delta pchA$ EHEC strain in which three *dicF* alleles were deleted ($\Delta pchA \Delta dicF1-3$). As expected, we measured decreased *espA* expression in the $\Delta dicF1-3$ and $\Delta pchA$ strains; however, no further decreases in *espA* transcript levels were measured in the $\Delta pchA \Delta dicF1-3$ strain compared to the $\Delta pchA$

strain (Fig. 2-6E). These findings demonstrated that DicF and PchA operate in the same pathway to promote LEE expression, with DicF being upstream of PchA.

DicF base-pairs with the *pchA* CDS to promote expression

To better understand DicF control of PchA expression, we used the program CopraRNA (167, 168) to identify predicted interaction sites. sRNAs usually bind to the 5' UTR of the target mRNA over short regions, e.g. 7-12 nucleotides, with imperfect complementarity (6). Notably, DicF was predicted to interact with the *pchA* CDS through extensive base-pairing (over 40 nucleotides) beginning at nucleotide +49 (based on the ATG site) (Fig. 2-8A). To test this predicted interaction, we performed RNA electrophoretic mobility shift assays (EMSAs) using *in vitro* transcribed and biotinylated DicF1 RNA. Upon addition of *pchA* transcript, we measured a shift in the labeled DicF RNA indicating direct base pairing (Fig. 2-8B). Moreover, mutation of six *pchA* nucleotides within the predicted DicF binding site (generating *pchA*^{mutA} RNA, Fig. 2-8A) resulted in diminished DicF-*pchA* RNA interaction (Fig. 2-8B). To further substantiate DicF base-pairing with the *pchA* CDS, we generated point mutations in the seed region of DicF (creating DicF^{mutA}) (Fig. 2-8A) that are expected to decrease interactions with the *pchA* transcript. Then, we performed competition RNA EMSAs using labeled WT DicF and increasing amounts of unlabeled DicF or DicF^{mutA} transcript. Unlabeled DicF competed with labeled DicF for binding; however, unlabeled DicF^{mutA} showed decreased competition (Fig. 2-9A). In the reciprocal experiment, unlabeled DicF^{mutA} effectively competed against labeled DicF^{mutA} for binding to the *pchA*^{mutA} transcript that harbors compensatory mutations, whereas unlabeled DicF did not compete for binding (Fig. 2-9B).

Next, we functionally interrogated the importance of DicF interaction with the *pchA* mRNA CDS. For these experiments, *pchA* or *pchA*^{mutB} (Fig. 2-8A), including the native 5'

UTR, was fused to a FLAG tag and cloned into an IPTG-inducible pUCP24 vector to specifically assay posttranscriptional regulation. We examined PchA::FLAG or PchA^{mutB}::FLAG expression in the $\Delta dicF1-4$ strain after *trans* complementation with DicF1 or mutated DicF^{mutB} (Fig. 2-10A and C). DicF1 complemented the $\Delta dicF1-4$ strain by restoring PchA expression, whereas DicF^{mutB} did not restore expression (Fig. 2-10A and B). Significantly, the DicF^{mutB} that contains compensatory mutations rescued PchA^{mutB}::FLAG expression in the $\Delta dicF1-4$ strain (Fig. 2-10C and D). Collectively, these data indicated that DicF binds directly and specifically to the *pchA* mRNA CDS to promote PchA expression.

DicF disrupts an anti-SD structure between the *pchA* mRNA CDS and 5' UTR to promote translation

To date, only a handful of sRNAs bind deep within the CDS (> 5 codons downstream of the start site (34)) of the target transcript to repress expression (36, 40, 169, 170). For example, in *Salmonella*, the sRNA MicC binds the *ompD* mRNA CDS and recruits RNase E, leading to degradation (40). To provide mechanistic insights into DicF regulation of PchA, we first examined whether DicF functions in the opposite manner to promote target transcript stability. After microaerobic growth of WT and the $\Delta dicF1-4$ strains, cultures were treated with rifampicin to halt further transcription. RNA samples were prepared from cells prior to and at indicated time points post-treatment. Chromosomal *pch* or plasmid-encoded *pchA* transcript abundance and stability was then determined by qPCR or Northern blot analyses, respectively. Both assays revealed that the *pch(A)* transcript was slightly more stable in the $\Delta dicF1-4$ strain compared to WT EHEC (Fig. 2-11A and B). These data suggested that DicF does not promote PchA expression by enhancing stability. Importantly, when *pchA* is overexpressed, transcript levels before the addition of rifampicin are equal (Fig. 2-11B), while protein levels are

decreased in the $\Delta dicF1-4$ strain compared to WT (Fig. 2-10A), indicating that the positive effect of DicF on PchA expression is due to increased translation of PchA.

A well-characterized mechanism of sRNAs positively regulating translation of target transcripts is through binding to the 5' UTR of a transcript to relieve secondary structures that occlude the RBS (26). Stem loop structures within the CDS of an mRNA transcript may also influence translation (36). Therefore, we performed *in silico* analyses to assess whether the *pchA* transcript harbors stem loop structures that may impact translation. Intriguingly, these queries revealed that the *pchA* CDS contains an anti-SD sequence that interacts with the 5' UTR and masks the *pchA* SD sequence (Fig. 2-12A and Fig. 2-13A). To test this prediction, we probed the structures of *pchA* or of *pchA*^{mutA} RNA that harbors mutations predicted to relieve *pchA* cis-interactions and expose the SD sequence (Fig. 2-12C and Fig. 2-13B). Comparison of cleavage patterns revealed guanine residues that were exposed in the *pchA*^{mutA} RBS but which were protected by secondary structures in the *pchA* RNA (Fig. 2-14A and B).

Significantly, the anti-SD sequence within the *pchA* RNA overlaps with the DicF base-pairing site (Fig. 2-12B). Therefore, we hypothesized that DicF disrupts anti-SD base-pairing between the *pchA* CDS and 5' UTR to promote translation. If our model is correct, point mutations that disrupt *pchA* interactions between the anti-SD site and the 5' UTR would be expected to restore PchA expression to WT levels in the $\Delta dicF1-4$ strain. To test this idea, we transformed WT and the $\Delta dicF1-4$ strains with a plasmid encoding *pchA*, *pchA*^{mutA}, or *pchA*^{mutC} alleles. *pchA*^{mutC} carries distinct mutations from *pchA*^{mutA} that are also predicted to unmask the SD sequence (Fig. 2-12F and Fig. 2-13D). In support of our model, although DicF was required for PchA expression, DicF was not required for robust expression of PchA^{mutA} or PchA^{mutC} (Fig. 2-12D, E, G, H). To ensure that the rescue of PchA expression was not due to nonspecific effects of the mutations, we also

generated the *pchA*^{mutD} allele that is predicted to strengthen *pchA cis* base-pairing (Fig. 2-13E and Fig. 2-15A). These mutations did not rescue PchA expression in the absence of DicF (Fig. 2-15B and C). Consistent with these findings, the *pchA*^{mutB} allele (shown in Fig. 2-8A and Fig. 2-13C) does not unmask the RBS, and its expression requires DicF (Fig. 2-10C and D). Altogether, these data substantiate our model, as although DicF was required for PchA expression, mutations that disrupted base-pairing between the *pchA* anti-SD and 5' UTR alleviated the requirement for DicF and resulted in robust PchA expression.

***pchA* mRNA *cis*-interactions impact translation initiation**

Secondary structures in the 5' UTR are able to inhibit translation completely, whereas RNA duplexes within the CDS do not restrict the ability of the ribosome to efficiently translate mRNA (171). In the previous experiment, PchA^{mutA} and PchA^{mutC} expression were similar in WT and $\Delta dicF1-4$ as well as to levels of PchA in WT (Fig. 2-12D, E, G, H). These data indicate that DicF interaction with the *pchA* CDS does not impair or enhance translation elongation and supports a role for DicF in disrupting intramolecular interactions between the *pchA* 5'UTR and CDS that inhibit translation initiation. To investigate how *cis*-interactions within the *pchA* transcript impact translation initiation, we measured progression of reverse transcriptase on the *pchA* or *pchA*^{mutA} (in which the anti-SD structure is disrupted) transcript. Addition of ribosomes to the reactions resulted in more rapid inhibition of reverse transcriptase on the *pchA*^{mutA} transcript and corresponding decrease in full length cDNA compared to the *pchA* transcript (Fig. 2-16A and B), indicating that *pchA cis*-interactions limit efficiency of ribosome binding. To support this idea, we performed *in vitro* translation assays using *pchA*, *pchA*^{mutA}, or *pchA*^{mutD} (in which the anti-SD structure is strengthened) transcripts as templates. These assays demonstrated that disruption of the anti-SD structure in the

pchA^{mutA} allele resulted in more rapid translation and accumulation of PchA^{mutA} compared to PchA or PchA^{mutD} (Fig. 2-16C and D). These data revealed that *pchA* cis-interactions between the CDS and 5' UTR control translation initiation.

DISCUSSION AND FUTURE DIRECTIONS

We discovered that the sRNA DicF plays an essential role in integrating oxygen sensing and virulence regulation in EHEC. DicF disrupts intrinsic silencing mechanisms within the *pchA* transcript to promote PchA expression, which ultimately results in global expression of the LEE and AE lesion formation. These data suggest a model in which DicF-dependent regulation of PchA enables EHEC to precisely time deployment of its T3SS and effectors within the colon, the site of EHEC host colonization (Fig. 2-17). Although oxygen was appreciated as an environmental signal that modulates EHEC virulence (147, 172), the underlying mechanisms were not fully understood, and the role of DicF in EHEC physiology and virulence was unknown. In addition to EHEC, other bacterial pathogens sense oxygen to coordinate virulence, including *Shigella*, enterotoxigenic *E. coli*, and *Salmonella* (173–175). In these examples, transcriptional adaptation through the regulatory factors FNR or ArcAB mediates changes in gene expression, including expression of sRNAs that modulate virulence (174). However, the ability to rapidly integrate this signal via RNA-based regulation may be an important and conserved strategy for bacterial pathogens to establish infection, and it is likely that further studies will uncover additional RNA-mediated mechanisms of oxygen sensing and virulence.

Bacteria have evolved to minimize binding between the CDS and respective SD sequences in order to promote efficient translation initiation and thus enhance fitness (176). Nevertheless, although much less common, long-distance *cis*-interactions

between the CDS and SD sequences have been reported to influence expression of genes important for thermo-stresses or growth rate (177–181). The mRNA of the heat shock sigma factor, *rpoH*, contains a secondary structure within the CDS that folds back on the translation initiation region, preventing translation during bacterial growth in low temperatures (181). Upon heat shock, the secondary structure is melted, leading to translation of *rpoH* mRNA (180). Similarly, the transcript encoding the cold shock protein CspA contains an inhibitory secondary structure in the CDS that allows for translation during growth in cold temperatures and inhibits translation during growth at 37°C (179). Apart from temperature-controlled mRNA structures, the *gnd* transcript encoding 6-phosphogluconate dehydrogenase contains a long-range inhibitory region in the CDS that blocks the RBS, leading to low rates of translation when the growth rate of *E. coli* is slow (177, 178). In these three examples, factors intrinsic to the mRNA or directly involved in its expression influence stability of the anti-SD structure and thus gene expression. Regulation of *pchA* expression via *cis*-interactions reveals that genes important to bacterial virulence are also regulated via anti-SD sequences within the CDS. Moreover, disruption of the anti-SD sequence also requires an external factor, the sRNA DicF.

Some sRNAs activate their target transcripts by binding to the 5' UTR to unravel inhibitory sequences on the RBS to allow for translation (21, 22, 26–29). While it has been suggested that sRNAs bind to the CDS to exert a similar effect (182, 183), the evidence was lacking. Falcone *et al.* demonstrated direct binding between the sRNA ErsA and the CDS of the transcriptional regulator *amrZ* *in vitro* and that ErsA promoted expression of *amrZ* *in vivo*. However, evidence of direct binding of ErsA to *amrZ* *in vivo* was not provided and the effects on the predicted secondary structure of *amrZ* were not tested (182). Similarly, Jones *et al.* suggested that the sRNA SolB binds to the CDS of

cftA, encoding a subunit of coenzyme A transferase, to relieve inhibitory structures that fold back on the RBS. To test this prediction, the RBS of *cftA* was changed to another functional *Clostridium* RBS that hypothetically prevented the inhibitory structure from forming. When expressed in the WT strain, the mutated *cftA* displayed increased activity compared to the WT *cftA*. The same phenotype is seen in the Δ *solB* strain; however, activity of the mutated *cftA* was still decreased in the Δ *solB* strain compared to the WT strain, suggesting that other factors affect *cftA* translation. Additionally, direct binding of SolB to *cftA* was not demonstrated (183). Although these previous two studies began to interrogate translation activation by sRNAs binding to the CDS, our study demonstrates a unique mechanism of target transcript regulation.

In non-pathogenic *E. coli*, DicF negatively regulates the cell division gene *ftsZ* as well as the xylose uptake gene *xylR* and maltose transporter gene *malX* (33, 35). DicF is encoded in multiple copies in pathogenic strains of *E. coli*, whereas non-pathogenic strains encode at most one copy of DicF. Whenever multicopy, or “sibling”, sRNAs are identified, a common question is why have bacteria evolved to maintain multiple identical or highly similar copies of the same sRNA (45)? Bacteria display a tendency towards reduced genomes and non-essential genes are generally lost over time (184). EHEC has acquired and maintained at least four copies of DicF (some strains have as many as six (54)), suggesting that DicF provides an evolutionary benefit to this pathogen. As we have demonstrated here, DicF is critical for the formation of AE lesions by EHEC, indicating that DicF promotes colonization in host niches. LEE expression is necessary for colonization of the bovine GI tract, the main environmental reservoir of EHEC (95, 185). That EHEC carries multiple copies of DicF suggests that DicF may be important to amplify bacterial virulence. In line with this idea, the other *pch* genes in EHEC, *pchB* and *pchC*, also promote Ler expression (126, 127). The DicF recognition sequence is

conserved in *pchA*, *pchB*, and *pchC*, hence it is likely that DicF promotes expression of all *pch* transcripts to activate T3SS expression.

Furthermore, we have shown that DicF also affects the expression of a phage-encoded virulence factor, Stx, by an unknown mechanism (Fig. 2-3C). Our RNAseq analysis demonstrated that genes throughout the phage insertion, including *stx2a* (encoding the A subunit of Stx), are upregulated in the absence of DicF. Our bioinformatic analysis of predicted DicF targets identified prophage genes that may be responsible for this phenotype. Future work will interrogate the mechanism of DicF regulation of Stx starting with these prophage targets. In addition to Stx, RNAseq analysis demonstrated that DicF affected the expression of >300 genes in EHEC (Fig. 2-3A). To further identify mechanisms of DicF regulation, we will prioritize the characterization of bioinformatically-predicted DicF targets that are differentially regulated in the RNAseq data set. For example, *oppA*, encoding a component of an oligopeptide transporter (186), was a predicted target of DicF and the entire *oppABCDF* operon was upregulated in the $\Delta dicF1-4$ strain in the RNAseq analysis. Additionally, we will determine the individual contributions of each DicF allele to EHEC gene expression. We will test the contribution of each DicF allele by generating triple deletion strains that are positive for only one copy of DicF. We will also use these strains to identify signals responsible for activation of each copy of DicF. These studies will expand our understanding of how multicopy sRNAs coordinate and modulate gene expression.

Somewhat contradictory to its role in promoting translation initiation of *pchA*, DicF also appears to moderately destabilize the *pchA* transcript (Fig. 2-11). Translation protects transcripts from degradation (17); however, here we demonstrated that *pchA* transcript stability exhibits an unconventional link with its translation status. It is possible that in affecting the secondary structure of *pchA*, DicF binding reveals RNase

degradation sites that are protected by the *pchA* structure. To test this, we will examine stability of the *pchA*^{mutA}, *pchA*^{mutC}, and *pchA*^{mutD} transcripts (Fig. 2-12 and 2-15) in the WT and the $\Delta dicF1-4$ strains to determine how the *pchA* structure affects stability. However, it is also evident that the effects of DicF on *pchA* stability are secondary to its activation of *pchA* translation, as deletion of DicF leads to overall decreased production of PchA and decreased expression of the LEE due to the translational repression of the *pchA* transcript.

To date, only a handful of sRNAs are known to regulate targets by binding deep within the CDS, and these inhibit gene expression (36, 40, 169, 170). DicF regulation of PchA expression is therefore unique in that base-pairing deep within the *pchA* CDS promotes translation. Notably, the ribosome is an RNA helicase, and although this activity does not function efficiently during translation initiation, the ribosome is able to disrupt RNA duplexes during elongation (187). Thus, we propose a model in which DicF interaction with the *pchA* CDS promotes ribosome loading to the 5' UTR and translation initiation. Subsequently, the ribosome displaces DicF during elongation. It is likely that the mechanism of DicF regulation will have broader implications for understanding sRNA functions in other bacteria. In summary, this work identifies an oxygen responsive feed-forward pathway and provides fundamental insights into RNA-mediated virulence regulation and environmental signaling in bacterial physiology and pathogenesis.

MATERIALS AND METHODS

Bacterial strains, plasmids, and growth conditions. Strains and plasmids are listed in Appendix Tables 1 and 2; primers are listed in Table 3. Unless indicated otherwise, bacteria were grown statically overnight in LB broth, diluted 1:100 in low-glucose DMEM (Invitrogen), and grown statically for 6 h at 37°C, 5% CO₂ (microaerobic conditions). For

aerobic growth conditions, cultures were grown shaking in DMEM to an O.D.₆₀₀ of 0.8 (late-logarithmic growth). Oxygen concentrations have been measured at >200 $\mu\text{mol O}_2/\text{L}$ or <10 $\mu\text{mol O}_2/\text{L}$ under the respective conditions (172). Deletion strains were constructed using lambda red mutagenesis (188). Point mutations were generated using the NEB Q5 Site-Directed Mutagenesis Kit. Deletions and mutations were confirmed by Sanger sequencing.

Growth experiment. WT and $\Delta\text{dicF1-4}$ EHEC strains were grown under microaerobic conditions in DMEM. At indicated time points, samples were serially diluted and plated on LB agar containing streptomycin (EHEC strain 86-24 is streptomycin resistant) to enumerate colony forming units. Doubling time was calculated as $\ln(2) / \text{growth rate}$ during linear growth phase.

RNA extraction and quantitative PCR (qPCR). RNA was extracted from three biological replicates using the PureLink RNA Mini Kit (Ambion) and treated with DNase (Ambion) according to manufacturer specifications. RNA purity was determined by measuring the A_{260}/A_{280} absorbance ratio and by performing PCR (35 cycles).

qPCR was performed in a one-step reaction using an ABI 7500-FAST sequence detection system and software (Applied Biosystems). For each 10- μl reaction mixture, 5 μl 2 \times SYBR master mix (Ambion), 0.05 μl Multi-Scribe reverse transcriptase (Invitrogen), and 0.05 μl RNase inhibitor (Invitrogen) were added. Primers were designed using Primer Blast (NCBI) to ensure no cross-reactivity to other genes in the EHEC chromosome. Amplicon length was approximately 100 bp. Amplification efficiency of each primer pair was verified using standard curves of known DNA concentrations. Melting-curve analysis was used to ensure template specificity by heating products to 95°C for 15 s, followed by cooling to 60°C and heating to 95°C while monitoring fluorescence. After the amplification efficiency and template specificity were determined

for each primer pair, relative quantification analysis was used to analyze the samples using the following conditions for cDNA generation and amplification: 1 cycle at 48°C for 30 min, 1 cycle at 95°C for 10 min, and 40 cycles at 95°C for 15 s and 60°C for 1 min. Two technical replicates of each biological replicate were included for each gene target. Data were normalized to the reference controls *rpoA*, or when indicated 16S rRNA, and analyzed using the comparative critical threshold (C_T) method (189). The expression level of the target genes was compared using the relative quantification method (189). Data are presented as the change (n -fold) in expression levels compared to WT levels. Error bars represent the standard deviations of the $\Delta\Delta C_T$ value.

RNAseq. RNA was extracted as described above. Ribosomal RNA was depleted before library preparation using the Ribo-Zero rRNA Removal Kit for Gram-Negative Bacteria (Illumina). Library preparation was performed using the NEBNext® Ultra™ Directional RNA Library Prep Kit (NEB). Libraries were pooled and sequenced using Illumina HiSeq4000 75PE.

RNAseq analysis was performed by the Informatics Resource Center, Institute for Genome Sciences, UMDSOM. Paired-end, strand-specific Illumina libraries were mapped to the EHEC EDL933 genome, using Bowtie v0.12.7. Read counts for each annotated gene were calculated using HTSeq. The DESeq Bioconductor package (v1.5.24) was used to estimate dispersion, normalize read counts by library size to generate the counts per million for each gene, and determine differentially expressed genes between sample groups. Differentially expressed transcripts with a FDR ≤ 0.05 and \log_2 fold change ≥ 1.5 were used for downstream analyses. Normalized read counts were used to compute the correlation between replicates for the same condition and compute the principal component analysis for all samples. RNAseq data have been deposited in Gene Expression Omnibus under accession number GSE123248.

***In vitro* transcription.** PCR products were purified using QIAquick PCR Purification Kit (Qiagen). DNA templates were transcribed with the HiScribe T7 High Yield RNA Synthesis Kit (NEB). Transcripts were DNase treated and purified using NucAway Spin Columns (Ambion). Probes for Northern blots were generated by incorporating biotinylated uridine into the *in vitro* transcription reaction.

RNA electrophoretic mobility shift assays (EMSAs). RNA EMSAs were performed using transcripts generated by *in vitro* transcription. DicF transcripts were 3' end-labeled with biotinylated cytidine (bis)phosphate using the Pierce RNA 3' End Biotinylation Kit. EMSA reactions included DicF and *pchA*, 1X structure buffer (Ambion), 2 ng/ μ l yeast RNA (Ambion), and RNase-free water (Ambion). Reactions were incubated for 2-3 min at 85°C, then at 37°C for 45 min. 5X RNA loading dye (50% glycerol, 0.1% bromophenol blue) was added to each sample. RNA was separated in 5% Mini-PROTEAN TBE gels (Bio-Rad), transferred to Zeta-Probe membranes, and visualized using the Chemiluminescent Nucleic Acid Detection Module Kit (Thermo Scientific). ImageJ was used to obtain raw numbers for band intensity. For Fig. 2-8B, data are presented as relative levels of shifted DicF compared to DicF shifted by addition of 0.2 μ M *pchA* RNA. For Fig. 2-9A and B, data are presented as relative levels of shifted DicF or DicF^{mutA} transcript, respectively, compared to shifted transcript in the absence of competitor RNA.

Fluorescein actin staining (FAS) assay. Assays were performed as previously described (190). Overnight bacterial cultures were diluted 1:150 to infect washed HeLa cells. Infected HeLa cells were grown on coverslips in low glucose DMEM for 3 h at 37°C, 5% CO₂. The coverslips were washed and fixed with formaldehyde, and cells were permeabilized with 0.2% Triton-X. Permeabilized cells were stained with fluorescein isothiocyanate-labeled phalloidin to visualize actin. Following RNase treatment, bacteria

and HeLa cell nuclei were stained with 4',6-diamidino-2-phenylindole. Samples were visualized with a Nikon E800 microscope with a Hamamatsu Orca-ER digital camera.

Western blotting. Standard procedures were used as described (134). Equal protein amounts (determined using Bradford reagent, Bio-Rad) were separated in 10 or 15% polyacrylamide gels. After electrophoresis, proteins were transferred to polyvinylidene difluoride membranes, and probed with indicated antibodies (EspA (Vanessa Sperandio)); DnaK (Abcam); FLAG (Sigma)). Samples were visualized with chemiluminescence and quantified with ImageJ. Expression levels were normalized to DnaK and shown relative to those of the WT strain.

Northern blotting. RNA was extracted as described above. Equal concentrations of RNA were mixed with 2X RNA loading dye (1X MOPS, 60% formamide, 1.85% formaldehyde, 0.3% bromophenol blue, 0.3% xylene cyanol), incubated at 65°C for 10 min, and immediately placed on ice. For stability assays, samples were separated in a 2% agarose gel (1X MOPS, 0.1% formaldehyde) in 1X MOPS buffer (Ambion) for the electrophoresis buffer. RNA was transferred overnight by capillary action onto Zeta-probe membranes (Bio-Rad) in 20X saline-sodium citrate (SSC) (Fisher). For DicF expression, samples were separated in 12% polyacrylamide TBE-urea gels using 1X TBE buffer for electrophoresis. RNA was transferred by electrophoresis to Zeta-Probe membranes. After UV crosslinking, the membranes were stained with 1% methylene blue to visualize 16S and 23S rRNA. Membranes were incubated in pre-warmed NorthernMax Prehybridization/Hybridization Buffer (Ambion) for 30 min at 68°C. RNA probes (0.2 pmol) were incubated with the membrane OVN at 68°C. The following day, membranes were washed twice with 2X SSC/0.1% SDS and then twice 1X SSC/0.1% SDS, and biotinylated probes were detected as described above.

Reverse transcriptase inhibition assays. Assays were performed using 0.5 pmol *in vitro* transcribed *pchA*. The biotinylated primer annealed at +30 to +51 nucleotides (based on ATG start codon) on the *pchA* RNA. The primer and *pchA* RNA were mixed in 1X AMV primer extension buffer (Promega) for 20 min at 60°C, and then for 10 min at RT. Subsequently, ribosomes and tRNA (PURExpress Δ (aa, tRNA) *In Vitro* Protein Synthesis Kit (NEB)) were added, and reactions were incubated at 37°C. RNA samples were collected prior to and at indicated time points post-incubation with ribosomes. Reverse transcription was then performed for 15 min at 37°C using AMV reverse transcriptase (Promega). Reactions were stopped using loading dye. Samples were separated in a 10% polyacrylamide TBE-urea gel, transferred to Zeta-Probe membrane, and visualized as described above.

***In vitro* translation.** *In vitro* translation using *pchA* RNA as templates was performed using the PURExpress *In Vitro* Protein Synthesis Kit (NEB). All reactions included *in vitro* transcribed *dnaK* RNA as a control. Proteins were separated in 15% polyacrylamide gels and analyzed by Western blotting. For quantification, levels of PchA, PchA^{mutA}, or PchA^{mutD} were normalized to respective levels of DnaK and shown relative to PchA at 15 min.

RNA structure probing. *pchA* and *pchA*^{mutA} RNA were *in vitro* transcribed as described above. The transcripts were treated with RNase T1 following manufacturer instructions (Invitrogen). Briefly, the *pchA* or *pchA*^{mutA} transcripts were mixed with structure buffer and yeast RNA, and treated with 0.2 U RNase T1 for 8 minutes at room temperature. Precipitation/Inactivation buffer was added to each reaction (including non-reacted controls). The reactions were incubated at -20°C for 15 minutes and pelleted by centrifugation. Pellets were air-dried and resuspended in 10 μ l RNase-free water. These reactions were used as templates for primer extension using the Primer Extension

System - AMV Reverse Transcriptase Kit (Promega) and biotinylated primer pchAPE. A sequencing ladder was generated using the pchAPE primer and PCR purified *pchA* as the template (USB Sequenase version 2.0 DNA polymerase kit (Affymetrix)). Reactions were separated in 10% TBE-Urea gels, transferred to a Zeta-probe membrane (Bio-Rad), and visualized as described above.

***In silico* analysis of predicted DicF and *pchA* mRNA interactions.** Predicted targets of DicF were identified using the program CopraRNA (167, 168). The EDL933, Sakai, and TW14359 genomes were used as the input reference genomes (55, 90, 191). Predicted structures of *pchA* and all point mutants were generated using RNAfold (192). In all analyses, default settings were used.

Quantification and statistical analysis. The students' t test was used to determine statistical significance. Number of biological samples can be found in the figure legends.

FIGURES

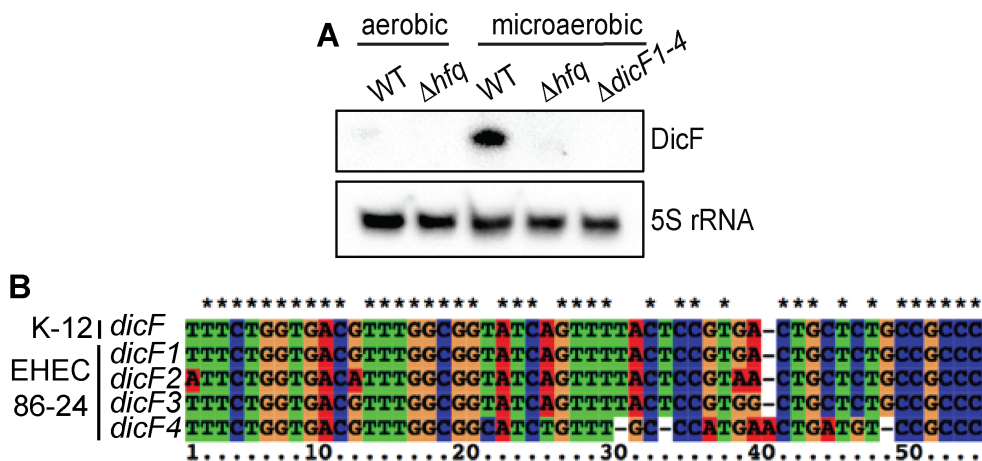


Fig. 2-1. DicF is expressed under microaerobic conditions. (A) Northern blot analysis of DicF in EHEC (WT or Δhfq) grown under aerobic conditions or in EHEC (WT, Δhfq , and $\Delta dicF1-4$) grown under microaerobic conditions. 5S rRNA is the loading control. n = 2. (B) Sequence alignment of *dicF* in *E. coli* K-12 and the four *dicF* copies in EHEC 86-24.

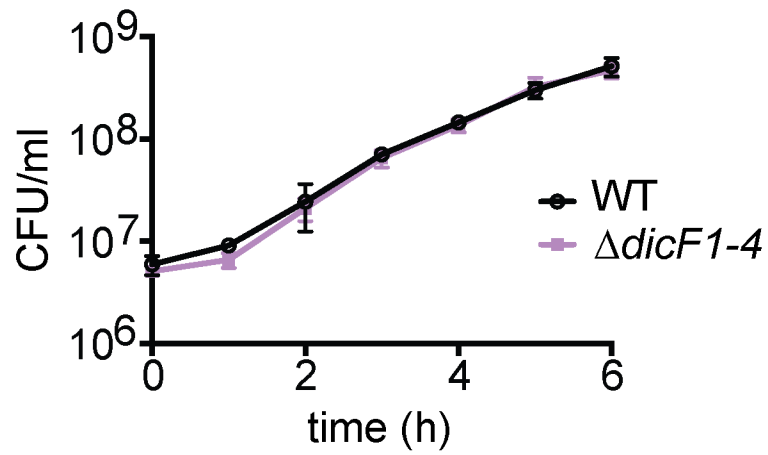


Fig. 2-2. Growth curves of WT and $\Delta dicF1-4$ EHEC grown under microaerobic conditions in DMEM. Doubling times were measured as 0.78 and 0.74 h for WT and $\Delta dicF1-4$, respectively. n=3. Error bars represent the mean \pm the standard deviation (SD).

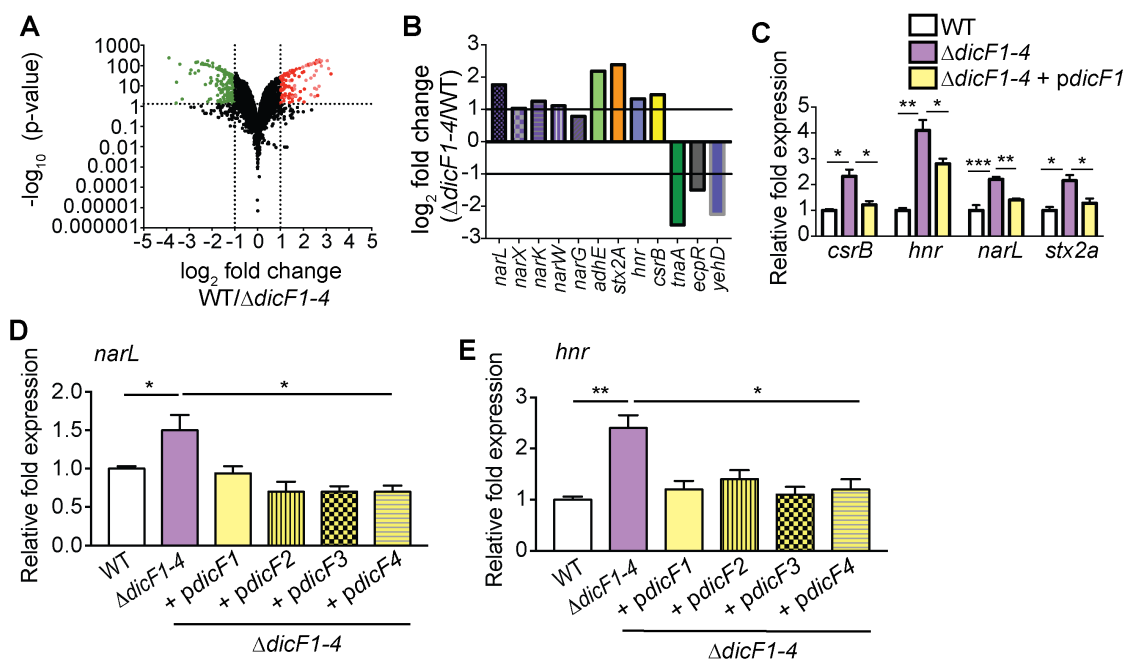


Fig. 2-3. DicF dependent gene expression. (A) Volcano plot of RNAseq data showing numbers of transcripts increased in expression (green dots) vs decreased in expression (red dots) more than two-fold in the $\Delta\text{dicF1-4}$ strain compared to WT EHEC. The line at $-\log_{10}(\text{p-value}) \sim 1$ indicates a p-value of < 0.05 . The lines at $\log_2 \text{fold change} = -1$ or 1 indicates fold change ≥ 2 . $n=3$. (B) RNAseq data showing a subset of differentially expressed transcripts in WT and $\Delta\text{dicF1-4}$ EHEC. $n=3$. (C) qPCR of genes identified as differentially expressed in the RNAseq data set in WT, $\Delta\text{dicF1-4}$, and complemented EHEC. WT and $\Delta\text{dicF1-4}$ EHEC strains were transformed with empty vectors. (D) qPCR of *narL* in WT, $\Delta\text{dicF1-4}$, and $\Delta\text{dicF1-4}$ complemented with the indicated *dicF* allele. (E) qPCR of *hnr* in WT, $\Delta\text{dicF1-4}$, and $\Delta\text{dicF1-4}$ complemented with the indicated *dicF* allele. For (D) and (E), WT and $\Delta\text{dicF1-4}$ EHEC strains were transformed with empty vectors (white and purple bars, respectively). 16S rRNA was used as the reference control. For (C), (D), and (E), $n=3$. Error bars represent the mean \pm SD. *, $p \leq 0.01$; **, $p \leq 0.001$; ***, $p \leq 0.0001$.

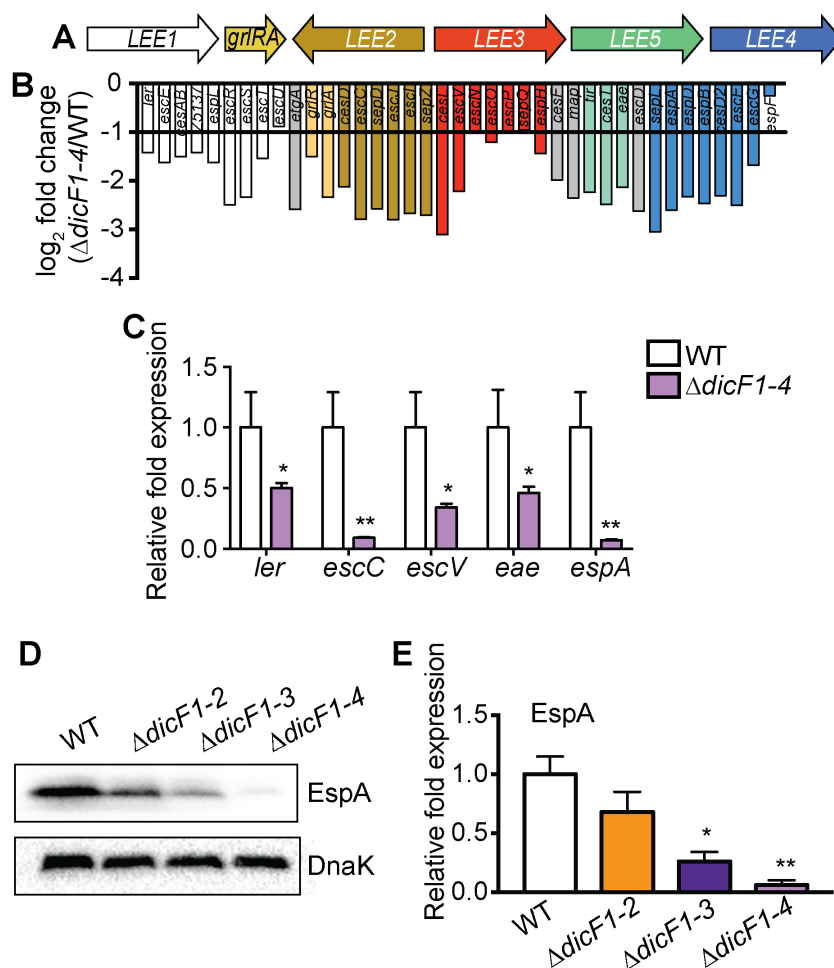


Fig. 2-4. DicF promotes LEE expression. (A) Schematic of the LEE. (B) RNAseq data comparing LEE gene expression in $\Delta dicF1-4$ to WT EHEC. $n=3$. Columns are color-coded according to operon (shown in (A)). The LEE-encoded regulators *grlA* and *grlR* are depicted in yellow, and genes not carried within the major operons are depicted in grey. (C) qPCR of LEE genes in WT and $\Delta dicF1-4$ EHEC. $n=3$. (D) Western blot of EspA expression in WT, $\Delta dicF1-2$, $\Delta dicF1-3$, and $\Delta dicF1-4$ EHEC. DnaK is the loading control. (E) Quantification of EspA expression in WT, $\Delta dicF1-2$, $\Delta dicF1-3$, and $\Delta dicF1-4$ EHEC. $n=9$. For (C, E) error bars represent the mean \pm SD. *, $p \leq 0.01$; **, $p \leq 0.001$.

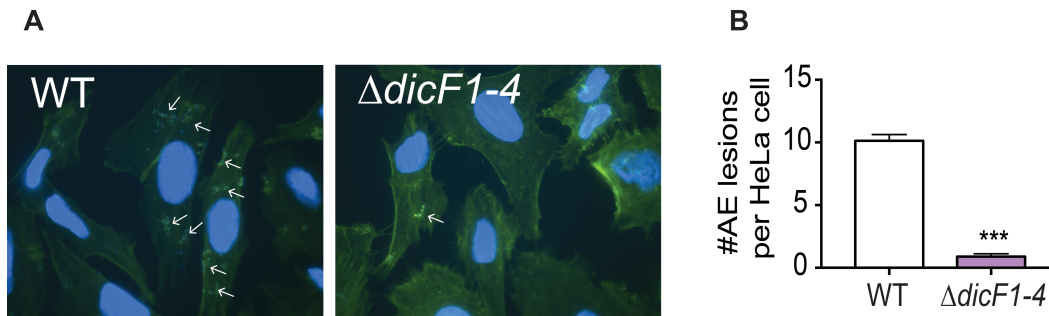


Fig. 2-5. DicF promotes AE lesion formation. (A) FAS assay showing AE lesions on HeLa cells infected with WT or $\Delta dicF1-4$. AE lesions are indicated by arrows. (B) Quantification of AE lesions on HeLa cells infected with WT or $\Delta dicF1-4$. n = 243-337 HeLa cells. Error bars represent the mean \pm SD. ***, $p \leq 0.0001$.

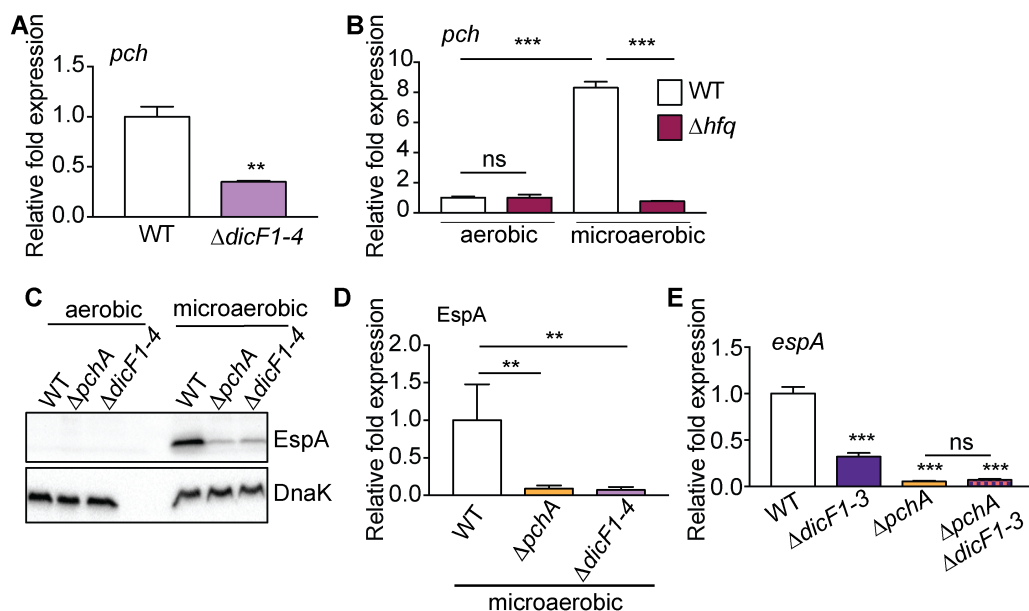


Fig. 2-6. DicF and PchA function in a feed-forward pathway. (A) qPCR of *pch* in WT and $\Delta dicF1-4$ EHEC. n=3. (B) qPCR of *pch* in WT and Δhfq after growth under aerobic or microaerobic conditions. 16S rRNA was used as the reference control. (C) Western blot of EspA in WT, $\Delta pchA$, and $\Delta dicF1-4$. DnaK is the loading control. (D) Quantification of EspA expression in WT, $\Delta pchA$, and $\Delta dicF1-4$ grown microaerobically. n=5. (E) qPCR of *espA* in WT, $\Delta dicF1-3$, $\Delta pchA$, and $\Delta pchA \Delta dicF1-3$. Significance are compared to WT or between the $\Delta pchA$ and $\Delta pchA \Delta dicF1-3$ strains. n=3. For (A, B, D, E), error bars show the mean \pm SD. *, $p \leq 0.01$; **, $p \leq 0.001$; ***, $p \leq 0.0001$; ns, $p > 0.05$.

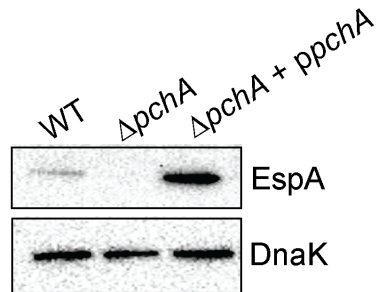


Fig. 2-7. PchA regulates EspA expression under microaerobic conditions.

Representative Western blot of EspA in WT, $\Delta pchA$, and complemented strains. DnaK is the loading control. WT and $\Delta pchA$ were transformed with empty vectors as controls.

n=3.

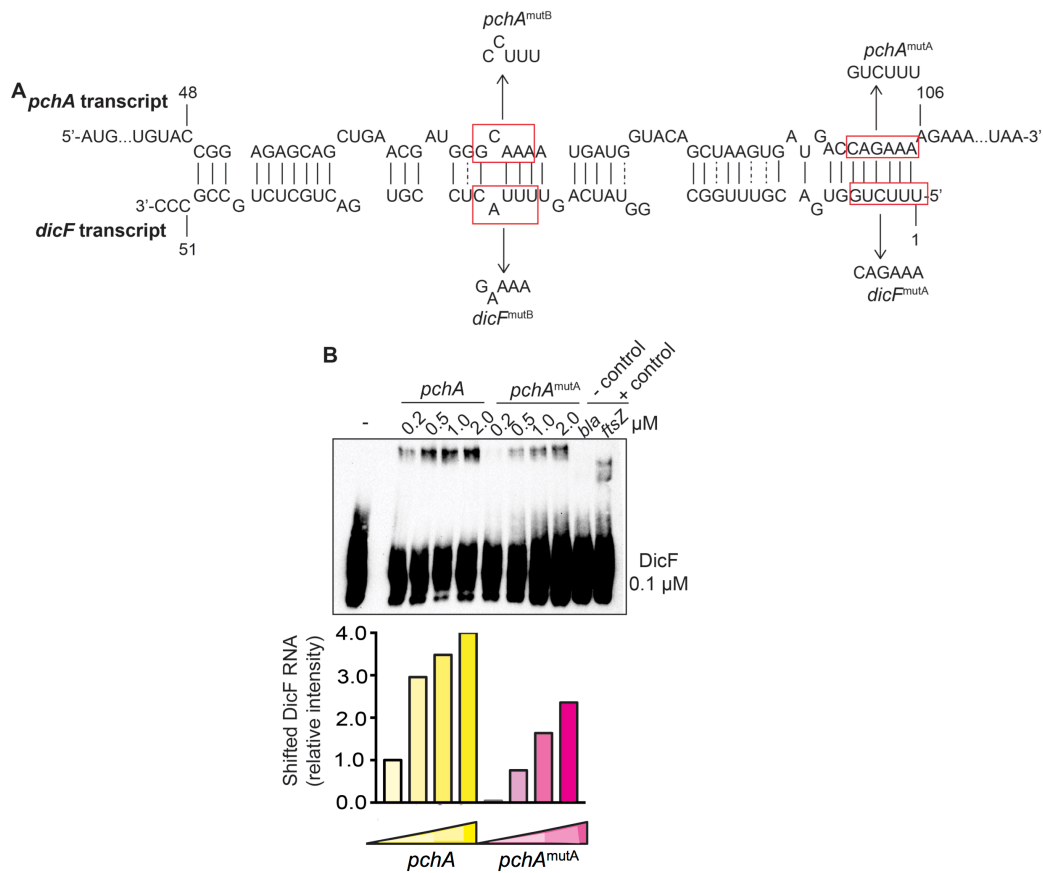


Fig. 2-8. DicF base-pairs with the *pchA* CDS. (A) Predicted DicF-*pchA* RNA base-pairing. Point mutations to generate the disrupted and compensatory alleles, DicF^{mutA} and *pchA*^{mutA} or DicF^{mutB} and *pchA*^{mutB} are indicated. (B) EMSA of DicF and *pchA* or *pchA*^{mutA} transcripts. *bla* and *ftsZ* transcripts (2 μM) are negative and positive controls. The graph shows quantification of shifted DicF.

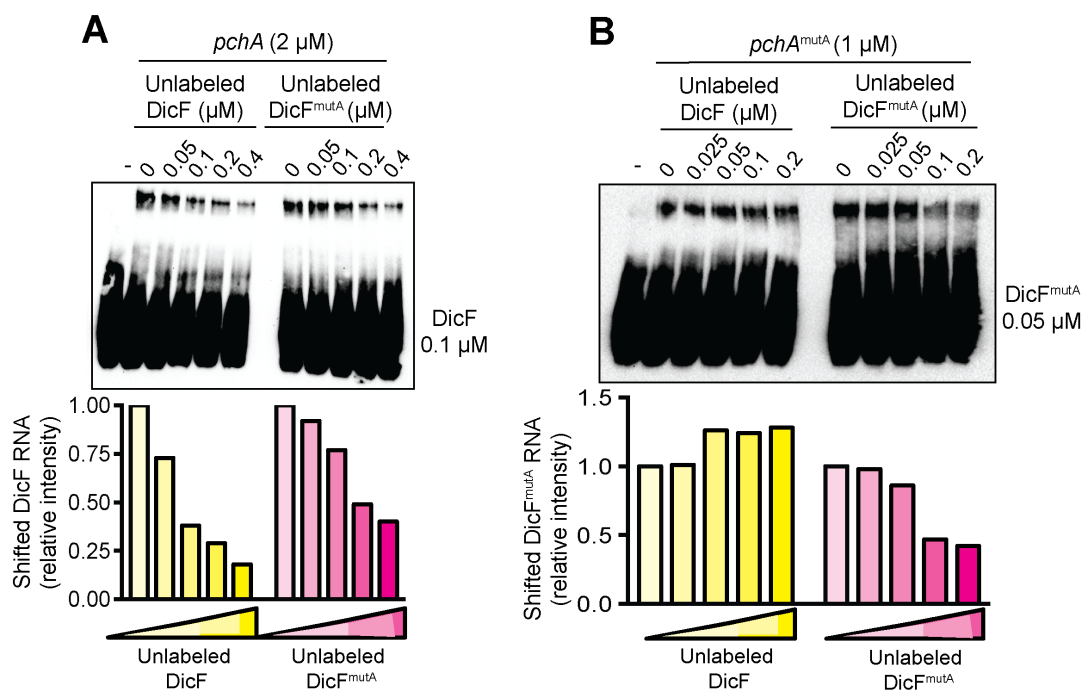


Fig. 2-9. DicF binds the CDS of the *pchA* transcript. (A) RNA EMSA of labeled DicF competing with DicF or DicF^{mutA} for base-pairing with the *pchA* transcript. (B) RNA EMSA of labeled DicF^{mutA} competing with DicF or DicF^{mutA} for binding to the *pchA^{mutA}* transcript. The associated graphs show quantification of shifted, labeled RNA as indicated.

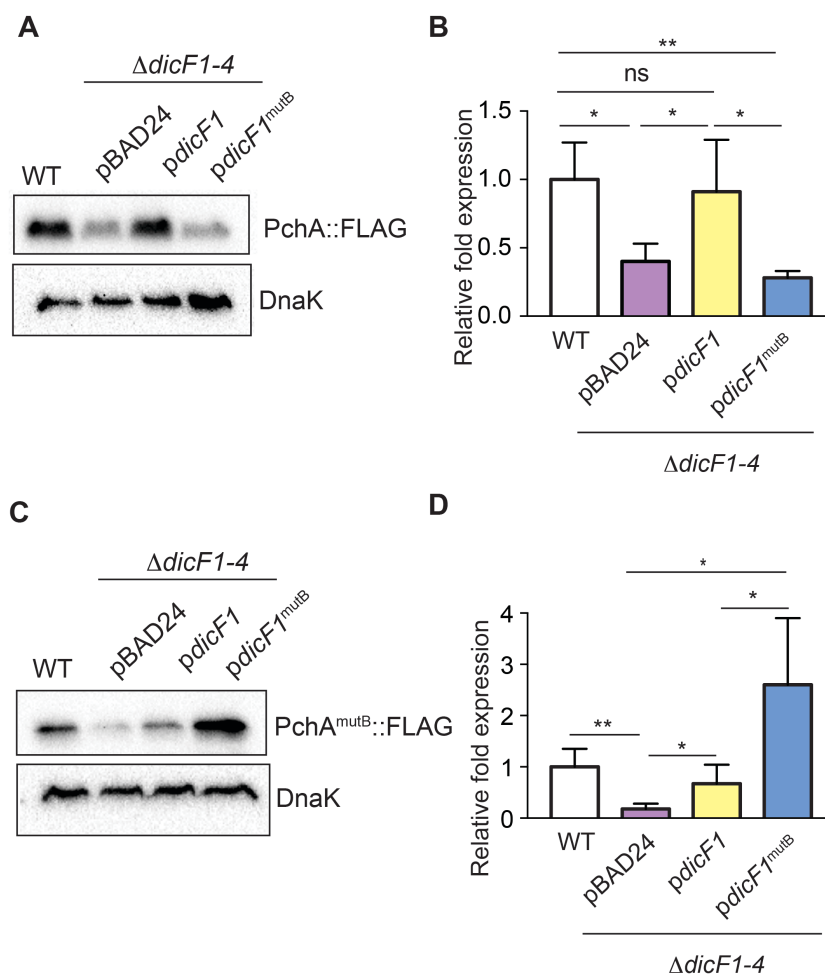


Fig. 2-10. DicF interacts with the CDS of the *pchA* transcript to promote *pchA* translation. (A) Western blot of PchA::FLAG in WT (carrying the pBAD24 vector), $\Delta dicF1-4$ + pBAD24, $\Delta dicF1-4$ + *pdicF1*, and $\Delta dicF1-4$ + *pdicF*^{mutB}. DnaK is the loading control. (B) Quantification PchA::FLAG in WT (carrying the pBAD24 vector), $\Delta dicF1-4$ + pBAD24, $\Delta dicF1-4$ + *pdicF1*, and $\Delta dicF1-4$ + *pdicF*^{mutB}. n=4. (C) Western blot of PchA^{mutB}::FLAG in WT (carrying the pBAD24 vector), $\Delta dicF1-4$ + pBAD24, $\Delta dicF1-4$ + *pdicF1*, and $\Delta dicF1-4$ + *pdicF*^{mutB}. DnaK is the loading control. (D) Quantification PchA^{mutB}::FLAG in WT (carrying the pBAD24 vector), $\Delta dicF1-4$ + pBAD24, $\Delta dicF1-4$ + *pdicF1*, and $\Delta dicF1-4$ + *pdicF*^{mutB}. n=4. For (B, D), error bars show the mean \pm SD. *, $p \leq 0.01$; **, $p \leq 0.001$; ns, $p > 0.05$.

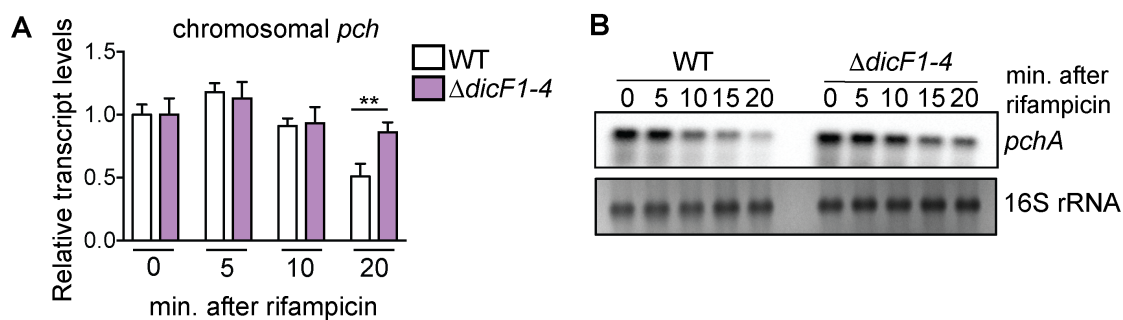


Fig. 2-11. *pch(A)* transcript stability in WT and $\Delta dicF1-4$ EHEC. (A) qPCR of chromosomal *pch* transcript levels in WT and $\Delta dicF1-4$ EHEC at indicated timepoints. Transcript levels are shown relative to levels at 0 min (which was normalized to 1 for each strain). 16S rRNA was used as the endogenous control. n=6. Error bars represent the mean \pm SD. **, $p \leq 0.001$. (B) Northern blot analysis of *pchA* transcripts expressed from an arabinose-inducible promoter in WT and $\Delta dicF1-4$ EHEC at indicated timepoints. 16S rRNA is shown as the loading control. n=4.

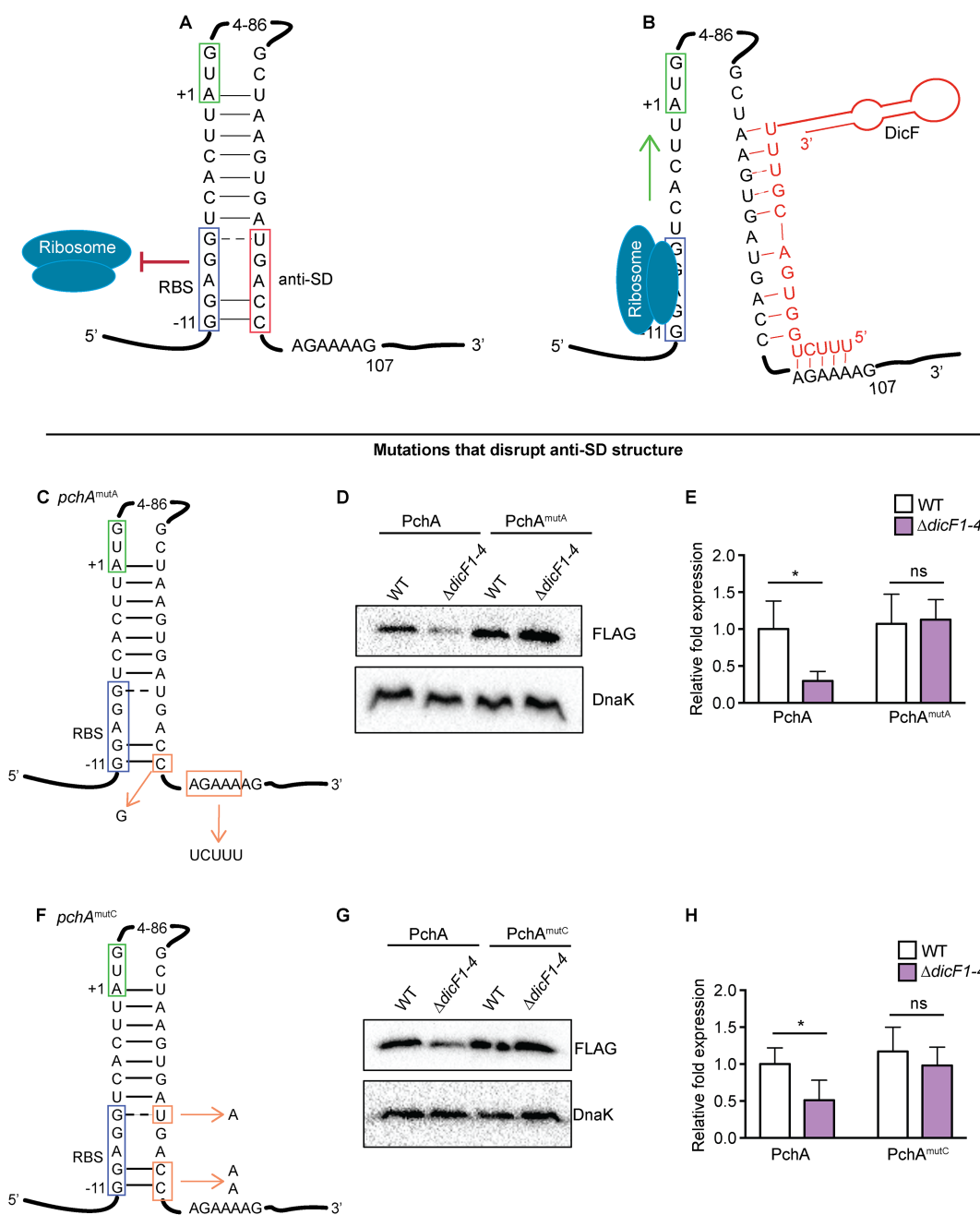


Fig. 2-12. DicF disrupts an anti-SD structure between the *pchA* mRNA CDS and 5' UTR. (A) Predicted base-pairing between the *pchA* mRNA CDS and 5' UTR. (B) Schematic showing DicF interaction with the *pchA* mRNA anti-SD site. (C) Schematic showing the mutated nucleotides in the *pchA^{mutA}* transcript. (D) Western of PchA::FLAG or PchA^{mutA}::FLAG in WT and $\Delta dicF1-4$. DnaK is the loading control. (E) Quantification of

PchA::FLAG or PchA^{mutA}::FLAG expression in WT and $\Delta dicF1-4$. n=5. (F) Schematic showing the mutated nucleotides in *pchA*^{mutC} transcript. (G) Western of PchA::FLAG or PchA^{mutC}::FLAG in WT and $\Delta dicF1-4$. DnaK is the loading control. (H) Quantification of PchA::FLAG or PchA^{mutC}::FLAG expression in WT and $\Delta dicF1-4$. n=5. For (E, H), data were normalized to PchA::FLAG expression in WT. Error bars show the mean \pm SD. *, $p \leq 0.01$; ns, $p > 0.05$.

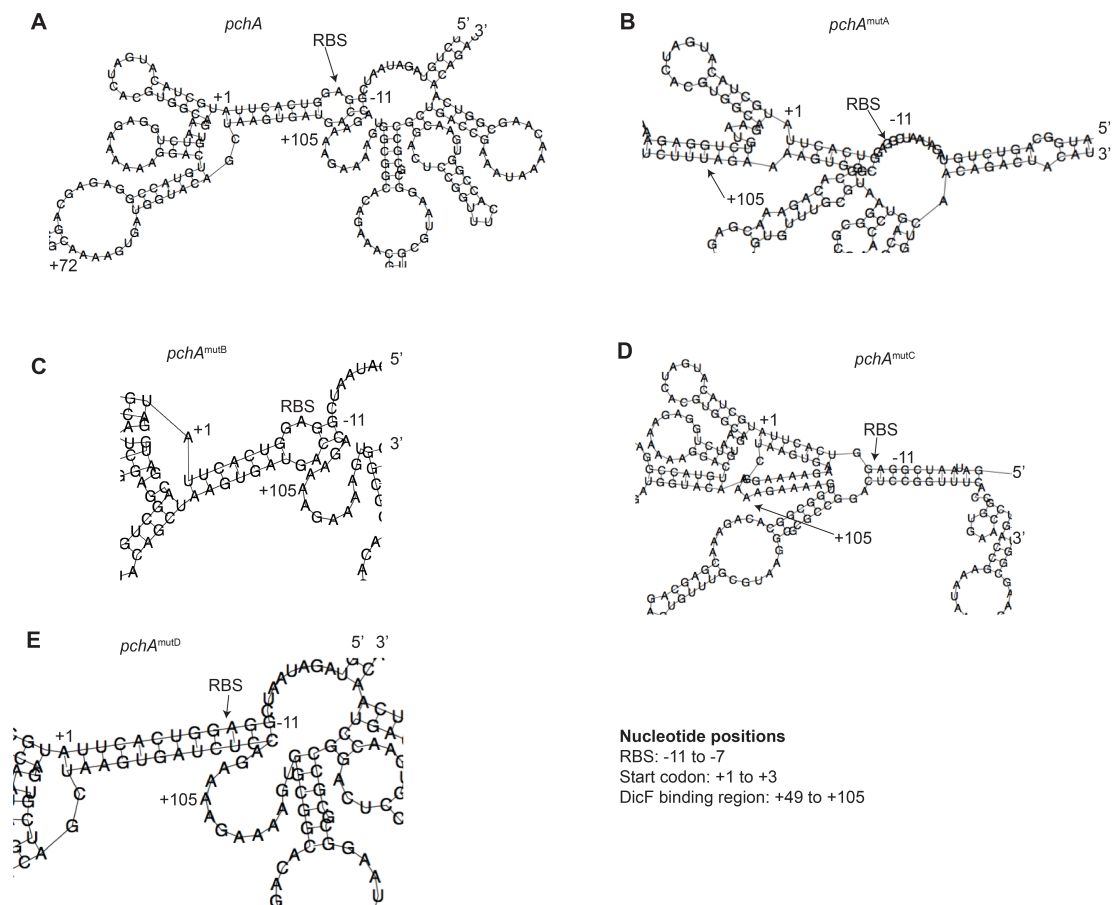


Fig. 2-13. Predicted secondary structures of *pchA* transcripts. Predicted RNA structures of (A) *pchA*; (B) *pchA^{mutA}*; (C) *pchA^{mutB}*; (D) *pchA^{mutC}*; and (E) *pchA^{mutD}*. The mutated nucleotides are indicated in Fig. 2-8, 2-12, and 2-15.

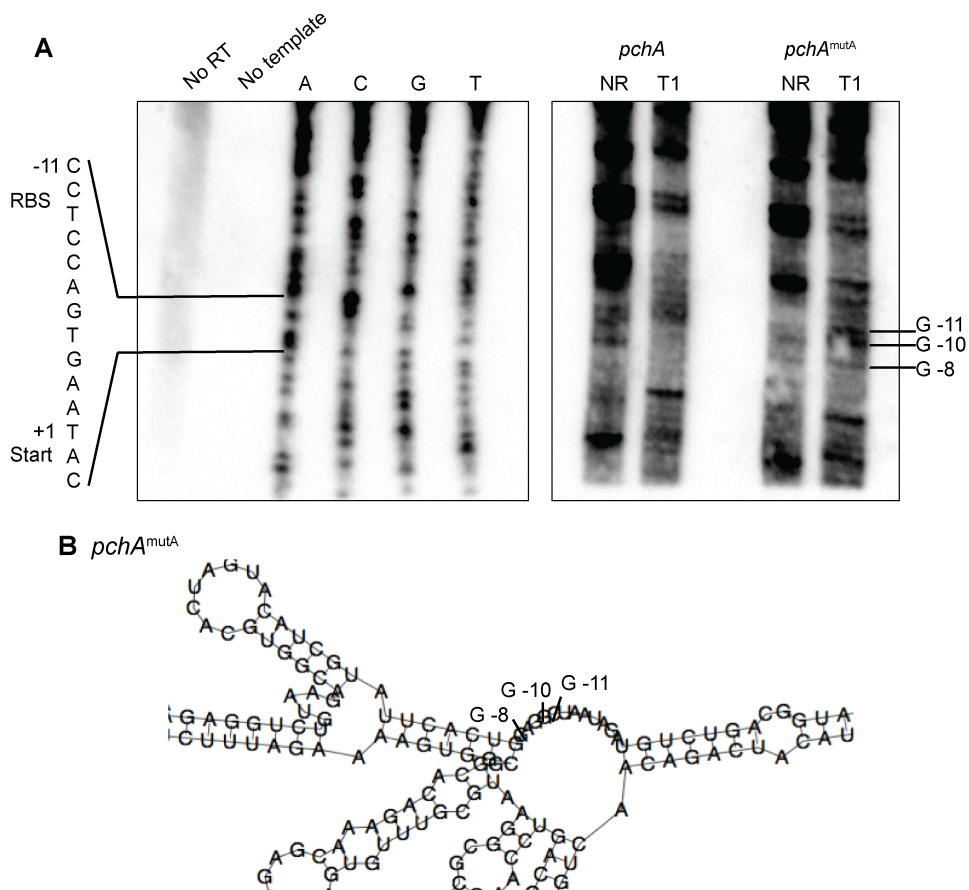


Fig. 2-14. Structure probing of *pchA* and *pchA*^{mutA} transcripts. (A) The area of the sequencing ladder that includes the RBS and the start codon is indicated on the left. RT = reverse transcriptase. *pchA* and *pchA*^{mutA} transcripts treated with RNase T1 are shown on the right. NR = non-reacted samples. T1 cleavage sites detected in the *pchA*^{mutA} transcript but absent in the *pchA* transcript are indicated. (B) Predicted secondary structures of *pchA*^{mutA} transcript with detected T1 cleavage sites identified in (A).

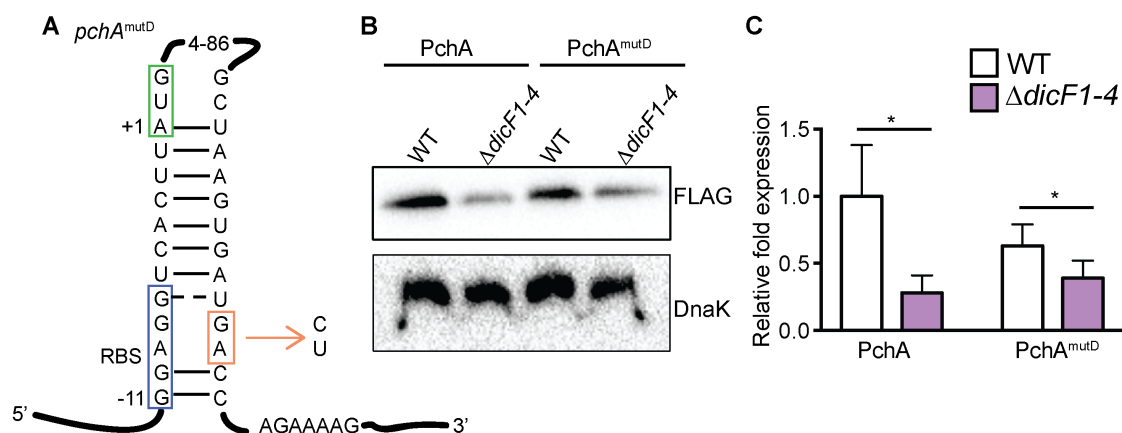


Fig. 2-15. Mutations that strengthen the anti-SD structure. (A) Schematic showing the mutated nucleotides in the *pchA^{mutD}* transcript. (B) Representative Western of PchA::FLAG or PchA^{mutD}::FLAG in WT and Δ *dicF1-4* EHEC. DnaK is the loading control. (C) Quantification of PchA::FLAG or PchA^{mutD}::FLAG expression in WT and Δ *dicF1-4* EHEC. $n=5$. Data were normalized to PchA::FLAG expression in WT. Error bars represent the mean \pm SD. *, $p \leq 0.01$; ns, $p > 0.05$.

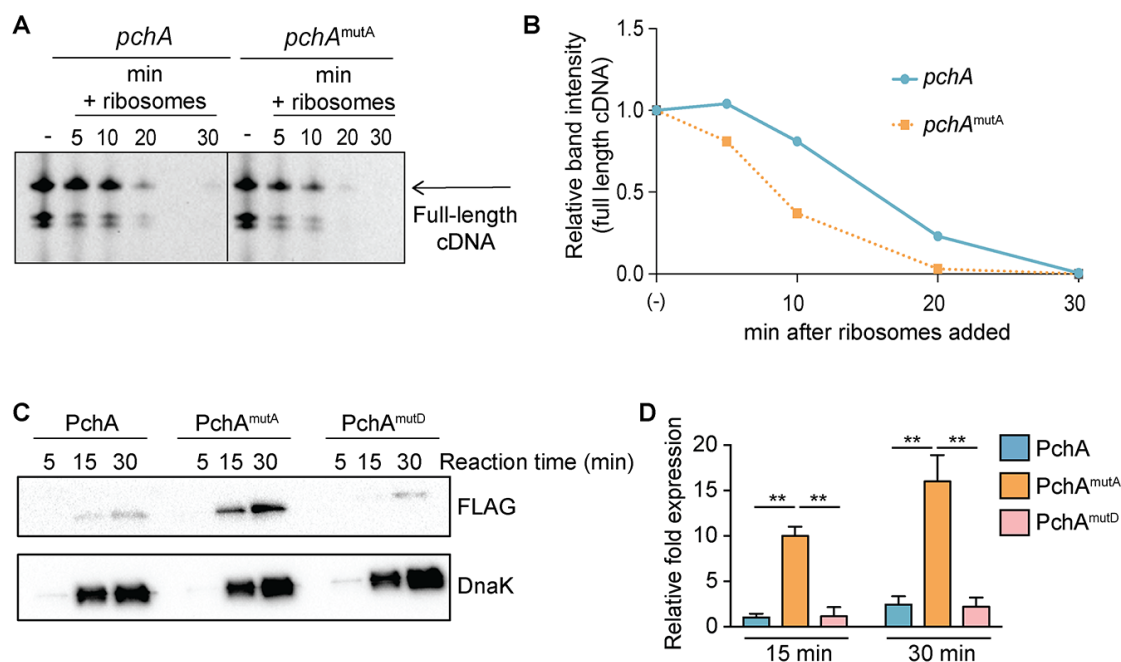


Fig. 2-16. *pchA* mRNA *cis*-interactions impact translation initiation. (A) Reverse transcription inhibition assay of *pchA* or *pchA^{mutA}* after incubation without or with ribosomes. The arrow indicates full length cDNA. (B) Relative levels of full length *pchA* or *pchA^{mutA}* cDNA after incubation without or with ribosomes. $n=3$. (C) Western blot of *in vitro* translated PchA::FLAG, PchA^{mutA}::FLAG, or PchA^{mutD}::FLAG. *In vitro* translated DnaK was used as a reaction control. (D) Quantification of *in vitro* translated PchA::FLAG, PchA^{mutA}::FLAG, or PchA^{mutD}::FLAG. Data are shown relative to PchA::FLAG at 15 min. $n=3$. Error bars show the mean \pm SD. **, $p \leq 0.001$.

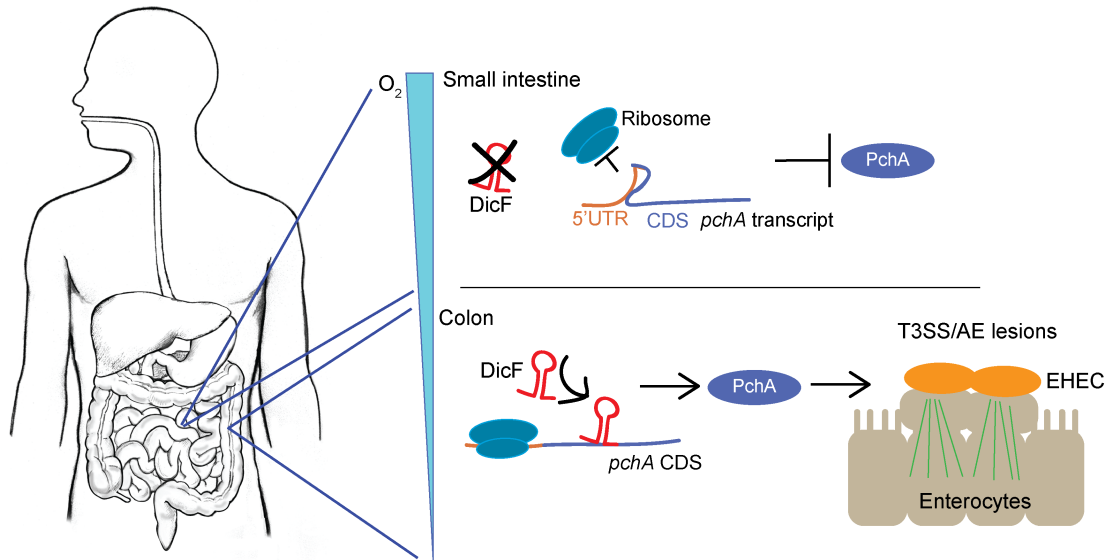


Fig. 2-17. Model of DicF-dependent oxygen sensing and virulence regulation. In the relatively oxygenated environment of the small intestine, DicF is not expressed, and PchA expression is inhibited by *cis*-interactions. Under oxygen-limited conditions in the colon, DicF is expressed and interacts with the *pchA* CDS to promote translation. This ultimately results in the expression of the T3SS and formation of AE lesions, with EHEC intimately adhering to enterocytes.

Chapter 3: RNA helicases promote virulence gene expression in EHEC

ABSTRACT

Post-transcriptional regulation of RNA is responsible for the rapid adaptation of bacteria to new environments, such as those encountered by a pathogen within a host organism. RNA-binding proteins, such as RNA helicases, are involved in all aspects of RNA metabolism. DEAD-box RNA helicases are a family of proteins that regulate ribosome maturation, RNA processing and degradation, and translation initiation. However, relatively little is known about how these helicases affect pathogenesis. The foodborne pathogen enterohemorrhagic *Escherichia coli* O157:H7 (EHEC) encodes a large pathogenicity island required for colonization of the colon known as the locus of enterocyte effacement (LEE) that is subject to post-transcriptional control. While EHEC encodes five DEAD-box RNA helicases, the effects of these helicases on pathogenesis have not been explored. Here, we demonstrate that RNA helicase E (RhIE) positively affects LEE expression through decreased expression of the negative LEE-regulator, RpoS. The *rpoS* transcript is destabilized in an *rhIE*-deletion strain by an RNase E-dependent manner. Additionally, we determine that RhIE positively affects the LEE in the related mouse pathogen *Citrobacter rodentium*, providing a tool to study this pathway of EHEC pathogenesis in a murine model of EHEC infection. Overall, this study identifies a previously unknown role for RNA helicases in regulating pathogenesis and contributes to a growing body of work demonstrating the importance of post-transcriptional regulation as a mechanism to control virulence.

INTRODUCTION

Post-transcriptional regulation of mRNA is appreciated as fundamentally important to rapid adaptation to changing environments (2). The RNA helicases are ubiquitous in all kingdoms of life, as well as encoded within viral genomes, and are involved in virtually all aspects of RNA metabolism, including RNA degradation or protection and translation (193, 194). The majority of RNA helicases belong to superfamily 2 of the nucleic acid helicases, which includes three subfamilies known as the DEAD, DEAH, and DExH RNA helicases, based on variations in the Asp-Glu-Ala-Asp domain critical for ATP hydrolysis (195). In bacteria, DEAD-box RNA helicases unwind short regions of double-stranded RNA via an ATP-dependent mechanism (196, 197). DEAD-box RNA helicases are involved in RNA processing and decay (87, 198), ribosome biogenesis and ribosomal RNA (rRNA) maturation (76, 199, 200), and translation initiation (77, 201). A handful of studies demonstrated roles for RNA helicases in virulence; however, the mechanisms remain poorly understood (78–80, 202).

To date, DEAD-box RNA helicases have not been implicated in EHEC virulence gene expression. *E. coli* species, including EHEC, encode five DEAD-box RNA helicases: RhIB, RhIE, CsdA, DpbA, and SrmB. All five DEAD-box helicases encode a common core of ~350 amino acids, with variation in their C-terminal ends (203). CsdA, DpbA, and SrmB are involved in ribosome maturation and translation initiation, particularly in response to cold shock (76, 77, 196, 199, 200). RhIB is unique in that it possesses no ATPase or helicase activity on its own, but rather requires other protein partners, such as ribonuclease (RNase) E, to stimulate its activity (204, 205). The C-terminal domain (CTD) of RNase E acts as a scaffold for binding of RhIB, enolase, and PNPase, which together form what is known as the RNA degradosome, responsible for degrading the majority of transcripts in *E. coli* (81, 87). As part of the RNA degradosome,

RhIB is involved in processing the *LEE4* operon in EHEC (143). Although a role for RhIE in ribosome assembly and maturation has been suggested (206), no specific function has been attributed to this RNA helicase in *E. coli*. For this reason, we chose to characterize RhIE function and activity in EHEC.

In this study, we demonstrate that RhIE promotes LEE expression in EHEC strain 86-24. RhIE activates LEE expression by repressing RpoS, an alternative sigma factor that binds RNA polymerase core enzyme under stress conditions to regulate the general stress response (44). While RpoS is reported to be both a positive and negative regulator of the LEE, depending on different strains and/or growth conditions (124, 129–132), we determine that RpoS negatively regulates the LEE in EHEC strain 86-24. RhIE destabilizes the *rpoS* transcript via an RNase E-dependent mechanism, leading to decreased RpoS expression and increased expression of the LEE. Furthermore, we identify a role for RhIB in LEE regulation distinct from processing of *LEE4*. Altogether, this study identifies a role for the DEAD-box RNA helicase RhIE, and expands on the body of work demonstrating the importance of post-transcriptional gene regulation in modulating virulence strategies in pathogens.

RESULTS

RhIE contributes to virulence gene expression in EHEC

The potential role of DEAD-box RNA helicases in regulating virulence gene expression in pathogenic *E. coli* has not been investigated. To determine whether RhIE affects virulence expression in EHEC, we measured EspA expression by western blot (Fig. 3-1A and B). EspA is encoded within *LEE4* and forms the filament of the T3SS (163). EspA expression was decreased in the $\Delta rhIE$ strain compared to the WT strain (Fig. 3-1A and B). Importantly, EspA expression was restored in the $\Delta rhIE$ strain when

RhIE was expressed *in trans* (Fig. 3-1A and B). Consistent with the EspA expression data, the $\Delta rhIE$ strain formed fewer AE lesions on epithelial cells compared to the WT strain (Fig. 3-2). To determine whether RhIE also affects Stx expression, we performed qPCR to examine *stx2a* (encoding the A subunit of Stx) levels in the $\Delta rhIE$ strain. However, RhIE did not have an effect on *stx2a* (Fig. 3-3). Altogether, these data suggest that RhIE affects virulence gene expression in EHEC by promoting LEE expression.

RhIE positively affects the LEE by repressing RpoS expression

Another DEAD-box RNA helicase, CsdA, promotes translation of the stress response sigma factor RpoS in non-pathogenic *E. coli* under cold shock conditions (77). RpoS is a known regulator of the LEE in some strains of EHEC (124, 129–132). Additionally, some RNA helicases display redundant functions (76, 196, 199, 203). To determine whether RhIE affects RpoS expression, we examined RpoS protein levels by Western blot from samples grown under microaerobic conditions, which promote LEE expression (30). Under these conditions, RpoS was undetectable in both the WT and the $\Delta rhIE$ strains (Fig. 3-4). ClpXP is a protease that degrades RpoS (44). We used a *clpXP*-deletion strain as a tool to detect RpoS expression by generating $\Delta clpXP$ and $\Delta rhIE\Delta clpXP$ strains. Surprisingly, RpoS was still undetectable in the $\Delta clpXP$ strain, but was robustly expressed in the $\Delta rhIE\Delta clpXP$ strain (Fig. 3-4). To determine whether RhIE affects *rpoS* transcript levels, we measured *rpoS* expression by Northern blot analysis. The *rpoS* transcript was significantly upregulated in the $\Delta rhIE$ strain compared to the WT strain (Fig. 3-5A and B). Altogether, these results indicate that RhIE represses RpoS expression.

Reports of the effect of RpoS on LEE expression are conflicting. In some cases, RpoS activates LEE expression (129–131), and in other examples RpoS is a repressor of LEE expression (124, 132). To determine how RpoS influences LEE expression in

EHEC strain 86-24 under microaerobic conditions, we examined EspA levels in the $\Delta rpoS$ strain by Western blot. EspA expression was significantly increased in the $\Delta rpoS$ strain compared to the WT strain, indicating that under physiologically relevant growth conditions, RpoS is a negative regulator of the LEE in EHEC strain 86-24 (Fig. 3-6A and B).

As RpoS repressed LEE expression (Fig. 3-6), and RhIE repressed *rpoS* (Fig. 3-4 and 3-5) and activated the LEE (Fig. 3-1), we hypothesized that RhIE promotes LEE expression through negative regulation of *rpoS*. To test this hypothesis, we generated a double deletion strain ($\Delta rhIE\Delta rpoS$) and examined EspA levels by Western blot. Deletion of *rpoS* in an $\Delta rhIE$ background phenocopied the $\Delta rpoS$ strain and restored EspA levels in the $\Delta rhIE$ strain, suggesting that decreased LEE expression in the $\Delta rhIE$ strain is due to aberrant RpoS expression (Fig. 3-6A and B). Furthermore, we examined *LEE* transcript levels by qPCR in the WT, $\Delta rhIE$, $\Delta rpoS$, and $\Delta rhIE\Delta rpoS$ strains and determined that expression of all LEE operons was decreased in the $\Delta rhIE$ strain (Fig. 3-7). *LEE1* (*ler*), *LEE2* (*escC*), and *LEE4* (*espA*) were increased in the $\Delta rpoS$ strain compared to WT (Fig. 3-7). With the exception of *LEE3* (*escV*), deletion of *rpoS* in the $\Delta rhIE$ background restored LEE expression to WT levels (Fig. 3-7). Altogether, these data suggest that RpoS represses LEE expression by a *ler*-mediated mechanism and RhIE promotes LEE expression by repressing *rpoS*. One study reported that RpoS repressed LEE expression by negatively regulating transcription of *pchA*, a transcriptional activator of the LEE (124). However, we did not detect differences in *pch* expression in the $\Delta rpoS$ strain compared to the WT strain, suggesting that RpoS regulates LEE expression independent of Pch (Fig. 3-8).

RhIE destabilizes the *rpoS* transcript

RNA helicases affect gene expression post-transcriptionally by modulating either RNA stability or translation (193). To determine whether RhIE affects *rpoS* stability, we performed an RNA stability assay. Briefly, we grew the WT and $\Delta rhIE$ strains under microaerobic conditions, added rifampicin to halt transcription and extracted RNA from samples collected at the indicated time points (Fig. 3-9). We performed Northern blot analysis to detect *rpoS* expression levels. Before rifampicin is added, *rpoS* expression was increased in the $\Delta rhIE$ strain compared to WT, as described previously (Fig. 3-5A and B, Fig. 3-9A). Additionally, the *rpoS* transcript was significantly more stable in the $\Delta rhIE$ strain compared to WT (half-life = 56.45 minutes vs. 39.94 minutes, respectively), suggesting that RhIE negatively regulates RpoS production by destabilizing the *rpoS* transcript (Fig. 3-9A and B).

RhIE destabilizes the *rpoS* transcript by an RNase E-dependent mechanism

To destabilize the *rpoS* transcript, RhIE must be recruiting or aiding in the activity of an RNase, as RhIE does not possess intrinsic RNase activity. RNase E is involved in the degradation of *rpoS* (23). However, RNase E is an essential gene, thus testing effects of RNase E is challenging. One approach around the essentiality of RNase E is the utilization of RNase E truncation mutants. The CTD of RNase E acts as a scaffold for the accessory proteins RhlB, enolase, and PNPase, which together with RNase E form the RNA degradosome (Fig. 3-10) (81). Deletion of the CTD of RNase E ($rne^{\Delta CTD}$) results in viable cells, but significantly affects the activity of RNase E (207, 208). To determine whether the effect of RhIE on *rpoS* is dependent on RNase E activity, we generated the $rne^{\Delta CTD}$ strain and the $\Delta rhIE rne^{\Delta CTD}$ strain to examine *rpoS* stability under these conditions. We planned to run this experiment under microaerobic conditions to match our LEE expression data; however, the $rne^{\Delta CTD}$ strain was not viable under these

conditions and no growth was detected up to 24 hours (data not shown). Therefore, we instead performed this experiment under aerobic growth conditions. Importantly, *rpoS* levels were increased in the $\Delta rhIE$ strain during aerobic growth before the addition of rifampicin, similar to the microaerobic growth conditions (Fig. 3-11). Furthermore, deletion of the RNase E CTD in both the WT and $\Delta rhIE$ backgrounds stabilized the *rpoS* transcript (Fig. 3-11), suggesting that the RhIE effect on *rpoS* stability is dependent on RNase E.

An alternative approach to this issue of non-viability of *rne*-deletion strains is the generation of temperature sensitive RNase E point mutations (209, 210). The RNase E temperature sensitive mutant (*rne*^{TS}) is the consequence of a single base-pair transition (C204T) resulting in the substitution of a phenylalanine for a leucine at amino acid position 68 (L68F) (Fig. 3-10) (210). At permissive temperatures ($\leq 37^\circ\text{C}$), RNase E activity is not affected. However, at higher temperatures, RNase E activity is depleted (209–211). The *rne*^{TS} strains are grown at the permissive temperature and then growth is switched to non-permissive temperatures to analyze effects of RNase E on RNA metabolism. To further attempt to analyze the contribution of RNase E to RhIE regulation of *rpoS* under microaerobic growth conditions, we expressed either the WT *rne* allele or the *rne*^{TS} allele in the *rne* ^{Δ CTD} and the $\Delta rhIE$ *rne* ^{Δ CTD} strain backgrounds. We grew the cultures under microaerobic conditions at 37°C (permissive temperature) for 5 hours, then shifted the temperature to 42°C (non-permissive temperature) for one additional hour of growth. We extracted RNA and analyzed the samples by Northern blot for *rpoS* expression (Fig. 3-12). If the *rne*^{TS} allele were temperature sensitive under these conditions, we would expect to see an increase in *rpoS* expression when the *rne*^{TS} allele is expressed in the *rne* ^{Δ CTD} background compared to when the *rne* allele is overexpressed (Fig. 3-12; compare the first and third lanes). The *rne*^{TS} allele did not

affect *rpoS* expression in either strain background under these conditions, suggesting that the L68F mutation does not inactivate RNase E under these growth conditions or in this strain of *E. coli*. Alternatively, these results may suggest that RNase E is not involved in *rpoS* degradation under microaerobic growth conditions.

Other RNA helicases may be involved in virulence gene expression in EHEC

There are five DEAD-box RNA helicases in *E. coli* (203); here, we described a role for RhIE in regulating the LEE in EHEC. Additionally, the effect of RhIE on *rpoS* expression is dependent on RNase E under aerobic growth conditions. Another DEAD-box RNA helicase, RhIB, binds to the CTD of RNase E as part of the RNA degradosome (81). To determine whether the effects of RhIE on the LEE are specific to RhIE, or are more broadly a function of RNA helicases, we generated an *rhIB*-deletion strain and examined EspA expression levels by Western blot. Interestingly, EspA was significantly decreased in the $\Delta rhIB$ strain compared to WT, as well as in the $\Delta rhIB$ strain compared to the $\Delta rhIE$ strain (Fig. 3-13A and B). The *espA* gene is encoded within *LEE4*, which undergoes post-transcriptional processing by the RNA degradosome (143). To determine whether the decrease in EspA expression in the $\Delta rhIB$ strain is solely related to the role of RhIB in the RNA degradosome processing of *LEE4*, or whether the effect on EspA is due to other effects on the LEE, we analyzed *ler* and *espA* expression by qPCR in the $\Delta rhIB$ strain. Interestingly, both *ler* and *espA* were decreased in the $\Delta rhIB$ strain compared to WT (Fig. 3-13C), indicating that in addition to its role in *LEE4* processing, RhIB affects LEE gene expression in a Ler-dependent manner, similar to RhIE. Additionally, *rpoS* expression was increased in the $\Delta rhIB$ strain compared to WT (Fig. 3-13C), suggesting that RhIB may affect LEE expression by a mechanism similar to that of RhIE.

RhIE contributes to virulence gene regulation in *Citrobacter rodentium*

As RhIE contributes to LEE gene expression and AE lesion formation in EHEC, we expect that the $\Delta rhIE$ strain would be attenuated during mammalian infection. EHEC does not produce similar signs of human infection in the mouse intestine, such as the formation of AE lesions on colonic epithelial cells, thus other models are necessary to study mammalian infection (155). *Citrobacter rodentium* is a mouse pathogen that causes colitis and transmissible colonic hyperplasia. Key regulatory pathways, including the LEE, are conserved between EHEC and *C. rodentium* (212, 213). In addition, *C. rodentium* forms AE lesions within the mouse GI tract (214). Due to expression of similar virulence factors and formation of AE lesions, *C. rodentium* has been adapted as a mouse model of EHEC infection (155). Analysis of the *C. rodentium* genome indicated that *C. rodentium* encodes an RhIE protein that is 96% identical to the EHEC RhIE from amino acids 1-389, with greater divergence in the C-terminal ends (Fig. 3-14A). To determine whether RhIE functions to regulate the LEE in *C. rodentium*, we generated a *C. rodentium* $\Delta rhIE$ strain and analyzed EspA expression from cultures grown under microaerobic conditions. Similar to our findings with EHEC, EspA expression was decreased in the *C. rodentium* $\Delta rhIE$ strain compared to the WT strain (Fig. 3-14B), suggesting that RhIE positively affects LEE expression in *C. rodentium*. This strain will be a useful tool to study the effects of RhIE on EHEC pathogenesis *in vivo*.

DISCUSSION AND FUTURE DIRECTIONS

Post-transcriptional modification of gene expression plays a critical role in rapid adaptation of bacteria to changing environments (1). Here, we demonstrated a role for the DEAD-box RNA helicase RhIE in EHEC pathogenesis. RhIE positively affects LEE expression by exerting a negative effect on RpoS, which we demonstrated negatively

regulates the LEE in EHEC strain 86-24 (Fig. 3-15). The *rpoS* transcript was stabilized in the absence of RhIE, suggesting that RhIE destabilizes *rpoS*. This effect on *rpoS* stability is likely mediated by RNase E during aerobic growth. Furthermore, the other five DEAD-box RNA helicases in EHEC may affect virulence gene regulation as well. RhIB, an RNA helicase that is part of the RNA degradosome, also positively influences the LEE. Interestingly, both RhIB and RhIE activate LEE expression by promoting *ler* expression (Fig. 3-15). Additionally, RhIB also has a negative effect on *rpoS* expression. We hypothesize that RpoS negatively regulates LEE expression by either directly binding to and repressing the *ler* promoter, or by affecting transcription of another LEE regulator. To test the former hypothesis, we will use DNA-protein electrophoretic mobility shift assays with purified RpoS protein and a PCR product of the *ler* promoter. To determine whether RpoS affects transcription of another LEE regulator, we will perform RNAseq comparing the WT and $\Delta rpoS$ strains. Additionally, we will interrogate whether the other three DEAD-box helicases (CsdA, DbpA, and SrmB) affect LEE and/or RpoS expression under microaerobic growth conditions and physiologically relevant temperatures. In some cases, the DEAD-box RNA helicases exhibit similar functions (196, 199, 203). Additionally, CsdA positively regulates *rpoS* translation during growth in cold temperatures in non-pathogenic *E. coli* (77). Therefore, examining the effects of the other DEAD-box RNA helicases to LEE and RpoS expression under microaerobic conditions will demonstrate whether other RNA helicases affect virulence gene expression in EHEC.

Although the involvement of RNA helicases in RNA processing is well-characterized, very little is known about the signals that promote expression of these proteins, with the exception of cold shock (215). Cold shock induces expression of RhIE or RhIE homologs in other bacteria (apart from *E. coli*) (74, 75, 216, 217). Cold

temperatures affect mRNA secondary structures, stabilizing the formation of double-stranded RNA which can limit translation (179). Therefore, it is not surprising that RNA helicases are expressed during cold shock, as they unwind RNA secondary structures (193). Our data demonstrate that in EHEC, RhIE regulates gene expression under both aerobic and microaerobic conditions at 37°C. Further work on this project will determine other signals that promote RNA helicase expression and/or activity in EHEC.

Experiments with the RNase E truncation strains demonstrated the effect of RhIE on *rpoS* stability is dependent on RNase E under aerobic growth conditions. The *rne*^{ΔCTD} strains do not grow under microaerobic growth conditions; therefore, to test the contribution of RNase E under these conditions we expressed the temperature sensitive *rne* allele (*rne*^{TS}) in the *rne*^{ΔCTD} strain backgrounds. However, the results suggest either this allele is not temperature sensitive in EHEC or in microaerobic conditions, or that RhIE regulation of *rpoS* stability is dependent on another RNase under these conditions (Fig. 3-12). To determine whether the *rne*^{TS} allele is temperature sensitive in EHEC, we will perform these same experiments on cultures grown aerobically. Membrane tethering of RNase E through its N-terminal domain is critical for its activity by maintaining an active conformation and protects RNase E from temperature-induced denaturation (85). RNase E is less stable and displays decreased activity under low oxygen conditions related to its localization in the cytoplasm during growth in low oxygen (54, 85). Therefore, perhaps RNase E activity of the *rne*^{TS} allele is not further affected by temperature during growth in low oxygen conditions. To test this possibility, we will utilize a well-characterized non-pathogenic *E. coli* strain that encodes a chromosomal *rne*^{TS} allele (209–211), generate an $\Delta rhIE$ strain in this background, and interrogate the contribution of RNase E to RhIE-dependent *rpoS* stability under both aerobic and microaerobic conditions.

RhIE (as well as SrmB and CsdA) binds to RNase E *in vitro* (218). CsdA also co-purifies with RNase E during growth in cold temperatures (219). RhIE binds to the CTD of RNase E at a position distinct from that of RhIB and functionally replaces RhIB activity *in vitro* (218). In *Caulobacter crescentus*, a model organism for studying the cell cycle, RhIE associates with RNase E *in vivo* during growth at cold temperatures, suggesting that RhIE is important for degradosome formation during cold shock in this bacterium (74). The RhIE-containing degradosomes also co-purified with RhIB, indicating that RhIE and RhIB are able to associate with the degradosome simultaneously (74). These studies highlight that other RNA helicases apart from or in addition to RhIB associate with the degradosome under certain conditions. We hypothesize that RhIE binds to RNase E and forms part of the degradosome in EHEC, under both aerobic and microaerobic conditions. We will test this hypothesis by performing protein interaction experiments (i.e. co-immunoprecipitation) *in vivo*. Additionally, although the *rpoS* transcript is more stable in the absence of RhIE, it is still degraded in the $\Delta rhIE$ strain (Fig. 3-9 and 3-11), suggesting other factors besides RhIE also affect RNase E-dependent *rpoS* degradation. As *rpoS* was also upregulated in the $\Delta rhIB$ strain (Fig. 3-13B) and RhIB forms part of the degradosome, we predict that RhIE and RhIB act in an additive manner. To test this hypothesis, we will generate an $\Delta rhIE\Delta rhIB$ strain and examine *rpoS* and EspA levels compared to the WT strain and the single deletion strains.

The effect of RhIE on LEE expression in *C. rodentium* is similar to EHEC, suggesting that virulence gene regulation by RhIE may be common in enteric pathogens. The *C. rodentium* $\Delta rhIE$ strain will be a useful tool to study the effects of RhIE on pathogenesis *in vivo*. However, it is possible that the mechanism of RhIE LEE regulation in *C. rodentium* is distinct from the mechanism of EHEC. In EHEC, we determined that RhIE positively regulates the LEE by repressing RpoS expression, which is a negative

regulator of the LEE in EHEC strain 86-24. In contrast, RpoS is reported to be a positive regulator of the LEE in *C. rodentium*, as demonstrated by decreased levels of secreted proteins (i.e. EspA) in the $\Delta rpoS$ strain compared to the WT strain (220). Additionally, the $\Delta rpoS$ strain was less virulent than the WT strain during mouse infection (220).

Furthermore, in mouse and cattle models of EHEC colonization, the $\Delta rpoS$ strain is recovered at lower numbers than the WT strain, suggesting that RpoS contributes to EHEC fitness in the GI tract (221). This colonization defect of the $\Delta rpoS$ strain is likely due to decreased acid resistance, as *rpoS* mutants are more sensitive to acid stress, such as the low pH levels in the stomach (221). Therefore, while LEE expression is decreased in the $\Delta rhIE$ strain and would hypothetically lead to decreased colonization of the $\Delta rhIE$ strain, increased RpoS expression in this strain may also cause increased stress resistance, particularly to acid stress, and positively affect colonization in the $\Delta rhIE$ strain. One could speculate that RpoS expression would be beneficial during early steps of infection as EHEC passes through the stomach and small intestine, but would be energetically wasteful when LEE expression is required to colonize the epithelial barrier of the colon. Therefore, RhIE may play a role in precise spatiotemporal control of RpoS during EHEC infection. Importantly, the cues that lead to RhIE production have not been identified, and elucidating these signals may shed light on how RhIE modulates EHEC pathogenesis. We will use the *C. rodentium* $\Delta rhIE$ strain to interrogate the physiological effect of RhIE on EHEC pathogenesis and begin to answer some of the remaining questions of this complex pathway.

In conclusion, we have identified an additional aspect of post-transcriptional control that regulates virulence gene expression in EHEC. Future studies will further explore the contribution of RNA helicases to virulence in enteric pathogens. Overall, this

work adds to our understanding of the complex regulatory networks that modulate pathogenesis.

MATERIALS AND METHODS

Bacterial strains, plasmids, and growth conditions. Strains and plasmids are listed in Appendix Tables 4 and 5; primers are listed in Table 6. Unless indicated otherwise, bacteria were grown statically overnight in LB broth, diluted 1:100 in low-glucose DMEM (Invitrogen), and grown statically for 6 h at 37°C, 5% CO₂ (microaerobic conditions). For aerobic growth conditions, cultures were grown shaking in DMEM to an O.D.₆₀₀ of 0.8 (late-logarithmic growth). Oxygen concentrations have been measured at >200 μmol O₂/L or <10 μmol O₂/L under the respective conditions (172). To induce expression of *rhIE* in pBAD-Myc/His for the complementation experiment or the *rne* alleles in pBAD24, arabinose was added to cultures to a final concentration of 0.2%. Deletion strains were constructed using lambda red mutagenesis (188). Point mutations were generated using the NEB Q5 Site-Directed Mutagenesis Kit. Deletions and mutations were confirmed by Sanger sequencing.

RNA extraction and quantitative PCR (qPCR). RNA was extracted from three biological replicates using the PureLink RNA Mini Kit (Ambion) and treated with Dnase (Ambion) according to manufacturer specifications. RNA purity was determined by measuring the A₂₆₀/A₂₈₀ absorbance ratio and by performing PCR (35 cycles).

qPCR was performed in a one-step reaction using an ABI 7500-FAST sequence detection system and software (Applied Biosystems). For each 10- μl reaction mixture, 5 μl 2× SYBR master mix (Ambion), 0.05 μl Multi-Scribe reverse transcriptase (Invitrogen), and 0.05 μl Rnase inhibitor (Invitrogen) were added. Primers were designed using Primer Blast (NCBI) to ensure no cross-reactivity to other genes in the EHEC

chromosome. Amplicon length was approximately 100 bp. Amplification efficiency of each primer pair was verified using standard curves of known DNA concentrations. Melting-curve analysis was used to ensure template specificity by heating products to 95°C for 15 s, followed by cooling to 60°C and heating to 95°C while monitoring fluorescence. After the amplification efficiency and template specificity were determined for each primer pair, relative quantification analysis was used to analyze the samples using the following conditions for cDNA generation and amplification: 1 cycle at 48°C for 30 min, 1 cycle at 95°C for 10 min, and 40 cycles at 95°C for 15 s and 60°C for 1 min. Two technical replicates of each biological replicate were included for each gene target. Data were normalized to the reference control 16S rRNA, and analyzed using the comparative critical threshold (C_T) method (189). The expression level of the target genes was compared using the relative quantification method (189). Data are presented as the change (n -fold) in expression levels compared to WT levels. Error bars represent the standard deviations of the $\Delta\Delta C_T$ value.

***In vitro* transcription.** PCR products were purified using QIAquick PCR Purification Kit (Qiagen). DNA templates were transcribed with the HiScribe T7 High Yield RNA Synthesis Kit (NEB). Transcripts were Dnase treated and purified using NucAway Spin Columns (Ambion). Probes for Northern blots were generated by incorporating biotinylated uridine into the *in vitro* transcription reaction.

Fluorescein actin staining (FAS) assay. Assays were performed as previously described (190). Overnight bacterial cultures were diluted 1:150 to infect washed HeLa cells. Infected HeLa cells were grown on coverslips in low glucose DMEM for 3 h at 37°C, 5% CO₂. The coverslips were washed and fixed with formaldehyde, and cells were permeabilized with 0.2% Triton-X. Permeabilized cells were stained with fluorescein isothiocyanate-labeled phalloidin to visualize actin. Following Rnase treatment, bacteria

and HeLa cell nuclei were stained with 4',6-diamidino-2-phenylindole. Samples were visualized with a Nikon E800 microscope with a Hamamatsu Orca-ER digital camera.

Western blotting. Standard procedures were used as described (134). Equal protein amounts (determined using Bradford reagent, Bio-Rad) were separated in 10 or 15% polyacrylamide gels. After electrophoresis, proteins were transferred to polyvinylidene difluoride membranes, and probed with indicated antibodies (EspA (Vanessa Sperandio); DnaK (Abcam)). Samples were visualized with chemiluminescence and quantified with ImageJ. Expression levels were normalized to DnaK and shown relative to those of the WT strain.

Northern blotting. RNA was extracted as described above. Equal concentrations of RNA were mixed with 2X RNA loading dye (1X MOPS, 60% formamide, 1.85% formaldehyde, 0.3% bromophenol blue, 0.3% xylene cyanol), incubated at 65°C for 10 min, and immediately placed on ice. Samples were separated in a 2% agarose gel (1X MOPS, 0.1% formaldehyde) in 1X MOPS buffer (Ambion) for the electrophoresis buffer. RNA was transferred overnight by capillary action onto Zeta-probe membranes (Bio-Rad) in 20X saline-sodium citrate (SSC) (Fisher). After UV crosslinking, the membranes were stained with 1% methylene blue to visualize 16S and 23S rRNA. Membranes were incubated in pre-warmed NorthernMax Prehybridization/Hybridization Buffer (Ambion) for 30 min at 68°C. RNA probes (0.2 pmol) were incubated with the membrane OVN at 68°C. The following day, membranes were washed twice with 2X SSC/0.1% SDS and then twice 1X SSC/0.1% SDS, and biotinylated probes were detected as described above. Northern blots were quantified using ImageJ, and fold changes were calculated using 16S rRNA as the reference control and are relative to expression before the addition of rifampicin. The half-life of the *rpoS* transcript was calculated in Prism using one phase exponential decay analysis.

Quantification and statistical analysis. The students' t test was used to determine statistical significance. Number of biological samples can be found in the figure legends.

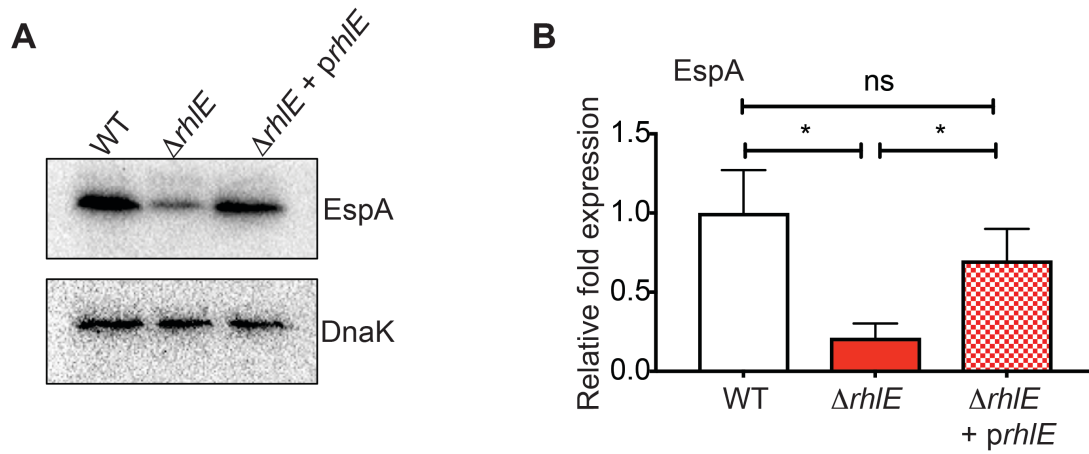
FIGURES

Fig. 3-1. RhIE positively affects LEE expression. (A) Western blot analysis of EspA in the WT, $\Delta rhIE$, and $\Delta rhIE$ complemented with *prhIE* strains grown under microaerobic conditions. The WT and $\Delta rhIE$ strains carry the empty vector. DnaK is the loading control. (B) Quantification of EspA in WT, $\Delta rhIE$, and $\Delta rhIE + prhIE$. $n=3$. For (B), error bars represent the mean \pm SD. *, $p \leq 0.01$.

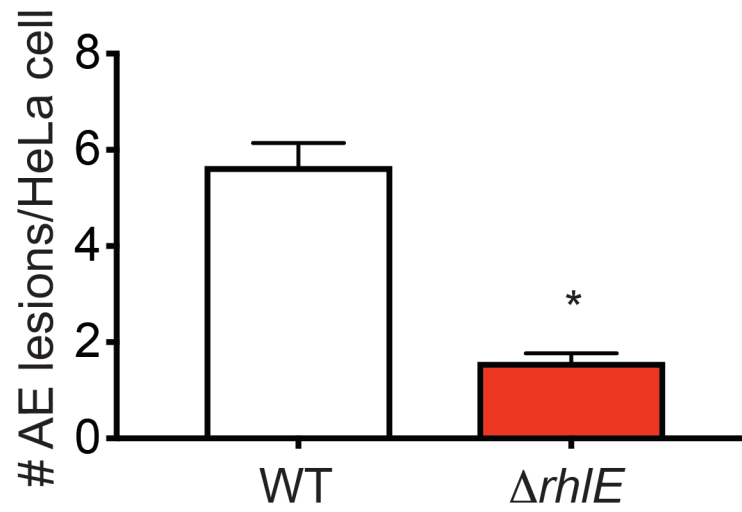


Fig. 3-2. RhIE promotes AE lesion formation. Quantification of AE lesions on HeLa cells infected with WT or $\Delta rhIE$. n=3. Error bars represent the mean \pm SD. *, p \leq 0.01.

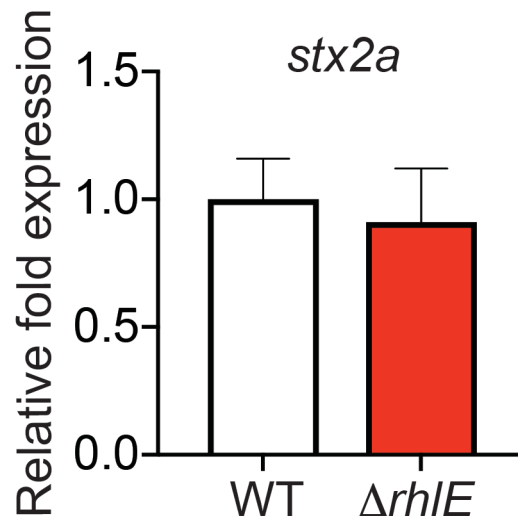


Fig. 3-3. RhIE is not involved in Stx expression. qPCR of *stx2a* in the WT and $\Delta rhIE$ strains grown under microaerobic conditions. n=3.

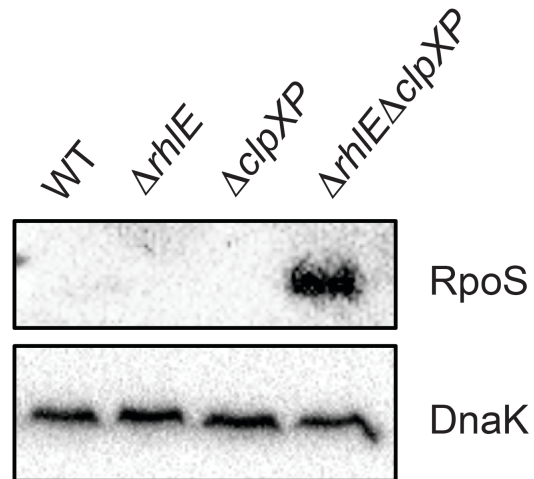


Fig. 3-4. RhIE negatively affects RpoS expression. Western blot analysis of RpoS in the WT, $\Delta rhIE$, $\Delta clpXP$, and $\Delta rhIE\Delta clpXP$ strains grown under microaerobic conditions. DnaK is the loading control. n=3.

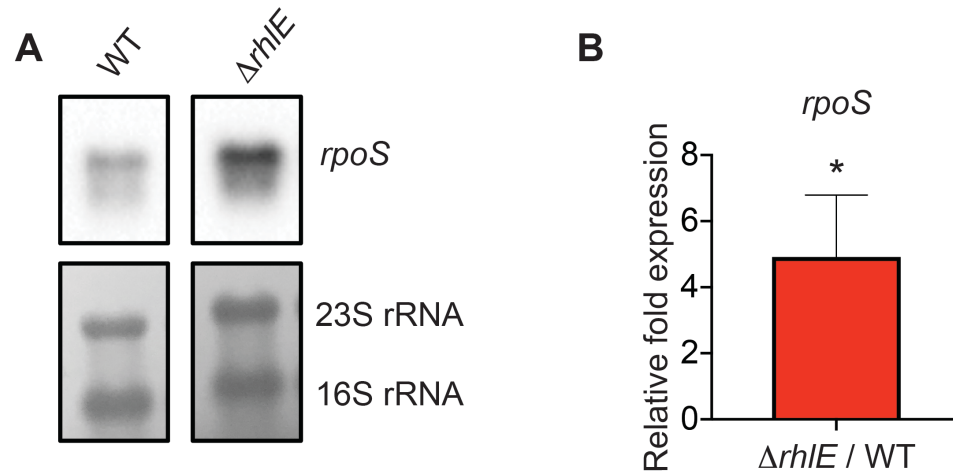


Fig. 3-5. RhIE negatively affects *rpoS* transcript levels. (A) Northern blot analysis of *rpoS* expression in RNA samples extracted from the WT and $\Delta rhIE$ strains. 23S and 16S rRNA are the loading controls. (B) Relative fold expression of *rpoS* in the $\Delta rhIE$ strain compared to the WT strain. Fold changes are in reference to the 16S rRNA control. $n=4$. Error bars represent the mean \pm SD. *, $p \leq 0.05$.

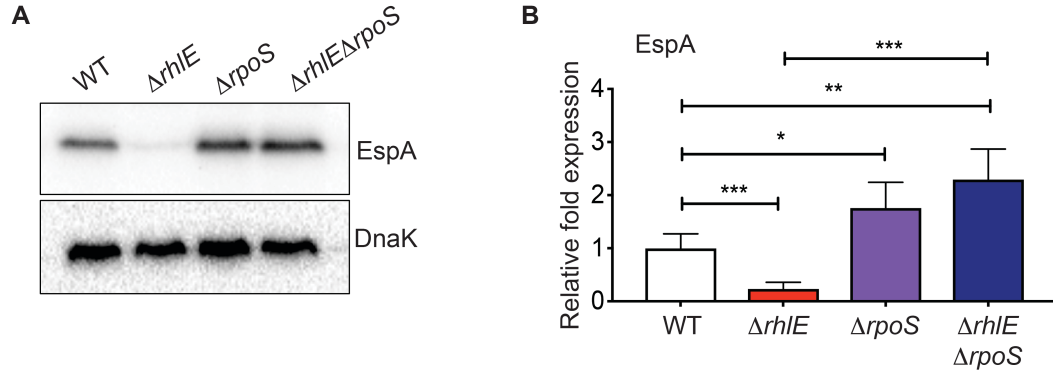


Fig. 3-6. RpoS negatively affects LEE expression and functions in the same pathway as RhIE. (A) Western blot analysis of EspA expression in the WT, $\Delta rhIE$, $\Delta rpoS$, and $\Delta rhIE \Delta rpoS$ strains. DnaK is the loading control. (B) Quantification of EspA in the WT, $\Delta rhIE$, $\Delta rpoS$, and $\Delta rhIE \Delta rpoS$ strains. n=6. For (B), error bars represent the mean \pm SD. *, $p \leq 0.01$; **, $p \leq 0.001$; ***, $p \leq 0.0001$.

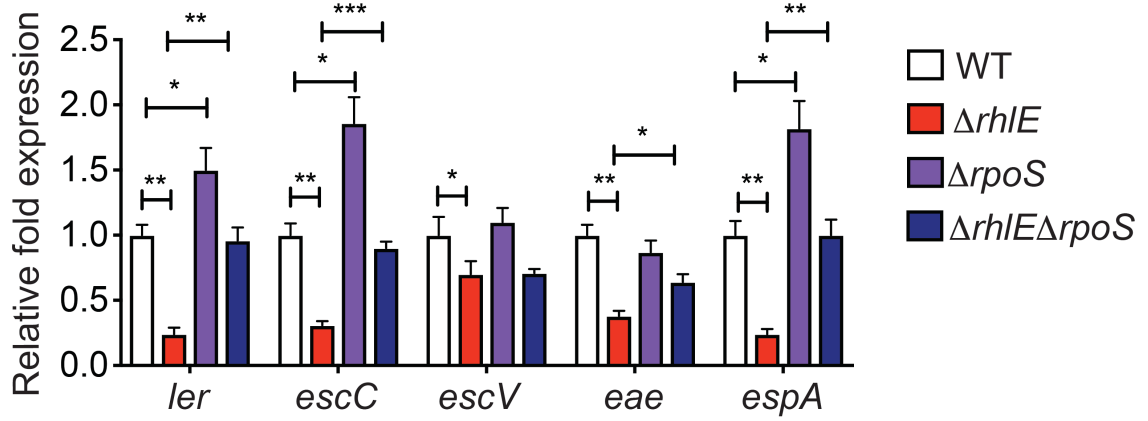


Fig. 3-7. RhIE and RpoS affect the LEE by modulating *ler* expression. qPCR of one gene from each LEE operon in the WT, $\Delta rhIE$, $\Delta rpoS$, and $\Delta rhIE\Delta rpoS$ strains. n=6.

Error bars represent the mean \pm SD. *, $p \leq 0.01$; **, $p \leq 0.001$; ***, $p \leq 0.0001$.

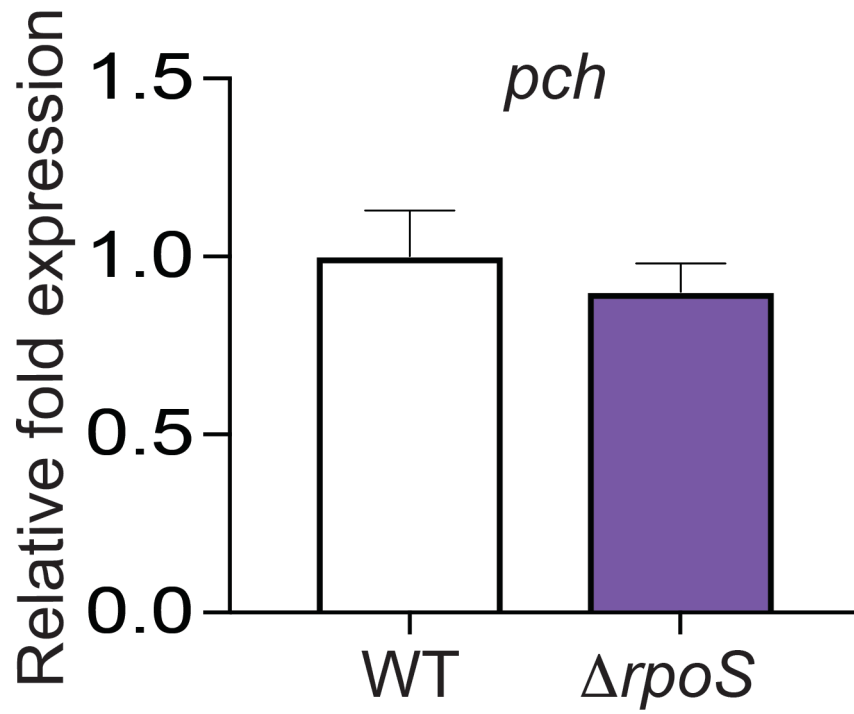


Fig. 3-8. RpoS does not affect *pch* expression. qPCR of *pch* in the WT and $\Delta rpoS$ strains. n=3.

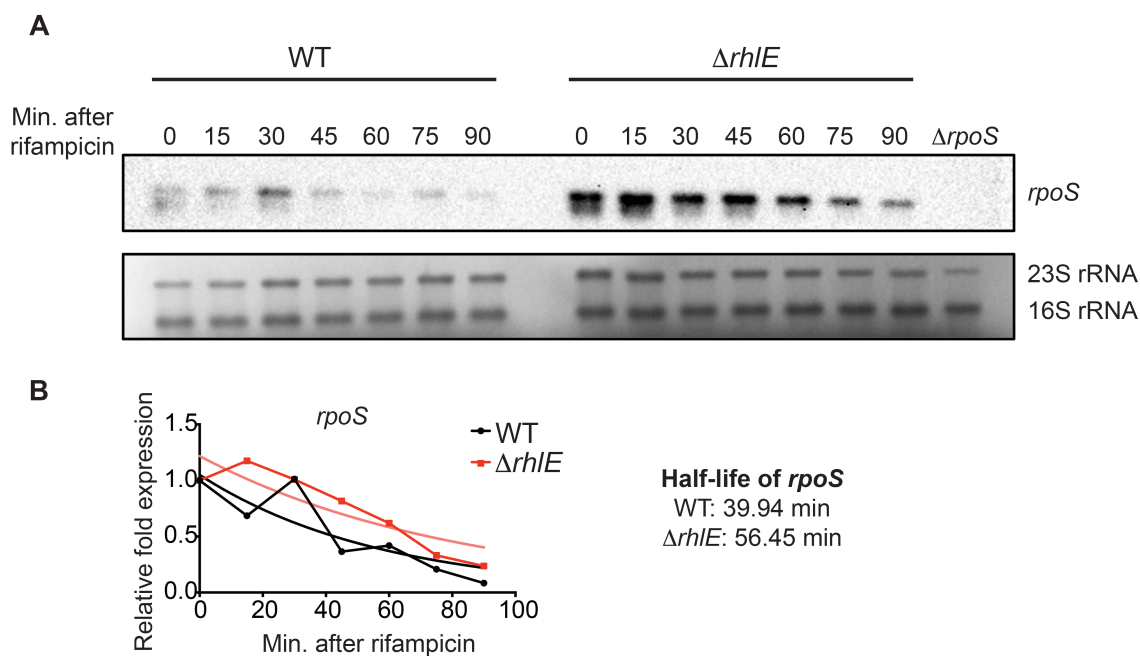


Fig. 3-9. RhIE destabilizes the *rpoS* transcript. (A) Northern blot analysis of *rpoS* expression in the WT and $\Delta rhIE$ strains grown under microaerobic conditions. After rifampicin was added to halt transcription, RNA was extracted from samples collected at the indicated time points. The $\Delta rpoS$ strain is used as a control to confirm probe specificity. 23S and 16S rRNA are used as loading controls. (B) Quantification of *rpoS* stability in the WT and $\Delta rhIE$ strains. The half-life of the *rpoS* transcript was calculated using one-phase decay analysis in Prism. n=2.

RNase E

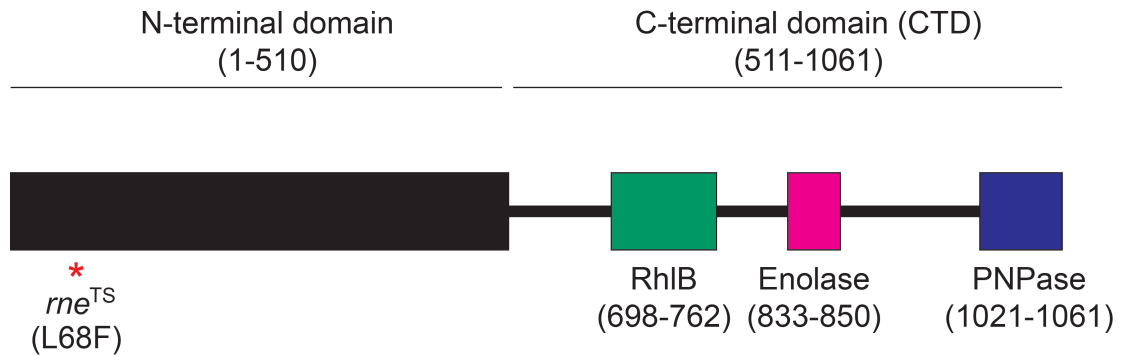


Fig. 3-10. Schematic of the RNA degradosome. The Rnase E C-terminal domain (CTD) contains binding sites for RhlB, enolase, and PNPase. The mutation that generates the temperature sensitive *rne* allele (*rne*^{TS}) is indicated in the N-terminal domain.

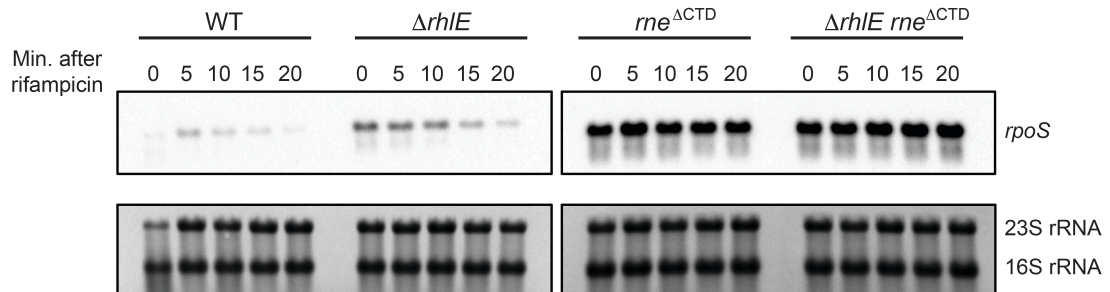


Fig. 3-11. The effect of RhIE on *rpoS* stability is dependent on RNase E. Northern blot analysis of *rpoS* stability in the WT, $\Delta rhIE$, $rne^{\Delta CTD}$, and $\Delta rhIE rne^{\Delta CTD}$ strains grown under aerobic conditions. After rifampicin was added to halt transcription, RNA was extracted from samples collected at the indicated time points. 23S and 16S rRNA are the loading controls.

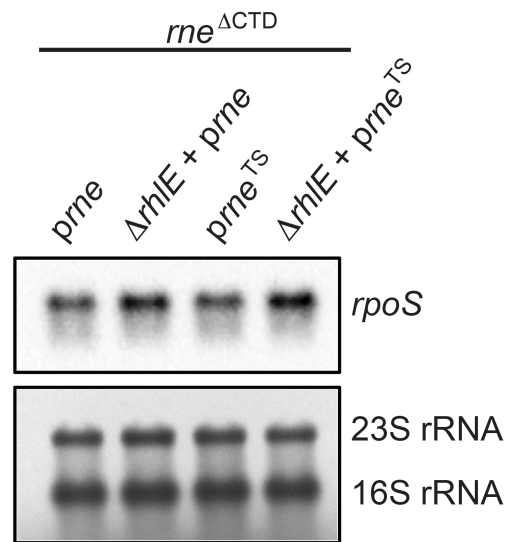


Fig. 3-12. The rne^{TS} allele is functional at 42°C in EHEC strain 86-24. Northern blot analysis of *rpoS* expression in the $rne^{\Delta CT D}$ strain with *prne* and *prne^{TS}*, and the $\Delta rhIE$ $rne^{\Delta CT D}$ strain with *prne* and *prne^{TS}* grown under microaerobic conditions. RNA was collected after cultures were grown for 5 hours at 37°C and shifted to 42°C for one hour. 23S and 16S rRNA are the loading controls.

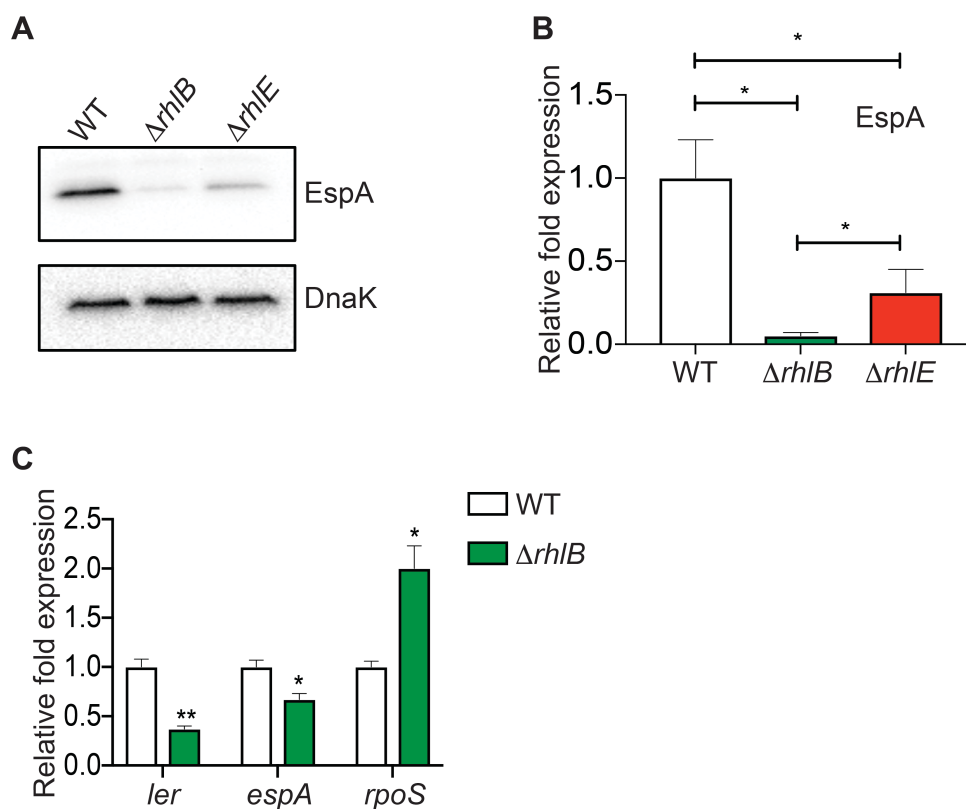


Fig. 3-13. RhIB promotes LEE expression and negatively affects *rpoS* expression.

(A) Western blot analysis of EspA expression in the WT, $\Delta rhIB$, and $\Delta rhIE$ strains grown under microaerobic conditions. (B) Quantification of EspA expression in the WT, $\Delta rhIB$, and $\Delta rhIE$ strains grown under microaerobic conditions. $n=3$. (C) qPCR of *ler*, *espA*, and *rpoS* expression in the WT and $\Delta rhIB$ strains grown under microaerobic conditions. $n=3$. For (B) and (C), Error bars represent the mean \pm SD. *, $p \leq 0.01$; **, $p \leq 0.001$.

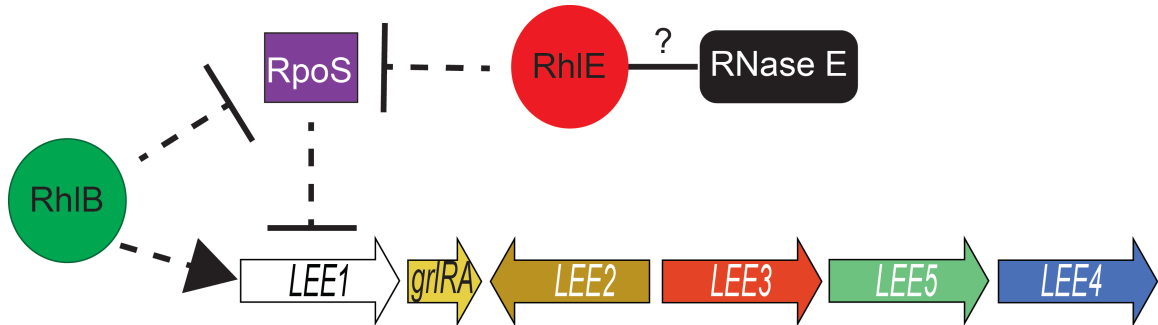


Fig. 3-15. Model of the effects of RhIE and RhIB on RpoS and the LEE. RhIE is a positive regulator of the LEE, and this effect is due to negative regulation of RpoS. RhIE regulation of RpoS is dependent on RNase E; however, it is unknown whether RhIE and RNase E interact *in vivo*. RhIB is also a positive regulator of the LEE and a negative regulator of RpoS. Whether the effect of RhIB on the LEE is dependent on RpoS is currently unknown. → indicates activation of expression; —| indicates inhibition of expression; - - - indicates effect may be indirect.

Chapter 4: Summary and Implications to the Field

SUMMARY

Post-transcriptional regulation is critical for rapid adaptation to new environments, such as those that a pathogen encounters when infecting a host. EHEC carries a critical pathogenicity island, the LEE, that encodes genes required for EHEC to intimately attach to host epithelial cells in the colon through the formation of AE lesions (89). Tight regulation of the LEE is required for precise spatiotemporal control of this virulence factor as expression of the LEE where it is not needed, such as the lumen of the colon, would be energetically unfavorable and would perhaps decrease EHEC fitness. Additionally, the low infectious dose of EHEC (~50 bacteria) (93) suggests that EHEC has evolved mechanisms to precisely regulate virulence factors.

Although it was previously demonstrated that low oxygen, or microaerobic, conditions influenced LEE expression (147), how EHEC responded to microaerobic conditions to promote AE lesion formation was not understood. Here, we demonstrated that the multicopy sRNA DicF is responsible for activating LEE expression under microaerobic conditions (30). DicF is expressed under low oxygen conditions (30, 54), due to the decreased activity of RNase E under these conditions (54). DicF promotes LEE expression by activating translation of the LEE transcriptional regulator, PchA. The CDS of *pchA* forms a secondary structure with its 5' UTR that limits its translation. DicF binds to the CDS of *pchA* to prevent the CDS from interacting with the *pchA* 5' UTR. Thus, DicF promotes translation of PchA, which activates transcription of the LEE. This study represents a novel mechanism of sRNA activation of translation that is responsible for appropriate spatiotemporal control of virulence gene expression in EHEC (30).

Although RNA helicases are ubiquitous in bacterial species, relatively few examples exist of RNA helicases affecting virulence factor production (78–80, 202). *E. coli* species, including EHEC, encode five DEAD-box RNA helicases, but the

contribution of these RNA helicases to EHEC pathogenesis remained unexplored. We determined that RhIE positively affects the LEE in EHEC. RhIE exerts its effect by destabilizing the *rpoS* transcript via an RNase E-dependent mechanism. RpoS is a negative regulator of the LEE in EHEC strain 86-24. Furthermore, we demonstrated that a related RNA helicase, RhIB, positively affects LEE expression by a mechanism distinct from that of its established role in processing *LEE4* (143), and also negatively affects *rpoS*. We generated a strain of *Citrobacter rodentium* that lacks RhIE that will be used to understand the ramifications of this pathway *in vivo*. Altogether, our work characterizes two important pathways of post-transcriptional virulence gene regulation in EHEC (Fig. 4-1).

IMPLICATIONS TO THE FIELD

The mechanism of DicF activation of *pchA* translation is unique: previously, sRNAs that promote translation of target transcripts by binding to the CDS had not been identified. Target transcript activation by sRNAs was thought to occur solely through binding of the sRNA to the 5' UTR of mRNA, to prevent secondary structures that occlude the RBS and inhibit translation (26). Therefore, our work identifies a novel mechanism of sRNA activity and it is likely that other sRNAs will be characterized that bind to the CDS to promote target transcript expression. Additionally, our research demonstrates that EHEC uses sRNAs to respond to oxygen levels in the environment and this may be a common mechanism among enteric pathogens that are exquisitely sensitive to oxygen levels in the GI tract. Moreover, many studies on the functions of sRNAs, including DicF (33, 35), are interpreted based on overexpression of the sRNA. These interpretations should be made with caution. Hfq is required for the activity of most *trans*-acting sRNAs and therefore overexpressed sRNAs can sequester Hfq and

may cause pleiotropic phenotypes (59, 65). Our study with DicF is distinct in that our interpretations are not based on overexpression of DicF, but rather involves analysis of deletion strains that display phenotypes under conditions known to promote virulence gene expression in EHEC (147).

Our work with DicF also provides further evidence that multicopy, or “sibling,” sRNAs are crucial regulators of bacterial virulence (45). EHEC strain 86-24 carries four nearly identical copies of DicF encoded within chromosome-integrated prophages (30). The effects of DicF on LEE expression are additive, suggesting that the acquisition and maintenance of multiple copies of DicF allows for the amplification of virulence. Indeed, EHEC also encodes three copies of the *pch* genes, which are targeted by DicF to promote LEE expression, indicating that the additive effects of multiple *dicF* and *pch* genes is evolutionarily advantageous to EHEC survival. The related LEE-encoding pathogen enteropathogenic *E. coli* (EPEC) also encodes at least two copies of DicF (54). The homolog of Pch in EPEC is PerC; however, *pch* and *perC* share little homology on the nucleotide level, and DicF is not predicted to bind to *perC*. Therefore, DicF may contribute to LEE expression in EPEC through a distinct mechanism. Interestingly, other intestinal and extraintestinal pathogenic *E. coli* strains that do not encode the LEE also carry multiple copies of DicF (33, 54), suggesting that DicF may target virulence genes in other pathogenic *E. coli* as well.

In the process of characterizing the mechanism of DicF activation of *pchA* translation, we discovered that the *pchA* CDS folds back on its RBS to inhibit translation. Although some examples exist of long-distance acting anti-SD sequences within the CDS (177–181), generally these types of interactions are selected against in bacteria (176). Our discovery with *pchA* indicates CDS interactions with the RBS may be more common than previously appreciated.

RNA helicases partake in diverse roles in post-transcriptional gene expression, particularly in response to cold temperatures (74–77). However, we characterized functions of RNA helicases under growth conditions that are relevant to human infection. Furthermore, both RhIE and RpoS are encoded in many bacterial genomes, and RpoS is expressed under different stress conditions and is the controller of the general stress response (44). The role of RhIE in regulating RpoS expression likely goes beyond effects on the LEE as the RpoS regulon includes at least 10% of the *E. coli* genome (44), and therefore RhIE could potentially contribute to stress responses in EHEC and other pathogens.

In total, our studies contribute to the understanding of how pathogens respond to their environments to modulate appropriate spatiotemporal control of virulence. We analyzed complex regulatory systems during EHEC growth in physiologically relevant conditions, suggesting that our work represents processes that occur during infection to promote EHEC pathogenesis. We characterized a novel mechanism of sRNA regulation and revealed the process of an RNA helicase affecting virulence gene expression, both of which may represent broadly conserved methods of genetic control and provide new insights into the role of post-transcriptional gene regulation in bacterial adaptation.

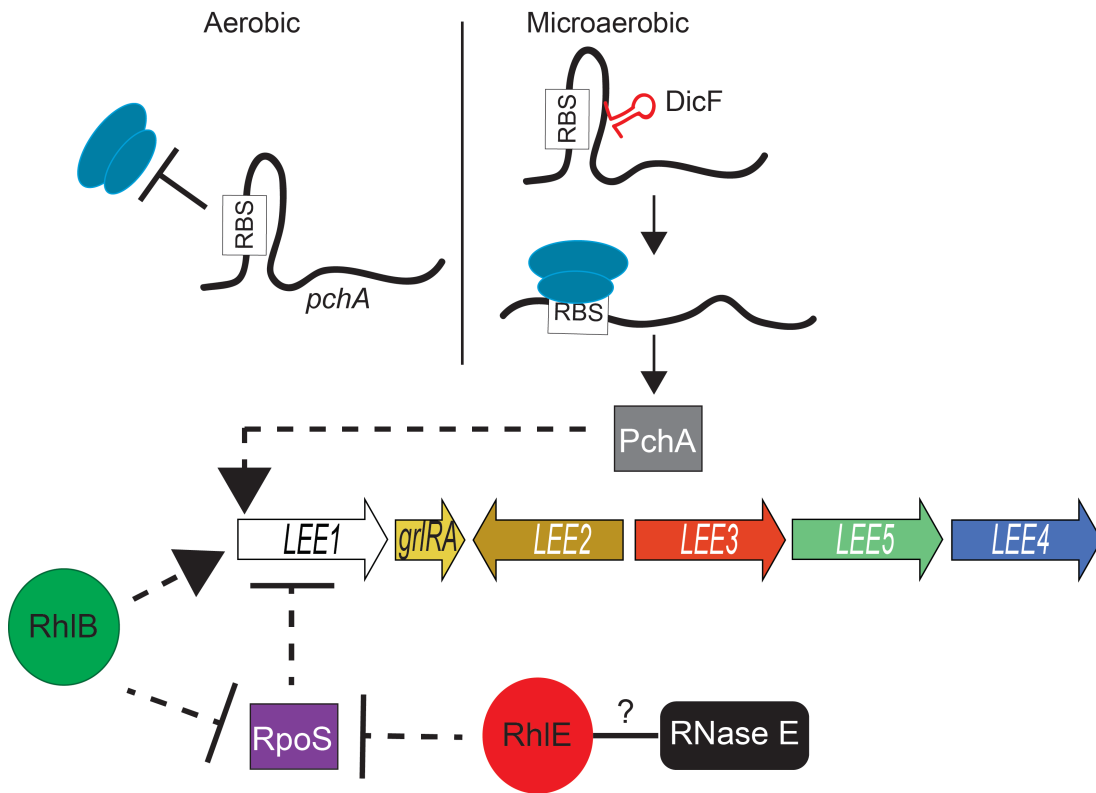


Fig. 4-1. Summary of the work described in Chapters 2 and 3. → indicates activation of expression; —| indicates inhibition of expression; - - - indicates effect may be indirect.

Appendix

Table 1. Bacterial strains used in Chapter 2.

Strain	Genotype or description	Source
86-24	Wild-type EHEC (serotype O157:H7)	(222)
MK80	EHEC 86-24 Δ <i>dicF1</i>	This study
MK86	EHEC 86-24 Δ <i>dicF1</i> with pKD46	This study
MK82	EHEC 86-24 Δ <i>dicF1/2</i>	This study
BM01	EHEC 86-24 Δ <i>dicF1/2</i> with pKD46	This study
BM02	EHEC 86-24 Δ <i>dicF1-3</i>	This study
BM03	EHEC 86-24 Δ <i>dicF1-3</i> with pKD46	This study
BM04	EHEC 86-24 Δ <i>dicF1-3 dicF4::Chl^R</i> (Δ <i>dicF1-4</i>)	This study
BM05	EHEC 86-24 <i>pchA::Kan^R</i> (Δ <i>pchA</i>)	This study
BM06	EHEC 86-24 Δ <i>dicF1-3 pchA::Kan^R</i> (Δ <i>pchA</i> Δ <i>dicF1-3</i>)	This study
BM07	EHEC 86-24 Δ <i>pchA</i> with pBAD-Myc/His A	This study
BM08	EHEC 86-24 Δ <i>pchA</i> with pBM09	This study
MK08	EHEC 86-24 Δ <i>hfq</i>	(134)
BM09	EHEC 86-24 with pBAD24	This study
BM10	EHEC 86-24 Δ <i>dicF1-4</i> with pBAD24	This study
BM11	EHEC 86-24 Δ <i>dicF1-4</i> with pBM01	This study
BM12	EHEC 86-24 with pBAD-Myc/His A	This study
BM13	EHEC 86-24 with pBAD24 and pBM10	This study
BM14	EHEC 86-24 Δ <i>dicF1-4</i> with pBAD24 and pBM10	This study
BM15	EHEC 86-24 Δ <i>dicF1-4</i> with pBM01 and pBM10	This study
BM16	EHEC 86-24 Δ <i>dicF1-4</i> with pBM03 and pBM10	This study
BM17	EHEC 86-24 with pBAD24 and pBM11	This study
BM18	EHEC 86-24 Δ <i>dicF1-4</i> with pBAD24 and pBM11	This study
BM19	EHEC 86-24 Δ <i>dicF1-4</i> with pBM01 and pBM11	This study
BM20	EHEC 86-24 Δ <i>dicF1-4</i> with pBM03 and pBM11	This study
BM21	EHEC 86-24 with pBM05	This study
BM22	EHEC 86-24 Δ <i>dicF1-4</i> with pBM05	This study
BM23	EHEC 86-24 with pBM06	This study
BM24	EHEC 86-24 Δ <i>dicF1-4</i> with pBM06	This study
BM25	EHEC 86-24 with pBM07	This study
BM26	EHEC 86-24 Δ <i>dicF1-4</i> with pBM07	This study
BM27	EHEC 86-24 with pBM08	This study
BM28	EHEC 86-24 Δ <i>dicF1-4</i> with pBM08	This study

Table 2. Plasmids used in Chapter 2.

Plasmid	Description	Source
pBAD24	Expression vector with arabinose-inducible promoter	(223)
pBM01	<i>dicF1</i> in pBAD24	This study
pBM02	<i>dicF1</i> ^{mutA} in pBAD24	This study
pBM03	<i>dicF1</i> ^{mutB} in pBAD24	This study
pBM04	SPA tag in pBAD24	This study
pBM05	<i>pchA</i> ^{WT} with 5' UTR fused in frame with SPA tag in pBM04	This study
pBM06	<i>pchA</i> ^{mutA} made from pBM05 with site-directed mutagenesis	This study
pBM07	<i>pchA</i> ^{mutC} made from pBM05 with site-directed mutagenesis	This study
pBM08	<i>pchA</i> ^{mutD} made from pBM05 with site-directed mutagenesis	This study
pBAD-Myc/His A	Expression vector with arabinose-inducible promoter and <i>Myc/His</i> tag	Invitrogen
pBM09	<i>pchA</i> in pBAD-Myc/His A	This study
pUCP24	Expression vector with IPTG-inducible promoter	(224)
pBM10	<i>pchA</i> with 5' UTR fused in frame with SPA tag in pUCP24	This study
pBM11	<i>pchA</i> ^{mutB} made from pBM10 with site-directed mutagenesis	This study
pKD46	Lambda red recombinase expression plasmid	(188)
pCP20	Temperature-sensitive replication and thermal induction of FLP synthesis	(188)
pKD4	pANTSI derivative containing FRT-flanked kanamycin resistance	(188)
pKD3	pANTSI derivative containing FRT-flanked chloramphenicol resistance	(188)
pJLD500	Vector carrying SPA tag	(225)

Table 3. Oligonucleotides used in Chapter 2.

Primer	Sequence (5' to 3')	Primer use	Template
Z6077_LR_F2	TTGACCATACGCTTAAGTGACAACCC CGCTGCAACGCCCTCTGTTATCAATT GTGTAGGCTGGAGCTGCTTC	Used with Z6077_LR_R 2 to delete <i>dicF1</i> from the chromosome	pKD4
Z6077_LR_R2	TGTTCCGCGTGCGCTCAGCCGCATT CACCGCATCACAAAATTCACCTTTAAAA CATATGAATATCCTCCTTAG	Used with Z6077_LR_F 2 to delete <i>dicF1</i> from the chromosome	pKD4
Z1327_LR_F2	GTTGACCATACGCTTAAGTGACAACC CCGCTGCAACGCCCTCTGTTATCAAT GTGTAGGCTGGAGCTGCTTC	Used with Z1327_LR_F 2 to delete <i>dicF2</i> from the chromosome	pKD4
Z1327_LR_R2	CCGCGTGCGCTGAGCCGCATTCACC GCATCACAAAATTCACCTTTAAAAAAG CATATGAATATCCTCCTTAG	Used with Z1327_LR_R 2 to delete <i>dicF2</i> from the chromosome	pKD4
DicF3LRF 1	TGACCATACGCTTAAGTGACAACCCC GCTGCAACGCCCTCTGTTATCAATGT GTAGGCTGGAGCTGCTTC	Used with DicF3LRR1 to delete <i>dicF3</i> from the chromosome	pKD4
DicF3LRR 1	TCCGCGTGCGCTTAGCCGCATTCAC CGCATCACAAAATTCACCTTTAAAAACA TATGAATATCCTCCTTAG	Used with DicF3LRF1 to delete <i>dicF3</i> from the chromosome	pKD4
DicF3upF 1	CGAATGCTGATTCTGTGAGCCTCAAC	Sequencing <i>dicF3</i> deletion	gDNA
DicF3downR1	AGTGCCTGGTGCCTCCAGGTGAC	Sequencing <i>dicF3</i> deletion	gDNA
DicF4LRR 1	TCCGCGTGCGCTTAGCCGCATTCAC GCATCACAAAATTCACCTTTAAAAACAT ATGAATATCCTCCTTAG	Used with DicF3LRF1 to delete <i>dicF4</i>	pKD3
DicF4upF 1	CGCGAATTGTA CT T GCTCTTTTCG	Sequencing <i>dicF4</i> deletion	gDNA

pBAD F	ATGCCATAGCATTTTTATCC	Sequencing vectors	
pBAD R	CTGATTTAATCTGTATCAGG	Sequencing vectors	
pBpchAM HF1	CTAGCTCGAGGCTACATGATCACGTG GCAGA	Cloning <i>pchA</i> into pBAD- <i>Myc/His A</i>	gDNA
pBpchAM HR1	CTAGAAGCTTGCATTTTTTTGACCGC GCGTTTC	Cloning <i>pchA</i> into pBAD- <i>Myc/His A</i>	gDNA
pchALRF1	TTCAGTAATTGCTCCCTCAAAAATAA TAAAATAAGGTGATTATTTTTGTGTGT AGGCTGGAGCTGCTTC	Used with pchALRR1 to delete <i>pchA</i> from the chromosome	pKD4
pchALRR 1	GGCGGTTCCATTAATTAATGAAAAATAT TCTCAATTTGTACCCAACAAAGACATA TGAATATCCTCCTTAG	Used with pchALRF1 to delete <i>pchA</i> from the chromosome	pKD4
pchAupF1	CCTGCTCCGGTACCGTGCGTGA	Sequencing <i>DpchA</i>	gDNA
pchAdown R1	GGTATAACAATCGACGATTGCTG	Sequencing <i>DpchA</i>	gDNA
pchAPM3 F1	TGACGTCTTTAGAAAAGTGGCGGC	Used to make <i>pchA</i> ^{mutA}	pBM05
pchAPM3 R1	TCACTTAGCTGTACCATCACTTTTGC	Used to make <i>pchA</i> ^{mutA}	pBM05
pchAPM8 F1	GGCCTTTAGTGATGGTACA	Used to make <i>pchA</i> ^{mutB}	pBM10
pchAPM8 R1	ATCGTTCAGCTGCTCTCCGGT	Used to make <i>pchA</i> ^{mutB}	pBM10
pchAPM5 F1	GTGAAGAAAAGAAAAGAAAAGTGGC GGC	Used to make <i>pchA</i> ^{mutC}	pBM05
pchAPM4 R1	TTAGCTGTACCATCACTTTTGCCC	Used to make <i>pchA</i> ^{mutC}	pBM05
pchAPM7 F1	GATCTCCAGAAAAGAAAAGTGGC	Used to make <i>pchA</i> ^{mutD}	pBM05
pchAPM7 R1	ACTTAGCTGTACCATCACTTTTG	Used to make <i>pchA</i> ^{mutD}	pBM05
dicFPM3F 1	TCAATAAAGACGTGACGTTTGCG	Used to make <i>dicF</i> ^{mutA}	pBM01
pB24dicF ptmtR2	TAACAGAGGGCGTTGCAGGG	Used to make <i>dicF</i> ^{mutA}	pBM01

dicFPM8F1	AGTAAAAGTCCGTGACTGCT	Used to make <i>dicF</i> ^{mutB}	pBM01
dicFPM8R1	GATACCGCCAAACGTCACC	Used to make <i>dicF</i> ^{mutB}	pBM01
pB24SPAF1	CTAGCTGCAGTCCATGGAAAAGAGAA GATGG	Used to clone SPA tag into pBAD24	pJLD500
pB24SPAR1	CTAGAAGCTTCTACTTGTCATCGTCA TCCTTG	Used to clone SPA tag into pBAD24	pJLD500
PchA5UTRSPAF1	CTAGGGATCCGGTTTGTTTTTTATTGT TATTTTCATTAAGGGAAGG	Used with PchAfullSPAR1 to clone <i>pchA</i> with the 5' UTR into pBM04	gDNA
PchAfullSPAR1	CTAGCTGCAGGCATTTTTTTGACCGC GCGTTTC	Used with PchA5UTRSPAF1 to clone <i>pchA</i> with the 5' UTR into pBM04	gDNA
pchAIVTT7F1	GCGAATTAATACGACTCACTATAGGG CTTAAGTATAAGGAGGAAAAAATATG CTACATGATCACGTGGCAGAATGT	Used with HisIVTR1 to make DNA template for <i>in vitro</i> transcription for EMSA	pBM09
HisIVTR1	AAACCCCTCCGTTTAGAGAGGGGTTA TGCTAGTTANNNNNNTCAATGATGAT GATGATGATGGTC	Used with pchAIVTT7F1 to make DNA template for <i>in vitro</i> transcription for EMSA	pBM09
pchAUTRIVTT7F1	GCGAATTAATACGACTCACTATAGGG CTTAAGTATATTAAGGGAAGGTAATT CAGGATGGC	Used with SPAIVTR1 to make DNA template for <i>in vitro</i> transcription/translation	pBM05
SPAIVTR1	AAACCCCTCCGTTTAGAGAGGGGTTA TGCTAGTTANNNNNNCTACTTGTCAT CGTCATCCTTGTA	Used with pchAUTRIVTT7F1 to make DNA template for <i>in vitro</i> transcription/tr	pBM05

		anslation	
Z6077NB F1	TTTCTGGTGACGTTTGGCGGT	Northern blot probe for DicF	pBM01
Z6077NB T7R1	TAATACGACTCACTATAGGGAGAGCG CTCAGCCGCATTCACCGCA	Northern blot probe for DicF	pBM01
pchANBF 1	TCCGAGCTCGAGGCTACATGA	Northern blot probe for <i>pchA</i>	pBM09
pchANBT 7R1	TAATACGACTCACTATAGGGAGACGG AGTCCGGCGCGCCTTACGC	Northern blot probe for <i>pchA</i>	pBM09
5S- rRNA_NB _fwd	CCCATGCCGAACTCAGAAGT	Northern blot probe for 5S rRNA	RNA
pchAPE	GCTCGTTTCTGTGCCGCCACT	DNA sequencing ladder and primer extension	
ler_RT_F1	CGACCAGGTCTGCCC	qPCR	cDNA
ler_RT_R 1	GCGCGGAACTCATC	qPCR	cDNA
escC_RT_ F1	GCGTAAACTGGTCCGGTACGT	qPCR	cDNA
escC_RT_ R1	TGCGGGTAGAGCTTTAAAGGCAAT	qPCR	cDNA
escV_RT_ F1	TCGCCCCGTCCATTGA	qPCR	cDNA
escV_RT_ R1	CGCTCCCGAGTGCAAAA	qPCR	cDNA
espA_RT_ F1	TCAGAATCGCAGCCTGAAAA	qPCR	cDNA
espA_RT_ R1	CGAAGGATGAGGTGGTTAAGCT	qPCR	cDNA
eae_RT_F 1	GCTGGCCCTTGGTTTGATCA	qPCR	cDNA
eae_RT_ R1	GCGGAGATGACTTCAGCACTT	qPCR	cDNA
rpoA_RT_ F1	GCGCTCATCTTCTTCCGAAT	qPCR	cDNA
rpoA_RT_ R1	CGCGGTCGTGGTTATCTG	qPCR	cDNA
stx2a _RT_F1	ACCCACCGGGCAGTT	qPCR	cDNA
stx2a _RT_R1	GGTCAAACGCGCCTGATA	qPCR	cDNA

narLqRTF 1	TGGTTGGCGAAGCGAGTAAT	qPCR	cDNA
narLqRTR 1	TGAATACCACAATGCGCCCT	qPCR	cDNA
csrBqRTF 1	GATTCGGTGGGTCAGGAAGG	qPCR	cDNA
csrBqRTR 1	TTGCTCCCTGCTCATCCTTG	qPCR	cDNA

Table 4. Bacterial strains used in Chapter 3.

Strain	Genotype or description	Source
86-24	Wild-type EHEC (serotype O157:H7)	(222)
BM29	EHEC 86-24 $\Delta rhIE$	This study
BM30	EHEC 86-24 $\Delta rhIE$ with pKD46	This study
BM12	EHEC 86-24 with pBAD-Myc/His A	(30)
BM31	EHEC 86-24 $\Delta rhIE$ with pBAD-Myc/His A	This study
BM32	EHEC 86-24 $\Delta rhIE$ with pBM12	This study
BM33	EHEC 86-24 $\Delta clpXP$	This study
BM34	EHEC 86-24 $\Delta rhIE\Delta clpXP$	This study
BM35	EHEC 86-24 $\Delta rpoS$	This study
BM36	EHEC 86-24 $\Delta rhIE\Delta rpoS$	This study
BM37	EHEC 86-24 $rne^{\Delta CTD}$	This study
BM38	EHEC 86-24 $\Delta rhIE rne^{\Delta CTD}$	This study
BM39	EHEC 86-24 $rne^{\Delta CTD}$ with $prne$	This study
BM40	EHEC 86-24 $rne^{\Delta CTD}$ with $prne^{TS}$	This study
BM41	EHEC 86-24 $\Delta rhIE rne^{\Delta CTD}$ with $prne$	This study
BM42	EHEC 86-24 $\Delta rhIE rne^{\Delta CTD}$ with $prne^{TS}$	This study
BM43	EHEC 86-24 $\Delta rhIB$	This study
C.r-j11	<i>Citrobacter rodentium</i> DBS100 with EHEC <i>ler</i> promoter	(226)
BM44	C.r-j11 $\Delta rhIE$	This study

Table 5. Plasmids used in Chapter 3.

Plasmid	Description	Source
pBAD24	Expression vector with arabinose-inducible promoter	(223)
pBAD- <i>Myc</i> /His A	Expression vector with arabinose-inducible promoter and <i>Myc</i> /His tag	Invitrogen
pBM12	<i>rhIE</i> in pBAD- <i>Myc</i> /His A	This study
pABS01	<i>rne</i> in pBAD24	This study
pABS02	<i>rne</i> ^{TS} in pBAD24	This study
pKD46	Lambda red recombinase expression plasmid	(188)
pCP20	Temperature-sensitive replication and thermal induction of FLP synthesis	(188)
pKD4	pANTSI derivative containing FRT-flanked kanamycin resistance	(188)
pKD3	pANTSI derivative containing FRT-flanked chloramphenicol resistance	(188)

Table 6. Oligonucleotides used in Chapter 3.

Primer	Sequence (5' to 3')	Primer use	Template
pBAD F	ATGCCATAGCATT TTTATCC	Sequencing vectors	pBAD vectors
pBAD R	CTGATTTAATCTGTATCAGG	Sequencing vectors	pBAD vectors
RhIELRF2	AACACCTGATCACTCGCCAGCCGCA CGCCAAAGGGCGTCGTCCGGTACGT GTGTAGGCTGGAGCTGCTTC	Used with RhIELRR2 to delete <i>rhIE</i> from the chromosome	pKD4
RhIELRR2	TGATTTGCGACCACCTTCTCCACGGC GTGGTTGCTGTTGACCGCGACCACC ATATGAATATCCTCCTTAG	Used with RhIELRF2 to delete <i>rhIE</i> from the chromosome	pKD4
rhIEupF1	CATGACATTGTGGTTTTTGTC	Used with rhIEdownR1 for sequencing the Δ <i>rhIE</i> strain	gDNA
rhIEdown R1	ATGTCATGCATGTCTGACCGTG	Used with rhIEupF1 for sequencing the Δ <i>rhIE</i> strain	gDNA
pBADrhIE MHF1	CTAGCTCGAGGTCTTTCGATTCTTTG GGTTTAAGC	Used with pBADrhIEMH R1 to clone <i>rhIE</i> into pBAD- <i>Myc/His</i>	gDNA
pBADrhIE MHR1	CTAGAAGCTTCTGCGCAGCGGCAGG TTTACGCGG	Used with pBADrhIEMH F1 to clone <i>rhIE</i> into pBAD- <i>Myc/His</i>	gDNA
ClpXP2LR	GGAGATAAAATCCCCCCTTTTTGGTT AACTAATTGTATGGGAATGGTTAACA TATGAATATCCTCCTTAGT	Used with ClpPP1LR to delete <i>clpXP</i> from the chromosome	pKD4
ClpPP1LR	AGGTTACAATCGGTACAGCAGGTTTT TTCAATTTTATCCAGGAGACGGAAGT GTAGGCTGGAGCTGCTTC	Used with ClpXP2LR to delete <i>clpXP</i> from the	pKD4

		chromosome	
ClpPupF1	TAGCTGATAATCCGTCCATA	Used with ClpXdownR1 to sequence the $\Delta clpXP$ strains	gDNA
ClpXdownR1	ACATTCAACGCCGAGAATAG	Used with ClpPupF1 to sequence the $\Delta clpXP$ strains	gDNA
rpoSNBF1	GCGCGTCGCGCACTGCGT	Used with rpoSNBT7R1 to generate template to <i>in vitro</i> transcribe for Northern blot probe	gDNA
rpoSNBT7R1	TAATACGACTCACTATAGGGAGAAAG GTCCAGCAACGCCAGA	Used with rpoSNBF1 to generate template to <i>in vitro</i> transcribe for Northern blot probe	gDNA
rhIBLRF1	CACCGGATACGCTTTCGTAAAGCAAT AGTAAGCTGATATTCTACCACACTGT GTAGGCTGGAGCTGCTTC	Used with rhIBLRR1 to delete <i>rhIB</i> from the chromosome	pKD4
rhIBLRR1	TCTTGCCATCTTGATACAGTTTGAATG ATTTTGAGTATGACATTTTTTATCATA TGAATATCCTCCTTAG	Used with rhIBLRF1 to delete <i>rhIB</i> from the chromosome	pKD4
rhIBupF1	TATAACTCCACAGGAATAA	Used with rhIBdownR1 to sequence the $\Delta rhIB$ strain	gDNA
rhIBdownR1	CTGTCTCTGTGTTGGCTGCA	Used with rhIBupF1 to sequence the $\Delta rhIB$ strain	gDNA
CrRhIELR F1	TATCTCCCTGAAAACGACACCGGGAA CGGTCGGGGCGGTTTCGGAGTAGTTG TGTAGGCTGGAGCTGCTTC	Used with CrRhIELRR1 to delete <i>rhIE</i>	pKD4

		from the <i>C. rodentium</i> chromosome	
CrRhIELR1	TACAGCTCATGCAGCCTGGATAAGGC GCAGCCGCCATTTCGGTAAAGAAAACA TATGAATATCCTCCTTAG	Used with CrRhIELRF1 to delete <i>rhIE</i> from the <i>C. rodentium</i> chromosome	pKD4
CrRhIEupF1	TCATGACATTGTGGTTTTTG	Used with CrRhIEdownR1 to sequence the <i>C.r. ΔrhIE</i> strain	gDNA
CrRhIEdownR1	CGCAATATGGATGCAGGGGTAAT	Used with CrRhIEdownF1 to sequence the <i>C.r. ΔrhIE</i> strain	gDNA
rpoS_LR_fwd	TTGAATGTTCCGTCAAGGGATCACGG GTAGGAGCCACCTTGTGTAGGCTGG AGCTGCTTC	Used with rpoS_LR_rev to delete <i>rpoS</i> from the chromosome	pKD4
rpoS_LR_rev	CCAGCCTCGCTTGAGACTGGCCTTTC TGACAGATGCTTACCATATGAATATC CTCCTTAG	Used with rpoS_LR_fwd to delete <i>rpoS</i> from the chromosome	pKD4
rpoS_fwd	TGTTCCGTCAAGGGATCACG	Used with rpoS_rev to sequence the <i>ΔrpoS</i> strains	gDNA
rpoS_rev	ATGCAAATTGCCGGGTAGGA	Used with rpoS_rev to sequence the <i>ΔrpoS</i> strains	gDNA
RneLRF1	CTGGCACCGTGCGTGACAACGAATC GCTGTGCTCTCTATTCTGCGTCTGG TGTAGGCTGGAGCTGCTTC	Used with RneLRR1 to generate the <i>rne^{ACTD}</i> strains	pKD4
RneLRR1	TTACTCAACAGGTTGCGGACGCGCA GGAGCGGCAGAGGCATGATGCGTTG CATATGAATATCCTCCTTAG	Used with RneLRF1 to generate the <i>rne^{ACTD}</i> strains	pKD4
RneseqF1	ACCGTGCGCGTATTCAAATCA	Used with RnedownR1	gDNA

		to sequence the <i>rne</i> ^{ACTD} strains	
Rnedown R1	CGATGAATTTTAATATGTTGATT	Used with RneseqF1 to sequence the <i>rne</i> ^{ACTD} strains	gDNA
rne_comp_fwd	TAGGGTACCGATAACCGTGAGGTTG GCGA	Used with rne_comp_rev to clone <i>rne</i> into pBAD24 (pABS01)	gDNA
rne_comp_rev	TAGAAGCTTGGCAGTTACCAGGGCTT GAT	Used with rne_comp_fwd to clone <i>rne</i> into pBAD24 (pABS01)	gDNA
rne_Tsmut_fwd	TCACGGTTTCTTCCCACTAAAAG	Used with rne_Tsmut_rev to generate the <i>rne</i> ^{TS} allele (pABS02)	pABS01
rne_Tsmut_rev	CGTTCAGCGCCGTAATCA	Used with rne_Tsmut_fwd to generate the <i>rne</i> ^{TS} allele (pABS02)	pABS01
EHEC16S qRTF2	TATTGCACAATGGGCGCAAG	qPCR	cDNA
EHEC16S qRTR2	GGAGTTAGCCGGTGCTTCTT	qPCR	cDNA
ler_RT_F1	CGACCAGGTCTGCCC	qPCR	cDNA
ler_RT_R1	GCGCGGAACTCATC	qPCR	cDNA
escC_RT_F1	GCGTAAACTGGTCCGGTACGT	qPCR	cDNA
escC_RT_R1	TGCGGGTAGAGCTTTAAAGGCAAT	qPCR	cDNA
escV_RT_F1	TCGCCCCGTCCATTGA	qPCR	cDNA
escV_RT_R1	CGCTCCCGAGTGCAAAA	qPCR	cDNA
espA_RT_F1	TCAGAATCGCAGCCTGAAAA	qPCR	cDNA

espA_RT_R1	CGAAGGATGAGGTGGTTAAGCT	qPCR	cDNA
eae_RT_F1	GCTGGCCCTTGGTTTGATCA	qPCR	cDNA
eae_RT_R1	GCGGAGATGACTTCAGCACTT	qPCR	cDNA
stx2a_RT_F1	ACCCACCCGGGCAGTT	qPCR	cDNA
stx2a_RT_R1	GGTCAAACGCGCCTGATA	qPCR	cDNA
rpoSqRTF1	ACCAAGTGCGGAAGAGATCG	qPCR	cDNA
rpoSqRTR1	TGTCCAGCAACGCTTTTTTCG	qPCR	cDNA

REFERENCES

1. Sauder AB, Kendall MM. 2018. After the fact(or): post-transcriptional gene regulation in enterohemorrhagic *Escherichia coli* O157:H7. *J Bacteriol*.
2. Shimoni Y, Friedlander G, Hetzroni G, Niv G, Altuvia S, Biham O, Margalit H. 2007. Regulation of gene expression by small non-coding RNAs: a quantitative view. *Mol Syst Biol* 3:138.
3. Holmqvist E, Vogel J. 2018. RNA-binding proteins in bacteria. *Nat Rev Microbiol* 16:601–615.
4. Quereda JJ, Cossart P. 2017. Regulating Bacterial Virulence with RNA. *Annu Rev Microbiol* 71:263–280.
5. Kawano M, Reynolds AA, Miranda-Rios J, Storz G. 2005. Detection of 5'- and 3'-UTR-derived small RNAs and cis-encoded antisense RNAs in *Escherichia coli*. *Nucleic Acids Res* 33:1040–1050.
6. Carrier M-C, Lalaouna D, Massé E. 2018. Broadening the Definition of Bacterial Small RNAs: Characteristics and Mechanisms of Action. *Annu Rev Microbiol* 72:141–161.
7. Holmqvist E, Wagner EGH. 2017. Impact of bacterial sRNAs in stress responses. *Biochem Soc Trans* 45:1203–1212.
8. Farnham PJ, Platt T. 1981. Rho-independent termination: dyad symmetry in DNA causes RNA polymerase to pause during transcription in vitro. *Nucleic Acids Res* 9:563–577.
9. Wilson KS, Hippel PH von. 1995. Transcription termination at intrinsic terminators: the role of the RNA hairpin. *Proc Natl Acad Sci* 92:8793–8797.
10. Chen J, Morita T, Gottesman S. 2019. Regulation of Transcription Termination of Small RNAs and by Small RNAs: Molecular Mechanisms and Biological Functions. *Front Cell Infect Microbiol* 9.
11. Ray-Soni A, Bellecourt MJ, Landick R. 2016. Mechanisms of Bacterial Transcription Termination: All Good Things Must End. *Annu Rev Biochem* 85:319–347.
12. Lowery-Goldhammer C, Richardson JP. 1974. An RNA-Dependent Nucleoside Triphosphate Phosphohydrolase (ATPase) Associated with Rho Termination Factor. *Proc Natl Acad Sci* 71:2003–2007.
13. Koslover DJ, Fazal FM, Mooney RA, Landick R, Block SM. 2012. Binding and Translocation of Termination Factor Rho Studied at the Single-Molecule Level. *J Mol Biol* 423:664–676.

14. Sedlyarova N, Shamovsky I, Bharati BK, Epshtein V, Chen J, Gottesman S, Schroeder R, Nudler E. 2016. sRNA-mediated control of transcription termination in *E. coli*. *Cell* 167:111-121.e13.
15. Silva IJ, Barahona S, Eyraud A, Lalaouna D, Figueroa-Bossi N, Massé E, Arraiano CM. 2019. SraL sRNA interaction regulates the terminator by preventing premature transcription termination of rho mRNA. *Proc Natl Acad Sci* 116:3042–3051.
16. Bossi L, Schwartz A, Guillemardet B, Boudvillain M, Figueroa-Bossi N. 2012. A role for Rho-dependent polarity in gene regulation by a noncoding small RNA. *Genes Dev* 26:1864–1873.
17. Massé E, Escorcia FE, Gottesman S. 2003. Coupled degradation of a small regulatory RNA and its mRNA targets in *Escherichia coli*. *Genes Dev* 17:2374–2383.
18. Dutta T, Srivastava S. 2018. Small RNA-mediated regulation in bacteria: A growing palette of diverse mechanisms. *Gene* 656:60–72.
19. Shine J, Dalgarno L. 1974. The 3'-Terminal Sequence of *Escherichia coli* 16S Ribosomal RNA: Complementarity to Nonsense Triplets and Ribosome Binding Sites. *Proc Natl Acad Sci U S A* 71:1342–1346.
20. Soper TJ, Woodson SA. 2008. The rpoS mRNA leader recruits Hfq to facilitate annealing with DsrA sRNA. *RNA N Y N* 14:1907–1917.
21. Soper T, Mandin P, Majdalani N, Gottesman S, Woodson SA. 2010. Positive regulation by small RNAs and the role of Hfq. *Proc Natl Acad Sci U S A* 107:9602–9607.
22. Majdalani N, Chen S, Murrow J, St John K, Gottesman S. 2001. Regulation of RpoS by a novel small RNA: the characterization of RprA. *Mol Microbiol* 39:1382–1394.
23. McCullen CA, Benhammou JN, Majdalani N, Gottesman S. 2010. Mechanism of positive regulation by DsrA and RprA small noncoding RNAs: pairing increases translation and protects rpoS mRNA from degradation. *J Bacteriol* 192:5559–5571.
24. Prévost K, Salvail H, Desnoyers G, Jacques J-F, Phaneuf E, Massé E. 2007. The small RNA RyhB activates the translation of shiA mRNA encoding a permease of shikimate, a compound involved in siderophore synthesis. *Mol Microbiol* 64:1260–1273.
25. Shao Y, Bassler BL. 2012. Quorum-sensing non-coding small RNAs use unique pairing regions to differentially control mRNA targets. *Mol Microbiol* 83:599–611.
26. Papenfort K, Vanderpool CK. 2015. Target activation by regulatory RNAs in bacteria. *FEMS Microbiol Rev* 39:362–378.

27. Hammer BK, Bassler BL. 2007. Regulatory small RNAs circumvent the conventional quorum sensing pathway in pandemic *Vibrio cholerae*. *Proc Natl Acad Sci U S A* 104:11145–11149.
28. Lease RA, Cusick ME, Belfort M. 1998. Riboregulation in *Escherichia coli*: DsrA RNA acts by RNA:RNA interactions at multiple loci. *Proc Natl Acad Sci U S A* 95:12456–12461.
29. Urban JH, Vogel J. 2008. Two Seemingly Homologous Noncoding RNAs Act Hierarchically to Activate *glmS* mRNA Translation. *PLOS Biol* 6:e64.
30. Melson EM, Kendall MM. 2019. The sRNA DicF integrates oxygen sensing to enhance enterohemorrhagic *Escherichia coli* virulence via distinctive RNA control mechanisms. *Proc Natl Acad Sci U S A* 116:14210–14215.
31. Argaman L, Altuvia S. 2000. *fhIA* repression by OxyS RNA: kissing complex formation at two sites results in a stable antisense-target RNA complex¹¹Edited by M. Gottesman. *J Mol Biol* 300:1101–1112.
32. Chen S, Zhang A, Blyn LB, Storz G. 2004. MicC, a Second Small-RNA Regulator of *Omp* Protein Expression in *Escherichia coli*. *J Bacteriol* 186:6689–6697.
33. Balasubramanian D, Rangunathan PT, Fei J, Vanderpool CK. 2016. A Prophage-Encoded Small RNA Controls Metabolism and Cell Division in *Escherichia coli*. *mSystems* 1.
34. Bouvier M, Sharma CM, Mika F, Nierhaus KH, Vogel J. 2008. Small RNA binding to 5' mRNA coding region inhibits translational initiation. *Mol Cell* 32:827–837.
35. Azam MS, Vanderpool CK. 2018. Translational regulation by bacterial small RNAs via an unusual Hfq-dependent mechanism. *Nucleic Acids Res* 46:2585–2599.
36. Jagodnik J, Chiaruttini C, Guillier M. 2017. Stem-Loop Structures within mRNA Coding Sequences Activate Translation Initiation and Mediate Control by Small Regulatory RNAs. *Mol Cell* 68:158-170.e3.
37. Ramirez-Peña E, Treviño J, Liu Z, Perez N, Sumbly P. 2010. The group A *Streptococcus* small regulatory RNA FasX enhances streptokinase activity by increasing the stability of the *ska* mRNA transcript. *Mol Microbiol* 78:1332–1347.
38. Obana N, Shirahama Y, Abe K, Nakamura K. 2010. Stabilization of *Clostridium perfringens* collagenase mRNA by VR-RNA-dependent cleavage in 5' leader sequence. *Mol Microbiol* 77:1416–1428.
39. Fröhlich KS, Papenfort K, Fekete A, Vogel J. 2013. A small RNA activates CFA synthase by isoform-specific mRNA stabilization. *EMBO J* 32:2963–2979.
40. Pfeiffer V, Papenfort K, Lucchini S, Hinton JCD, Vogel J. 2009. Coding sequence targeting by MicC RNA reveals bacterial mRNA silencing downstream of translational initiation. *Nat Struct Mol Biol* 16:840–846.

41. Wroblewska Z, Olejniczak M. 2016. Hfq assists small RNAs in binding to the coding sequence of *ompD* mRNA and in rearranging its structure. *RNA* 22:979–994.
42. Bandyra KJ, Said N, Pfeiffer V, Górna MW, Vogel J, Luisi BF. 2012. The Seed Region of a Small RNA Drives the Controlled Destruction of the Target mRNA by the Endoribonuclease RNase E. *Mol Cell* 47:943–953.
43. Prévost K, Desnoyers G, Jacques J-F, Lavoie F, Massé E. 2011. Small RNA-induced mRNA degradation achieved through both translation block and activated cleavage. *Genes Dev* 25:385–396.
44. Battesti A, Majdalani N, Gottesman S. 2011. The RpoS-Mediated General Stress Response in *Escherichia coli*. *Annu Rev Microbiol* 65:189–213.
45. Caswell CC, Oglesby-Sherrouse AG, Murphy ER. 2014. Sibling rivalry: related bacterial small RNAs and their redundant and non-redundant roles. *Front Cell Infect Microbiol* 4.
46. Pannekoek Y, Veld RAGH in 't, Schipper K, Bovenkerk S, Kramer G, Brouwer MC, Beek D van de, Speijer D, Ende A van der. 2017. *Neisseria meningitidis* Uses Sibling Small Regulatory RNAs To Switch from Cataplerotic to Anaplerotic Metabolism. *mBio* 8:e02293-16.
47. Sheehan LM, Caswell CC. 2017. A 6-Nucleotide Regulatory Motif within the AbcR Small RNAs of *Brucella abortus* Mediates Host-Pathogen Interactions. *mBio* 8:e00473-17.
48. Dos Santos PT, Menendez-Gil P, Sabharwal D, Christensen J-H, Brunhede MZ, Lillebæk EMS, Kallipolitis BH. 2018. The Small Regulatory RNAs LhrC1-5 Contribute to the Response of *Listeria monocytogenes* to Heme Toxicity. *Front Microbiol* 9:599.
49. Ross JA, Thorsing M, Lillebæk EMS, Teixeira Dos Santos P, Kallipolitis BH. 2019. The LhrC sRNAs control expression of T cell-stimulating antigen TcsA in *Listeria monocytogenes* by decreasing *tcsA* mRNA stability. *RNA Biol* 1–12.
50. Skippington E, Ragan MA. 2012. Evolutionary dynamics of small RNAs in 27 *Escherichia coli* and *Shigella* genomes. *Genome Biol Evol* 4:330–345.
51. Gottesman S, Storz G. 2011. Bacterial Small RNA Regulators: Versatile Roles and Rapidly Evolving Variations. *Cold Spring Harb Perspect Biol* 3.
52. Mollerup MS, Ross JA, Helfer A-C, Meistrup K, Romby P, Kallipolitis BH. 2016. Two novel members of the LhrC family of small RNAs in *Listeria monocytogenes* with overlapping regulatory functions but distinctive expression profiles. *RNA Biol* 13:895–915.

53. Lenz DH, Mok KC, Lilley BN, Kulkarni RV, Wingreen NS, Bassler BL. 2004. The Small RNA Chaperone Hfq and Multiple Small RNAs Control Quorum Sensing in *Vibrio harveyi* and *Vibrio cholerae*. *Cell* 118:69–82.
54. Murashko ON, Lin-Chao S. 2017. *Escherichia coli* responds to environmental changes using enolase degradosomes and stabilized DicF sRNA to alter cellular morphology. *Proc Natl Acad Sci* 201703731.
55. Hayashi T, Makino K, Ohnishi M, Kurokawa K, Ishii K, Yokoyama K, Han CG, Ohtsubo E, Nakayama K, Murata T, Tanaka M, Tobe T, Iida T, Takami H, Honda T, Sasakawa C, Ogasawara N, Yasunaga T, Kuhara S, Shiba T, Hattori M, Shinagawa H. 2001. Complete genome sequence of enterohemorrhagic *Escherichia coli* O157:H7 and genomic comparison with a laboratory strain K-12. *DNA Res Int J Rapid Publ Rep Genes Genomes* 8:11–22.
56. Franze de Fernandez MT, Eoyang L, August JT. 1968. Factor fraction required for the synthesis of bacteriophage Qbeta-RNA. *Nature* 219:588–590.
57. Sun X, Zhulin I, Wartell RM. 2002. Predicted structure and phyletic distribution of the RNA-binding protein Hfq. *Nucleic Acids Res* 30:3662–3671.
58. Tsui HC, Leung HC, Winkler ME. 1994. Characterization of broadly pleiotropic phenotypes caused by an hfq insertion mutation in *Escherichia coli* K-12. *Mol Microbiol* 13:35–49.
59. Brennan RG, Link TM. 2007. Hfq structure, function and ligand binding. *Curr Opin Microbiol* 10:125–133.
60. Kajitani M, Kato A, Wada A, Inokuchi Y, Ishihama A. 1994. Regulation of the *Escherichia coli* hfq gene encoding the host factor for phage Q beta. *J Bacteriol* 176:531–534.
61. Møller T, Franch T, Højrup P, Keene DR, Bächinger HP, Brennan RG, Valentin-Hansen P. 2002. Hfq: a bacterial Sm-like protein that mediates RNA-RNA interaction. *Mol Cell* 9:23–30.
62. Schumacher MA, Pearson RF, Møller T, Valentin-Hansen P, Brennan RG. 2002. Structures of the pleiotropic translational regulator Hfq and an Hfq-RNA complex: a bacterial Sm-like protein. *EMBO J* 21:3546–3556.
63. Zhang A, Altuvia S, Tiwari A, Argaman L, Hengge-Aronis R, Storz G. 1998. The OxyS regulatory RNA represses rpoS translation and binds the Hfq (HF-I) protein. *EMBO J* 17:6061–6068.
64. Otaka H, Ishikawa H, Morita T, Aiba H. 2011. PolyU tail of rho-independent terminator of bacterial small RNAs is essential for Hfq action. *Proc Natl Acad Sci U S A* 108:13059–13064.
65. Hussein R, Lim HN. 2011. Disruption of small RNA signaling caused by competition for Hfq. *Proc Natl Acad Sci U S A* 108:1110–1115.

66. Kunte HJ, Crane RA, Culham DE, Richmond D, Wood JM. 1999. Protein ProQ influences osmotic activation of compatible solute transporter ProP in *Escherichia coli* K-12. *J Bacteriol* 181:1537–1543.
67. Smirnov A, Förstner KU, Holmqvist E, Otto A, Günster R, Becher D, Reinhardt R, Vogel J. 2016. Grad-seq guides the discovery of ProQ as a major small RNA-binding protein. *Proc Natl Acad Sci* 113:11591–11596.
68. Smirnov A, Wang C, Drewry LL, Vogel J. 2017. Molecular mechanism of mRNA repression in trans by a ProQ-dependent small RNA. *EMBO J* 36:1029–1045.
69. Holmqvist E, Li L, Bischler T, Barquist L, Vogel J. 2018. Global Maps of ProQ Binding In Vivo Reveal Target Recognition via RNA Structure and Stability Control at mRNA 3' Ends. *Mol Cell* 70:971-982.e6.
70. Romeo T, Babitzke P. 2018. Global regulation by CsrA and its RNA antagonists. *Microbiol Spectr* 6.
71. Liu MY, Gui G, Wei B, Preston JF, Oakford L, Yüksel U, Giedroc DP, Romeo T. 1997. The RNA molecule CsrB binds to the global regulatory protein CsrA and antagonizes its activity in *Escherichia coli*. *J Biol Chem* 272:17502–17510.
72. Weilbacher T, Suzuki K, Dubey AK, Wang X, Gudapaty S, Morozov I, Baker CS, Georgellis D, Babitzke P, Romeo T. 2003. A novel sRNA component of the carbon storage regulatory system of *Escherichia coli*. *Mol Microbiol* 48:657–670.
73. Khemici V, Linder P. 2016. RNA helicases in bacteria. *Curr Opin Microbiol* 30:58–66.
74. Aguirre AA, Vicente AM, Hardwick SW, Alvelos DM, Mazzon RR, Luisi BF, Marques MV. 2017. Association of the Cold Shock DEAD-Box RNA Helicase RhIE to the RNA Degradosome in *Caulobacter crescentus*. *J Bacteriol* 199:e00135-17.
75. Chamot D, Magee WC, Yu E, Owttrim GW. 1999. A cold shock-induced cyanobacterial RNA helicase. *J Bacteriol* 181:1728–1732.
76. Charollais J, Dreyfus M, Iost I. 2004. CsdA, a cold-shock RNA helicase from *Escherichia coli*, is involved in the biogenesis of 50S ribosomal subunit. *Nucleic Acids Res* 32:2751–2759.
77. Resch A, Večerek B, Palavra K, Bläsi U. 2010. Requirement of the CsdA DEAD-box helicase for low temperature riboregulation of *rpoS* mRNA. *RNA Biol* 7:796–802.
78. El Mortaji L, Aubert S, Galtier E, Schmitt C, Anger K, Redko Y, Quentin Y, De Reuse H. 2018. The Sole DEAD-Box RNA Helicase of the Gastric Pathogen *Helicobacter pylori* Is Essential for Colonization. *mBio* 9.

79. Intile PJ, Balzer GJ, Wolfgang MC, Yahr TL. 2015. The RNA Helicase DeaD Stimulates ExsA Translation To Promote Expression of the *Pseudomonas aeruginosa* Type III Secretion System. *J Bacteriol* 197:2664–2674.
80. Netterling S, Bäreclöv C, Vaitkevicius K, Johansson J. 2015. RNA Helicase Important for *Listeria monocytogenes* Hemolytic Activity and Virulence Factor Expression. *Infect Immun* 84:67–76.
81. Mackie GA. 2013. RNase E: at the interface of bacterial RNA processing and decay. *Nat Rev Microbiol* 11:45–57.
82. McDowall KJ, Lin-Chao S, Cohen SN. 1994. A+U content rather than a particular nucleotide order determines the specificity of RNase E cleavage. *J Biol Chem* 269:10790–10796.
83. Caruthers JM, Feng Y, McKay DB, Cohen SN. 2006. Retention of Core Catalytic Functions by a Conserved Minimal Ribonuclease E Peptide That Lacks the Domain Required for Tetramer Formation. *J Biol Chem* 281:27046–27051.
84. Callaghan AJ, Marcaida MJ, Stead JA, McDowall KJ, Scott WG, Luisi BF. 2005. Structure of *Escherichia coli* RNase E catalytic domain and implications for RNA turnover. *Nature* 437:1187–1191.
85. Murashko ON, Kaberdin VR, Lin-Chao S. 2012. Membrane binding of *Escherichia coli* RNase E catalytic domain stabilizes protein structure and increases RNA substrate affinity. *Proc Natl Acad Sci U S A* 109:7019–7024.
86. Liou GG, Jane WN, Cohen SN, Lin NS, Lin-Chao S. 2001. RNA degradosomes exist in vivo in *Escherichia coli* as multicomponent complexes associated with the cytoplasmic membrane via the N-terminal region of ribonuclease E. *Proc Natl Acad Sci U S A* 98:63–68.
87. Miczak A, Kaberdin VR, Wei CL, Lin-Chao S. 1996. Proteins associated with RNase E in a multicomponent ribonucleolytic complex. *Proc Natl Acad Sci U S A* 93:3865–3869.
88. Mohanty BK, Kushner SR. 2000. Polynucleotide phosphorylase functions both as a 3' right-arrow 5' exonuclease and a poly(A) polymerase in *Escherichia coli*. *Proc Natl Acad Sci U S A* 97:11966–11971.
89. Kaper JB, Nataro JP, Mobley HLT. 2004. Pathogenic *Escherichia coli*. *Nat Rev Microbiol* 2:123–140.
90. Perna NT, Plunkett G, Burland V, Mau B, Glasner JD, Rose DJ, Mayhew GF, Evans PS, Gregor J, Kirkpatrick HA, Pósfai G, Hackett J, Klink S, Boutin A, Shao Y, Miller L, Grotbeck EJ, Davis NW, Lim A, Dimalanta ET, Potamousis KD, Apodaca J, Anantharaman TS, Lin J, Yen G, Schwartz DC, Welch RA, Blattner FR. 2001. Genome sequence of enterohaemorrhagic *Escherichia coli* O157:H7. *Nature* 409:529–533.

91. McDaniel TK, Jarvis KG, Donnenberg MS, Kaper JB. 1995. A genetic locus of enterocyte effacement conserved among diverse enterobacterial pathogens. *Proc Natl Acad Sci U S A* 92:1664–1668.
92. Mellies JL, Barron AMS, Carmona AM. 2007. Enteropathogenic and Enterohemorrhagic *Escherichia coli* Virulence Gene Regulation. *Infect Immun* 75:4199–4210.
93. Tuttle J, Gomez T, Doyle MP, Wells JG, Zhao T, Tauxe RV, Griffin PM. 1999. Lessons from a large outbreak of *Escherichia coli* O157:H7 infections: insights into the infectious dose and method of widespread contamination of hamburger patties. *Epidemiol Infect* 122:185–192.
94. Goldwater PN, Bettelheim KA. 2012. Treatment of enterohemorrhagic *Escherichia coli* (EHEC) infection and hemolytic uremic syndrome (HUS). *BMC Med* 10:12.
95. Nguyen Y, Sperandio V. 2012. Enterohemorrhagic *E. coli* (EHEC) pathogenesis. *Front Cell Infect Microbiol* 2.
96. Price SB, Wright JC, DeGraves FJ, Castanie-Cornet M-P, Foster JW. 2004. Acid Resistance Systems Required for Survival of *Escherichia coli* O157:H7 in the Bovine Gastrointestinal Tract and in Apple Cider Are Different. *Appl Environ Microbiol* 70:4792–4799.
97. Pacheco AR, Sperandio V. 2012. Shiga toxin in enterohemorrhagic *E. coli*: regulation and novel anti-virulence strategies. *Front Cell Infect Microbiol* 2:81.
98. Riley LW, Remis RS, Helgerson SD, McGee HB, Wells JG, Davis BR, Hebert RJ, Olcott ES, Johnson LM, Hargrett NT, Blake PA, Cohen ML. 1983. Hemorrhagic colitis associated with a rare *Escherichia coli* serotype. *N Engl J Med* 308:681–685.
99. Callaway TR, Carr MA, Edrington TS, Anderson RC, Nisbet DJ. 2009. Diet, *Escherichia coli* O157:H7, and cattle: a review after 10 years. *Curr Issues Mol Biol* 11:67–79.
100. Shere JA, Bartlett KJ, Kaspar CW. 1998. Longitudinal Study of *Escherichia coli* O157:H7 Dissemination on Four Dairy Farms in Wisconsin. *Appl Environ Microbiol* 64:1390–1399.
101. Callejón RM, Rodríguez-Naranjo MI, Ubeda C, Hornedo-Ortega R, Garcia-Parrilla MC, Troncoso AM. 2015. Reported Foodborne Outbreaks Due to Fresh Produce in the United States and European Union: Trends and Causes. *Foodborne Pathog Dis* 12:32–38.
102. Wadamori Y, Gooneratne R, Hussain MA. 2017. Outbreaks and factors influencing microbiological contamination of fresh produce. *J Sci Food Agric* 97:1396–1403.

103. Zimmerhackl LB. 2000. E. coli, antibiotics, and the hemolytic-uremic syndrome. *N Engl J Med* 342:1990–1991.
104. Wong CS, Mooney JC, Brandt JR, Staples AO, Jelacic S, Boster DR, Watkins SL, Tarr PI. 2012. Risk factors for the hemolytic uremic syndrome in children infected with *Escherichia coli* O157:H7: a multivariable analysis. *Clin Infect Dis Off Publ Infect Dis Soc Am* 55:33–41.
105. Grif K, Dierich MP, Karch H, Allerberger F. 1998. Strain-Specific Differences in the Amount of Shiga Toxin Released from Enterohemorrhagic *Escherichia coli* O157 following Exposure to Subinhibitory Concentrations of Antimicrobial Agents. *Eur J Clin Microbiol Infect Dis* 17:761–766.
106. Neely MN, Friedman DI. 1998. Functional and genetic analysis of regulatory regions of coliphage H-19B: location of shiga-like toxin and lysis genes suggest a role for phage functions in toxin release. *Mol Microbiol* 28:1255–1267.
107. Stein PE, Boodhoo A, Tyrrell GJ, Brunton JL, Read RJ. 1992. Crystal structure of the cell-binding B oligomer of verotoxin-1 from *E. coli*. *Nature* 355:748–750.
108. Fraser ME, Fujinaga M, Cherney MM, Melton-Celsa AR, Twiddy EM, O'Brien AD, James MNG. 2004. Structure of Shiga Toxin Type 2 (Stx2) from *Escherichia coli* O157:H7. *J Biol Chem* 279:27511–27517.
109. Beddoe T, Paton AW, Le Nours J, Rossjohn J, Paton JC. 2010. Structure, Biological Functions and Applications of the AB5 Toxins. *Trends Biochem Sci* 35:411–418.
110. Lindberg AA, Brown JE, Strömberg N, Westling-Ryd M, Schultz JE, Karlsson KA. 1987. Identification of the carbohydrate receptor for Shiga toxin produced by *Shigella dysenteriae* type 1. *J Biol Chem* 262:1779–1785.
111. Endo Y, Tsurugi K, Yutsudo T, Takeda Y, Ogasawara T, Igarashi K. 1988. Site of action of a Vero toxin (VT2) from *Escherichia coli* O157:H7 and of Shiga toxin on eukaryotic ribosomes. RNA N-glycosidase activity of the toxins. *Eur J Biochem FEBS* 171:45–50.
112. Elliott SJ, Wainwright LA, McDaniel TK, Jarvis KG, Deng Y, Lai L-C, McNamara BP, Donnenberg MS, Kaper JB. 1998. The complete sequence of the locus of enterocyte effacement (LEE) from enteropathogenic *Escherichia coli* E2348/69. *Mol Microbiol* 28:1–4.
113. Lai Y, Rosenshine I, Leong JM, Frankel G. 2013. Intimate host attachment: enteropathogenic and enterohaemorrhagic *Escherichia coli*. *Cell Microbiol* 15:1796–1808.
114. Mellies JL, Elliott SJ, Sperandio V, Donnenberg MS, Kaper JB. 1999. The Per regulon of enteropathogenic *Escherichia coli*: identification of a regulatory cascade and a novel transcriptional activator, the locus of enterocyte effacement (LEE)-encoded regulator (Ler). *Mol Microbiol* 33:296–306.

115. Elliott SJ, Sperandio V, Girón JA, Shin S, Mellies JL, Wainwright L, Hutcheson SW, McDaniel TK, Kaper JB. 2000. The Locus of Enterocyte Effacement (LEE)-Encoded Regulator Controls Expression of Both LEE- and Non-LEE-Encoded Virulence Factors in Enteropathogenic and Enterohemorrhagic *Escherichia coli*. *Infect Immun* 68:6115–6126.
116. Bustamante VH, Santana FJ, Calva E, Puente JL. 2001. Transcriptional regulation of type III secretion genes in enteropathogenic *Escherichia coli*: Ler antagonizes H-NS-dependent repression. *Mol Microbiol* 39:664–678.
117. Dorman CJ. 2004. H-NS: a universal regulator for a dynamic genome. *Nat Rev Microbiol* 2:391–400.
118. Lucchini S, Rowley G, Goldberg MD, Hurd D, Harrison M, Hinton JCD. 2006. H-NS Mediates the Silencing of Laterally Acquired Genes in Bacteria. *PLOS Pathog* 2:e81.
119. Deng W, Puente JL, Gruenheid S, Li Y, Vallance BA, Vázquez A, Barba J, Ibarra JA, O'Donnell P, Metalnikov P, Ashman K, Lee S, Goode D, Pawson T, Finlay BB. 2004. Dissecting virulence: systematic and functional analyses of a pathogenicity island. *Proc Natl Acad Sci U S A* 101:3597–3602.
120. Creasey EA, Delahay RM, Daniell SJ, Frankel G. 2003. Yeast two-hybrid system survey of interactions between LEE-encoded proteins of enteropathogenic *Escherichia coli*. *Microbiol Read Engl* 149:2093–2106.
121. Russell RM, Sharp FC, Rasko DA, Sperandio V. 2007. QseA and GrlR/GrlA Regulation of the Locus of Enterocyte Effacement Genes in Enterohemorrhagic *Escherichia coli*. *J Bacteriol* 189:5387–5392.
122. Padavannil A, Jobichen C, Mills E, Velazquez-Campoy A, Li M, Leung KY, Mok YK, Rosenshine I, Sivaraman J. 2013. Structure of GrlR-GrlA complex that prevents GrlA activation of virulence genes. *Nat Commun* 4:2546.
123. Barba J, Bustamante VH, Flores-Valdez MA, Deng W, Finlay BB, Puente JL. 2005. A Positive Regulatory Loop Controls Expression of the Locus of Enterocyte Effacement-Encoded Regulators Ler and GrlA. *J Bacteriol* 187:7918–7930.
124. Iyoda S, Watanabe H. 2005. ClpXP protease controls expression of the type III protein secretion system through regulation of RpoS and GrlR levels in enterohemorrhagic *Escherichia coli*. *J Bacteriol* 187:4086–4094.
125. Furniss RCD, Clements A. 2017. Regulation of the Locus of Enterocyte Effacement in Attaching and Effacing Pathogens. *J Bacteriol* 200.
126. Porter ME, Mitchell P, Free A, Smith DGE, Gally DL. 2005. The LEE1 Promoters from both Enteropathogenic and Enterohemorrhagic *Escherichia coli* Can Be Activated by PerC-Like Proteins from Either Organism. *J Bacteriol* 187:458–472.

127. Iyoda S, Watanabe H. 2004. Positive effects of multiple pch genes on expression of the locus of enterocyte effacement genes and adherence of enterohaemorrhagic *Escherichia coli* O157:H7 to HEp-2 cells. *Microbiology* 150:2357–2571.
128. Fukui N, Oshima T, Ueda T, Ogasawara N, Tobe T. 2016. Gene Activation through the Modulation of Nucleoid Structures by a Horizontally Transferred Regulator, Pch, in Enterohemorrhagic *Escherichia coli*. *PLOS ONE* 11:e0149718.
129. Dong T, Chiang SM, Joyce C, Yu R, Schellhorn HE. 2009. Polymorphism and selection of rpoS in pathogenic *Escherichia coli*. *BMC Microbiol* 9:118.
130. Sperandio V, Mellies JL, Nguyen W, Shin S, Kaper JB. 1999. Quorum sensing controls expression of the type III secretion gene transcription and protein secretion in enterohemorrhagic and enteropathogenic *Escherichia coli*. *Proc Natl Acad Sci* 96:15196–15201.
131. Beltrametti F, Kresse AU, Guzmán CA. 1999. Transcriptional regulation of the esp genes of enterohemorrhagic *Escherichia coli*. *J Bacteriol* 181:3409–3418.
132. Tomoyasu T, Takaya A, Handa Y, Karata K, Yamamoto T. 2005. ClpXP controls the expression of LEE genes in enterohaemorrhagic *Escherichia coli*. *FEMS Microbiol Lett* 253:59–66.
133. Lange R, Hengge-Aronis R. 1994. The cellular concentration of the sigma S subunit of RNA polymerase in *Escherichia coli* is controlled at the levels of transcription, translation, and protein stability. *Genes Dev* 8:1600–1612.
134. Kendall MM, Gruber CC, Rasko DA, Hughes DT, Sperandio V. 2011. Hfq Virulence Regulation in Enterohemorrhagic *Escherichia coli* O157:H7 Strain 86-24 ▽. *J Bacteriol* 193:6843–6851.
135. Hansen A-M, Kaper JB. 2009. Hfq affects the expression of the LEE pathogenicity island in enterohaemorrhagic *Escherichia coli*. *Mol Microbiol* 73:446–465.
136. Shakhnovich EA, Davis BM, Waldor MK. 2009. Hfq negatively regulates type III secretion in EHEC and several other pathogens. *Mol Microbiol* 74:347–363.
137. Islam MS, Bingle LEH, Pallen MJ, Busby SJW. 2011. Organization of the LEE1 operon regulatory region of enterohaemorrhagic *Escherichia coli* O157:H7 and activation by GrlA. *Mol Microbiol* 79:468–483.
138. Sharp FC, Sperandio V. 2007. QseA directly activates transcription of LEE1 in enterohemorrhagic *Escherichia coli*. *Infect Immun* 75:2432–2440.
139. Sperandio V, Li CC, Kaper JB. 2002. Quorum-sensing *Escherichia coli* regulator A: a regulator of the LysR family involved in the regulation of the locus of enterocyte effacement pathogenicity island in enterohemorrhagic *E. coli*. *Infect Immun* 70:3085–3093.

140. Wang S, Yang F, Yang B. 2017. Global effect of CsrA on gene expression in enterohemorrhagic *Escherichia coli* O157:H7. *Res Microbiol* 168:700–709.
141. Bhatt S, Edwards AN, Nguyen HTT, Merlin D, Romeo T, Kalman D. 2009. The RNA Binding Protein CsrA Is a Pleiotropic Regulator of the Locus of Enterocyte Effacement Pathogenicity Island of Enteropathogenic *Escherichia coli*. *Infect Immun* 77:3552–3568.
142. Bhatt S, Romeo T, Kalman D. 2011. Honing the message: post-transcriptional and post-translational control in attaching and effacing pathogens. *Trends Microbiol* 19:217–224.
143. Lodato PB, Kaper JB. 2009. Post-transcriptional processing of the LEE4 operon in enterohaemorrhagic *Escherichia coli*. *Mol Microbiol* 71:273–290.
144. Gruber CC, Sperandio V. 2014. Posttranscriptional Control of Microbe-Induced Rearrangement of Host Cell Actin. *mBio* 5:e01025-13.
145. Gruber CC, Sperandio V. 2015. Global analysis of posttranscriptional regulation by GlmY and GlmZ in enterohemorrhagic *Escherichia coli* O157:H7. *Infect Immun* 83:1286–1295.
146. Wang D, McAteer SP, Wawarczyk AB, Russell CD, Tahoun A, Elmi A, Cockroft SL, Tollervey D, Granneman S, Tree JJ, Gally DL. 2018. An RNA-dependent mechanism for transient expression of bacterial translocation filaments. *Nucleic Acids Res* 46:3366–3381.
147. Schüller S, Phillips AD. 2010. Microaerobic conditions enhance type III secretion and adherence of enterohaemorrhagic *Escherichia coli* to polarized human intestinal epithelial cells. *Environ Microbiol* 12:2426–2435.
148. Tropini C, Earle KA, Huang KC, Sonnenburg JL. 2017. The Gut Microbiome: Connecting Spatial Organization to Function. *Cell Host Microbe* 21:433–442.
149. Bäumlner AJ, Sperandio V. 2016. Interactions between the microbiota and pathogenic bacteria in the gut. *Nature* 535:85–93.
150. Albenberg L, Esipova TV, Judge CP, Bittinger K, Chen J, Laughlin A, Grunberg S, Baldassano RN, Lewis JD, Li H, Thom SR, Bushman FD, Vinogradov SA, Wu GD. 2014. Correlation between intraluminal oxygen gradient and radial partitioning of intestinal microbiota. *Gastroenterology* 147:1055-1063.e8.
151. Belzer C, de Vos WM. 2012. Microbes inside--from diversity to function: the case of Akkermansia. *ISME J* 6:1449–1458.
152. Friedman ES, Bittinger K, Esipova TV, Hou L, Chau L, Jiang J, Mesaros C, Lund PJ, Liang X, FitzGerald GA, Goulian M, Lee D, Garcia BA, Blair IA, Vinogradov SA, Wu GD. 2018. Microbes vs. chemistry in the origin of the anaerobic gut lumen. *Proc Natl Acad Sci U S A* 115:4170–4175.

153. Sperandio V. 2018. Pathogens' adaptation to the human host. *Proc Natl Acad Sci U S A* 115:9342–9343.
154. Karmali MA, Petric M, Lim C, Fleming PC, Steele BT. 1983. *Escherichia coli* cytotoxin, haemolytic-uraemic syndrome, and haemorrhagic colitis. *Lancet Lond Engl* 2:1299–1300.
155. Collins JW, Keeney KM, Crepin VF, Rathinam VAK, Fitzgerald KA, Finlay BB, Frankel G. 2014. *Citrobacter rodentium*: infection, inflammation and the microbiota. *Nat Rev Microbiol* 12:612–623.
156. Luzader DH, Kendall MM. 2016. Commensal “trail of bread crumbs” provide pathogens with a map to the intestinal landscape. *Curr Opin Microbiol* 29:68–73.
157. Kendall MM, Gruber CC, Parker CT, Sperandio V. 2012. Ethanolamine controls expression of genes encoding components involved in interkingdom signaling and virulence in enterohemorrhagic *Escherichia coli* O157:H7. *mBio* 3.
158. Bouché F, Bouché JP. 1989. Genetic evidence that DicF, a second division inhibitor encoded by the *Escherichia coli* *dicB* operon, is probably RNA. *Mol Microbiol* 3:991–994.
159. Faubladiet M, Cam K, Bouché JP. 1990. *Escherichia coli* cell division inhibitor DicF-RNA of the *dicB* operon. Evidence for its generation in vivo by transcription termination and by RNase III and RNase E-dependent processing. *J Mol Biol* 212:461–471.
160. Tétart F, Albigot R, Confer A, Mulder E, Bouché J-P. 1992. Involvement of FtsZ in coupling of nucleoid separation with septation. *Mol Microbiol* 6:621–627.
161. Tétart F, Bouché J-P. 1992. Regulation of the expression of the cell-cycle gene *ftsZ* by DicF antisense RNA. Division does not require a fixed number of FtsZ molecules. *Mol Microbiol* 6:615–620.
162. Curtis MM, Hu Z, Klimko C, Narayanan S, Deberardinis R, Sperandio V. 2014. The Gut Commensal *Bacteroides thetaiotaomicron* Exacerbates Enteric Infection through Modification of the Metabolic Landscape. *Cell Host Microbe* 16:759–769.
163. Garmendia J, Frankel G, Crepin VF. 2005. Enteropathogenic and enterohemorrhagic *Escherichia coli* infections: translocation, translocation, translocation. *Infect Immun* 73:2573–2585.
164. Bustamante VH, Villalba MI, García-Angulo VA, Vázquez A, Martínez LC, Jiménez R, Puente JL. 2011. PerC and GrIA independently regulate Ler expression in enteropathogenic *Escherichia coli*. *Mol Microbiol* 82:398–415.
165. Gómez-Duarte OG, Kaper JB. 1995. A plasmid-encoded regulatory region activates chromosomal *eaeA* expression in enteropathogenic *Escherichia coli*. *Infect Immun* 63:1767–1776.

166. Honda N, Iyoda S, Yamamoto S, Terajima J, Watanabe H. 2009. LrhA positively controls the expression of the locus of enterocyte effacement genes in enterohemorrhagic *Escherichia coli* by differential regulation of their master regulators PchA and PchB. *Mol Microbiol* 74:1393–1341.
167. Wright PR, Richter AS, Papenfort K, Mann M, Vogel J, Hess WR, Backofen R, Georg J. 2013. Comparative genomics boosts target prediction for bacterial small RNAs. *Proc Natl Acad Sci U S A* 110:E3487-3496.
168. Wright PR, Georg J, Mann M, Sorescu DA, Richter AS, Lott S, Kleinkauf R, Hess WR, Backofen R. 2014. CopraRNA and IntaRNA: predicting small RNA targets, networks and interaction domains. *Nucleic Acids Res* 42:W119-123.
169. Fröhlich KS, Papenfort K, Berger AA, Vogel J. 2012. A conserved RpoS-dependent small RNA controls the synthesis of major porin OmpD. *Nucleic Acids Res* 40:3623–3640.
170. Lalaouna D, Morissette A, Carrier M-C, Massé E. 2015. DsrA regulatory RNA represses both *hns* and *rbsD* mRNAs through distinct mechanisms in *Escherichia coli*. *Mol Microbiol* 98:357–369.
171. Lingelbach K, Dobberstein B. 1988. An extended RNA/RNA duplex structure within the coding region of mRNA does not block translational elongation. *Nucleic Acids Res* 16:3405–3414.
172. Carlson-Banning KM, Sperandio V. 2016. Catabolite and Oxygen Regulation of Enterohemorrhagic *Escherichia coli* Virulence. *mBio* 7.
173. Crofts AA, Giovanetti SM, Rubin EJ, Poly FM, Gutiérrez RL, Talaat KR, Porter CK, Riddle MS, DeNearing B, Brubaker J, Maciel M, Alcalá AN, Chakraborty S, Prouty MG, Savarino SJ, Davies BW, Trent MS. 2018. Enterotoxigenic *E. coli* virulence gene regulation in human infections. *Proc Natl Acad Sci U S A* 115:E8968–E8976.
174. Kim K, Golubeva YA, Vanderpool CK, Slauch JM. 2019. Oxygen-dependent regulation of SPI1 type three secretion system by small RNAs in *Salmonella enterica* serovar Typhimurium. *Mol Microbiol* 111:570–587.
175. Marteyn B, West NP, Browning DF, Cole JA, Shaw JG, Palm F, Mounier J, Prévost M-C, Sansonetti P, Tang CM. 2010. Modulation of *Shigella* virulence in response to available oxygen in vivo. *Nature* 465:355–358.
176. Bhattacharyya S, Jacobs WM, Adkar BV, Yan J, Zhang W, Shakhnovich EI. 2018. Accessibility of the Shine-Dalgarno Sequence Dictates N-Terminal Codon Bias in *E. coli*. *Mol Cell* 70:894-905.e5.
177. Carter-Muenchau P, Wolf RE. 1989. Growth-rate-dependent regulation of 6-phosphogluconate dehydrogenase level mediated by an anti-Shine-Dalgarno sequence located within the *Escherichia coli* *gnd* structural gene. *Proc Natl Acad Sci* 86:1138–1142.

178. Chang JT, Green CB, Wolf RE. 1995. Inhibition of translation initiation on *Escherichia coli* *gnd* mRNA by formation of a long-range secondary structure involving the ribosome binding site and the internal complementary sequence. *J Bacteriol* 177:6560–6567.
179. Giuliadori AM, Di Pietro F, Marzi S, Masquida B, Wagner R, Romby P, Gualerzi CO, Pon CL. 2010. The *cspA* mRNA Is a Thermosensor that Modulates Translation of the Cold-Shock Protein CspA. *Mol Cell* 37:21–33.
180. Morita M, Kanemori M, Yanagi H, Yura T. 1999. Heat-Induced Synthesis of σ^{32} in *Escherichia coli*: Structural and Functional Dissection of *rpoH* mRNA Secondary Structure. *J Bacteriol* 181:401–410.
181. Morita MT, Tanaka Y, Kodama TS, Kyogoku Y, Yanagi H, Yura T. 1999. Translational induction of heat shock transcription factor σ^{32} : evidence for a built-in RNA thermosensor. *Genes Dev* 13:655–665.
182. Falcone M, Ferrara S, Rossi E, Johansen HK, Molin S, Bertoni G. 2018. The Small RNA *ErsA* of *Pseudomonas aeruginosa* Contributes to Biofilm Development and Motility through Post-transcriptional Modulation of *AmrZ*. *Front Microbiol* 9.
183. Jones AJ, Fast AG, Clupper M, Papoutsakis ET. 2018. Small and Low but Potent: the Complex Regulatory Role of the Small RNA *SolB* in Solventogenesis in *Clostridium acetobutylicum*. *Appl Environ Microbiol* 84:e00597-18.
184. Ochman H, Lawrence JG, Groisman EA. 2000. Lateral gene transfer and the nature of bacterial innovation. *Nature* 405:299–304.
185. Dziva F, van Diemen PM, Stevens MP, Smith AJ, Wallis TS. 2004. Identification of *Escherichia coli* O157 : H7 genes influencing colonization of the bovine gastrointestinal tract using signature-tagged mutagenesis. *Microbiol Read Engl* 150:3631–3645.
186. Klepsch MM, Kovermann M, Löw C, Balbach J, Permentier HP, Fusetti F, de Gier JW, Slotboom DJ, Berntsson RP-A. 2011. *Escherichia coli* peptide binding protein *OppA* has a preference for positively charged peptides. *J Mol Biol* 414:75–85.
187. Takyar S, Hickerson RP, Noller HF. 2005. mRNA helicase activity of the ribosome. *Cell* 120:49–58.
188. Datsenko KA, Wanner BL. 2000. One-step inactivation of chromosomal genes in *Escherichia coli* K-12 using PCR products. *Proc Natl Acad Sci U S A* 97:6640–6645.
189. Lovak K. 1997. ABI Prism 7700 Sequence Detection System. User Bulletin no. 2, PE Applied Biosystems 4303859B(bulletin reference 1997):777802-778002.
190. Knutton S, Baldwin T, Williams PH, McNeish AS. 1989. Actin accumulation at sites of bacterial adhesion to tissue culture cells: basis of a new diagnostic test for

- enteropathogenic and enterohemorrhagic *Escherichia coli*. *Infect Immun* 57:1290–1298.
191. Kulasekara BR, Jacobs M, Zhou Y, Wu Z, Sims E, Saenphimmachak C, Rohmer L, Ritchie JM, Radey M, McKeivitt M, Freeman TL, Hayden H, Haugen E, Gillett W, Fong C, Chang J, Beskhlebnaya V, Waldor MK, Samadpour M, Whittam TS, Kaul R, Brittnacher M, Miller SI. 2009. Analysis of the genome of the *Escherichia coli* O157:H7 2006 spinach-associated outbreak isolate indicates candidate genes that may enhance virulence. *Infect Immun* 77:3713–3721.
 192. Lorenz R, Bernhart SH, Höner Zu Siederdisen C, Tafer H, Flamm C, Stadler PF, Hofacker IL. 2011. ViennaRNA Package 2.0. *Algorithms Mol Biol* 6:26.
 193. Owtrim GW. 2013. RNA helicases. *RNA Biol* 10:96–110.
 194. Rocak S, Linder P. 2004. DEAD-box proteins: the driving forces behind RNA metabolism. *Nat Rev Mol Cell Biol* 5:232–241.
 195. Fairman-Williams ME, Guenther U-P, Jankowsky E. 2010. SF1 and SF2 helicases: family matters. *Curr Opin Struct Biol* 20:313–324.
 196. Diges CM, Uhlenbeck OC. 2001. *Escherichia coli* DbpA is an RNA helicase that requires hairpin 92 of 23S rRNA. *EMBO J* 20:5503–5512.
 197. Bizebard T, Ferlenghi I, Iost I, Dreyfus M. 2004. Studies on Three *E. coli* DEAD-Box Helicases Point to an Unwinding Mechanism Different from that of Model DNA Helicases. *Biochemistry* 43:7857–7866.
 198. Py B, Higgins CF, Krisch HM, Carpousis AJ. 1996. A DEAD-box RNA helicase in the *Escherichia coli* RNA degradosome. *Nature* 381:169–172.
 199. Charollais J, Pflieger D, Vinh J, Dreyfus M, Iost I. 2003. The DEAD-box RNA helicase SrmB is involved in the assembly of 50S ribosomal subunits in *Escherichia coli*. *Mol Microbiol* 48:1253–1265.
 200. Proux F, Dreyfus M, Iost I. 2011. Identification of the sites of action of SrmB, a DEAD-box RNA helicase involved in *Escherichia coli* ribosome assembly. *Mol Microbiol* 82:300–311.
 201. Lu J, Aoki H, Ganoza MC. 1999. Molecular characterization of a prokaryotic translation factor homologous to the eukaryotic initiation factor eIF4A. *Int J Biochem Cell Biol* 31:215–229.
 202. Oun S, Redder P, Didier J-P, François P, Corvaglia A-R, Buttazzoni E, Giraud C, Girard M, Schrenzel J, Linder P. 2013. The CshA DEAD-box RNA helicase is important for quorum sensing control in *Staphylococcus aureus*. *RNA Biol* 10:157–165.
 203. Iost I, Dreyfus M. 2006. DEAD-box RNA helicases in *Escherichia coli*. *Nucleic Acids Res* 34:4189–4197.

204. Khemici V, Poljak L, Toesca I, Carpousis AJ. 2005. Evidence in vivo that the DEAD-box RNA helicase RhlB facilitates the degradation of ribosome-free mRNA by RNase E. *Proc Natl Acad Sci U S A* 102:6913–6918.
205. Vanzo NF, Li YS, Py B, Blum E, Higgins CF, Raynal LC, Krisch HM, Carpousis AJ. 1998. Ribonuclease E organizes the protein interactions in the *Escherichia coli* RNA degradosome. *Genes Dev* 12:2770–2781.
206. Jain C. 2008. The *E. coli* RhlE RNA helicase regulates the function of related RNA helicases during ribosome assembly. *RNA N Y N* 14:381–389.
207. Kido M, Yamanaka K, Mitani T, Niki H, Ogura T, Hiraga S. 1996. RNase E polypeptides lacking a carboxyl-terminal half suppress a mukB mutation in *Escherichia coli*. *J Bacteriol* 178:3917–3925.
208. Ow MC, Liu Q, Kushner SR. 2000. Analysis of mRNA decay and rRNA processing in *Escherichia coli* in the absence of RNase E-based degradosome assembly. *Mol Microbiol* 38:854–866.
209. Apirion D, Lassar AB. 1978. A conditional lethal mutant of *Escherichia coli* which affects the processing of ribosomal RNA. *J Biol Chem* 253:1738–1742.
210. McDowall KJ, Hernandez RG, Lin-Chao S, Cohen SN. 1993. The *ams-1* and *rne-3071* temperature-sensitive mutations in the *ams* gene are in close proximity to each other and cause substitutions within a domain that resembles a product of the *Escherichia coli* *mre* locus. *J Bacteriol* 175:4245–4249.
211. Perwez T, Hami D, Maples VF, Min Z, Wang B-C, Kushner SR. 2008. Intragenic suppressors of temperature-sensitive *rne* mutations lead to the dissociation of RNase E activity on mRNA and tRNA substrates in *Escherichia coli*. *Nucleic Acids Res* 36:5306–5318.
212. Deng W, Li Y, Vallance BA, Finlay BB. 2001. Locus of Enterocyte Effacement from *Citrobacter rodentium*: Sequence Analysis and Evidence for Horizontal Transfer among Attaching and Effacing Pathogens. *Infect Immun* 69:6323–6335.
213. Petty NK, Bulgin R, Crepin VF, Cerdeño-Tárraga AM, Schroeder GN, Quail MA, Lennard N, Corton C, Barron A, Clark L, Toribio AL, Parkhill J, Dougan G, Frankel G, Thomson NR. 2010. The *Citrobacter rodentium* Genome Sequence Reveals Convergent Evolution with Human Pathogenic *Escherichia coli*. *J Bacteriol* 192:525–538.
214. Johnson E, Barthold SW. 1979. The ultrastructure of transmissible murine colonic hyperplasia. *Am J Pathol* 97:291–313.
215. Redder P, Hausmann S, Khemici V, Yasrebi H, Linder P. 2015. Bacterial versatility requires DEAD-box RNA helicases. *FEMS Microbiol Rev* 39:392–412.

216. Li S, Xiao X, Sun P, Wang F. 2008. Screening of genes regulated by cold shock in *Shewanella piezotolerans* WP3 and time course expression of cold-regulated genes. *Arch Microbiol* 189:549–556.
217. Bergholz PW, Bakermans C, Tiedje JM. 2009. *Psychrobacter arcticus* 273-4 uses resource efficiency and molecular motion adaptations for subzero temperature growth. *J Bacteriol* 191:2340–2352.
218. Khemici V, Toesca I, Poljak L, Vanzo NF, Carpousis AJ. 2004. The RNase E of *Escherichia coli* has at least two binding sites for DEAD-box RNA helicases: functional replacement of RhlB by RhlE. *Mol Microbiol* 54:1422–1430.
219. Prud'homme-Généreux A, Beran RK, Iost I, Ramey CS, Mackie GA, Simons RW. 2004. Physical and functional interactions among RNase E, polynucleotide phosphorylase and the cold-shock protein, CsdA: evidence for a “cold shock degradosome.” *Mol Microbiol* 54:1409–1421.
220. Dong T, Coombes BK, Schellhorn HE. 2009. Role of RpoS in the Virulence of *Citrobacter rodentium*. *Infect Immun* 77:501–507.
221. Price SB, Cheng C-M, Kaspar CW, Wright JC, DeGraves FJ, Penfound TA, Castanie-Cornet M-P, Foster JW. 2000. Role of rpoS in Acid Resistance and Fecal Shedding of *Escherichia coli* O157:H7. *Appl Environ Microbiol* 66:632–637.
222. Griffin PM, Ostroff SM, Tauxe RV, Greene KD, Wells JG, Lewis JH, Blake PA. 1988. Illnesses associated with *Escherichia coli* O157:H7 infections. A broad clinical spectrum. *Ann Intern Med* 109:705–712.
223. Guzman LM, Belin D, Carson MJ, Beckwith J. 1995. Tight regulation, modulation, and high-level expression by vectors containing the arabinose PBAD promoter. *J Bacteriol* 177:4121–4130.
224. West SE, Schweizer HP, Dall C, Sample AK, Runyen-Janecky LJ. 1994. Construction of improved *Escherichia-Pseudomonas* shuttle vectors derived from pUC18/19 and sequence of the region required for their replication in *Pseudomonas aeruginosa*. *Gene* 148:81–86.
225. Zeghouf M, Li J, Butland G, Borkowska A, Canadien V, Richards D, Beattie B, Emili A, Greenblatt JF. 2004. Sequential Peptide Affinity (SPA) System for the Identification of Mammalian and Bacterial Protein Complexes. *J Proteome Res* 3:463–468.
226. Hernandez-Doria JD, Sperandio V. 2018. Bacteriophage Transcription Factor Cro Regulates Virulence Gene Expression in Enterohemorrhagic *Escherichia coli*. *Cell Host Microbe* 23:607-617.e6.